



Universidad Autónoma de Querétaro  
Facultad de ingeniería  
Doctorado en ingeniería

Desarrollo de un sistema de fitocontrol basado en la respuesta fotosintética  
y de transpiración de la planta.

**TESIS**

Que como parte de los requisitos para obtener el grado de  
Doctor en Ingeniería

**Presenta:**

M. en C. Carlos Duarte Galván

**Dirigido por:**

Dr. Jesús Roberto Millán Almaraz

**SINODALES**


Dr. Jesús Roberto Millán Almaraz  
Presidente


Dr. Irineo Torres Pacheco  
Secretario

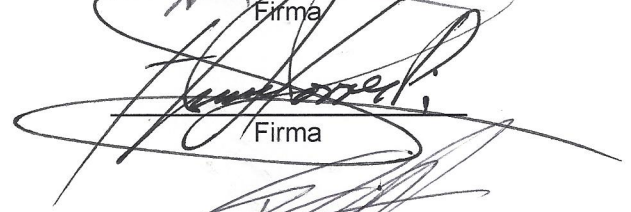
Dr. Ramón Gerardo Guevara González  
Vocal


Dr. René de Jesús Romero Troncoso  
Suplente

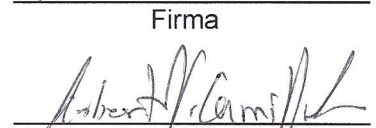
Dr. Roberto Valentín Carrillo Serrano  
Suplente


  
Dr. Aurelio Domínguez González  
Director de la Facultad


  
Firma

  
Firma

  
Firma

  
Firma

  
Firma

  
Dr. Irineo Torres Pacheco  
Director de Investigación y Posgrado

Centro Universitario  
Querétaro, Qro.  
Octubre del 2014  
México

# **Desarrollo de un sistema de fitocontrol basado en la respuesta fotosintética y de transpiración de la planta.**

**Por Carlos Duarte Galván**

## RESUMEN

Entre la variedad de estrés bióticos y abióticos que las plantas padecen, la sequía es el más peligroso, en poco tiempo impacta el rendimiento y calidad de los cultivos y si no se detecta oportunamente puede provocar la pérdida total del cultivo. Sin embargo, se ha comprobado que para determinadas especies de plantas, un estrés moderado mejora algunas características de interés como el sabor y el contenido de sustancias bioactivas. Es por eso que es deseable contar con equipos con la capacidad de detectar y monitorear en tiempo real el estrés que sufre un cultivo. El presente trabajo se enfoca en probar como el monitoreo de procesos fisiológicos de la planta como fotosíntesis y transpiración proporcionan la información suficiente para detectar y cuantificar el daño del estrés en las plantas. El experimento consistió en utilizar un conjunto de sensores basados en la metodología de intercambio de gases y vapor de agua, para monitorear plantas bajo condiciones controladas de estrés por sequía. Los objetivos principales fueron utilizar los equipos de monitoreo llamados en este trabajo fitomonitores, bajo condiciones operativas reales así como utilizar una metodología de índices de variables para compensar las variaciones espaciales dentro del invernadero y lograr comparaciones entre tratamientos más confiables.

**Palabras clave:** detección de sequía, sensor inteligente, dinámica de transpiración, estimación de fotosíntesis, monitoreo de estrés hídrico en plantas.

## **SUMMARY**

Among the variety of biotic and abiotic stress plants suffer, soil drought represents the most dangerous stress for plants. It impacts the yield and quality of crops, and if it remains undetected for long time the entire crop could be lost. However, for determinate plants a certain amount of drought stress improves specific characteristics. Then, a device which opportunely detects and quantifies the impact of drought stress in plants is desirable. The current work focuses in testing how the monitoring of physiological process through a gas exchange methodology provides enough information to detect drought stress conditions in plants. The experiment consisted in using a set of smart sensors previously designed, for monitoring a stage of plants under controlled drought conditions. The major goals are to use the monitoring devices under real operative conditions and to apply an index-based methodology in the analysis to compensate the spatial variation inside the greenhouse. In this way, differences between treatments will be independent of longitudinal climate variations inside the greenhouse.

**Keywords:** drought detection, smart sensor, transpiration dynamic, photosynthesis measurement, plant water stress monitoring.

## DEDICATORIA

A mi Padre y Madre.

## **AGRADECIMIENTOS**

Agradezco a mi Director de tesis, el Dr. Jesús Roberto Millán Almaraz por su apoyo y por la confianza depositada en mí para cumplir con este proyecto.

El Dr. Rene de Jesús Romero Troncoso merece una mención especial por el tiempo que dedicó en ayudarme con la parte técnica de este trabajo.

A los Doctores Irineo Torres pacheco, Ramón Guevara González y Roberto Valentín Carrillo Serrano les agradezco el tiempo dedicado a la revisión de mi trabajo y las observaciones que dieron la calidad final que este proyecto doctoral necesitaba.

Agradezco también a los profesores del programa de Doctorado en Ingeniería; Juan Carlos Jáuregui Correa, Carlos Fuentes Ruíz y Rebeca del Rocío Peniche Vera, y al Dr. Mario Enrique Rodríguez García por sus valiosos y útiles consejos.

Agradezco a mi amigo, el Dr. Ismael Urrutia por apoyarme con la parte biológica de este trabajo.

Agradezco a la Universidad Autónoma de Sinaloa por aceptarme para una estancia y proporcionarme los recursos y espacios necesarios para mi investigación.

Quiero agradecer a mi familia. A mi madre, a mi padre y a mis hermanos por su gran apoyo.

Es importante agradecer a mis tíos, Margarita Galván y Venancio Ramírez por recibirme en su hogar cuando llegué a Querétaro.

Agradezco también a mi compañera Belén Pérez por su tiempo y apoyo incondicional.

Finalmente pero no menos importante, agradezco a mis compañeros Montserrat Campos, Lina Mier, Verónica Picazo, Yajaira Esquivel, Jannette Alonso, Nelly Jiménez, Alejandro García Vidales, Luis Contreras y Arturo Fernández por hacer grata e interesante esta experiencia.

# ÍNDICE DE CONTENIDO

RESUMEN .....	i
SUMMARY .....	ii
AGRADECIMIENTOS .....	iv
ÍNDICE DE CONTENIDO.....	v
ÍNDICE DE TABLAS .....	vii
ÍNDICE DE FIGURAS .....	viii
I INTRODUCCIÓN .....	9
I.1 Antecedentes y justificación .....	9
I.2 Planteamiento del problema.....	12
I.3 Hipótesis y objetivos .....	13
I.3.1 Hipótesis general.....	13
I.3.2 Objetivo general .....	13
I.3.3 Objetivos específicos.....	13
II REVISIÓN DE LITERATURA.....	14
II.1 Estrés en plantas .....	14
II.2 Estrés hídrico .....	14
II.3 Fitomonitorio .....	17
II.4 Fitocontrol .....	20
III METODOLOGÍA .....	23
III.1 Estimación de procesos fisiológicos .....	23
III.1.1 Estimación de fotosíntesis .....	24
III.1.2 Estimación de transpiración.....	25
III.1.3 Estimación de conductancia estomática.....	26

III.1.4	Estimación del déficit de presión de vapor .....	27
III.1.5	Cálculo de la diferencia de temperatura aire-hoja .....	28
III.2	Sensor inteligente para fitomonitorio .....	28
III.2.1	Sistema neumático .....	29
III.2.2	Sistema de adquisición de datos (DAS) .....	31
III.2.3	Unidad de procesamiento de señales .....	33
III.3	Sistema de comunicación inalámbrica.....	37
III.4	Software para adquisición de datos .....	40
III.5	Calibración y validación de sensores de sensores .....	41
III.6	Calibración por estrés químico .....	42
III.7	Diseño del experimento .....	43
IV	RESULTADOS Y DISCUSIÓN.....	46
IV.1	Resultados del filtrado digital .....	46
IV.2	Señales ambientales.....	47
IV.3	Señales de procesos fisiológicos.....	49
IV.4	Análisis con Transformada Wavelet Discreta (DWT).....	52
IV.5	Conclusiones y perspectivas .....	56
	BIBLIOGRAFÍA .....	58
	ARTÍCULOS INTERNACIONALES PUBLICADOS .....	64



## ÍNDICE DE TABLAS

<b>Tabla</b>		<b>Página</b>
1.1	Producción de tomate en invernadero.	10
2.1	Rangos óptimos para el desarrollo de los cultivos (Baert et al., 2013).	15
3.1	Características del sensor SHT75.	32
4.1	Resultados del análisis de correlación de radiación contra fotosíntesis.	47
4.2	Resultados de las correlaciones de Fotosíntesis contra Radiación con y sin filtrado Wavelet (DWT).	55

## ÍNDICE DE FIGURAS

<b>Figura</b>		<b>Página</b>
3.1	Diagrama a bloques del fitomonitor.	29
3.2	Diseño del sistema neumático para intercambio de CO <sub>2</sub> .	30
3.3	Cámara foliar y disposición de sensores de temperatura y radiación.	32
3.4	Arquitectura del sensor inteligente para monitoreo fisiológico.	34
3.5	Estandarización de la transmisión de datos.	39
3.6	Software para adquisición de datos.	41
3.7	Prueba de validación de sensores de CO <sub>2</sub> .	42
3.8	Resultados de estimación de fotosíntesis en plantas con herbicida.	43
3.9	Instalación del sistema de detección de sequía en un experimento bajo condiciones reales de operación.	44
4.1	Resultados del filtrado digital en la estimación de fotosíntesis.	46
4.2	Lecturas del clima dentro del invernadero en las posiciones de los Nodos 1, 2 y 3 de la WSN.	48
4.3	Imagen ampliada de dos días de radiación.	49
4.4	Señales de procesos fisiológicos.	50
4.5	Wavelets de los índices Procesos/Radiación.	54
4.6	Balance de Carbono en Tiempo Real (RT-CB).	56

# I INTRODUCCIÓN

## I.1 Antecedentes y justificación

La agricultura (del latín *agri*, 'campo o tierra de labranza' y *cultura*, 'cultivo, crianza') es el conjunto de técnicas y conocimientos para cultivar la tierra. En ella se engloban los diferentes trabajos para tratamiento del suelo y manejo de cultivos, y comprende el conjunto de acciones humanas que transforma el medio ambiente natural. Este conjunto de conocimientos se formalizaron en la agronomía, ciencia que estudia la práctica de la agricultura.

Debido a la creciente necesidad de alimentos, es necesario tener una alta productividad y calidad en los mismos. Estas demandas han vuelto indispensable el uso de tecnología de punta en la producción alimentaria, buscando la optimización del espacio de cultivo y consumo de agua a través del mejoramiento constante de las prácticas agrícolas (Ton, 1997; Ton y Kopyt, 2003).

Existe también una gran necesidad de manipular los tiempos de producción y de poder cultivar en lugares con climas desfavorables y con escasas de agua; atender estos problemas requiere un nivel de tecnificación muy alto en las prácticas agrícolas. Surge entonces el esquema de agricultura de precisión, es decir la aplicación de alta tecnología mecatrónica y biotecnológica al campo. Un ejemplo claro de agricultura de precisión es el invernadero tecnificado. La agricultura protegida permite incrementar la eficiencia en el manejo de recursos para reducir costos a largo plazo, aumentar ganancias y tener mayor producción. Además de reducir pérdidas por enfermedades, insectos y maleza que ascienden al 36% de la producción mundial, ó 550 mil millones de dólares, (Agrios, 2005; Baptista *et al.*, 2010).

Por otro lado el problema de la sequía se complica cada vez más. A nivel mundial el 69% del agua dulce se emplea en agricultura, 10% se destina para consumo doméstico y 21% por la industria. Hablando de México estas cifras son más alarmantes ya que al ser un país que basa su producto interno bruto (PIB) en actividades primarias como la agricultura, la distribución del consumo de agua es de 77-14-9

respectivamente (CONAGUA, 2013; FAOstat, 2013). Este problema ha forzado la tecnificación del campo, pasando de agricultura convencional a protegida y de precisión donde, el consumo de agua es manejado de manera eficiente a través de sistemas de riego automatizados que proporcionan la cantidad justa de agua que requieren los cultivos.

Otras estadísticas muestran que hay un notable crecimiento en la superficie que se cultiva bajo invernaderos en México, como ejemplo puede mencionarse que en 2004 había en el país 2,306 hectáreas sembradas en invernadero, mientras que en 2007 hay aproximadamente 12,530 hectáreas, y se estima que desde entonces la tasa de crecimiento fue de 2500 hectáreas por año (INEGI, 2013). De acuerdo con la Tabla 1.1, a pesar del incremento en el uso de invernaderos para producción agrícola, los rendimientos reportados al año 2011 están muy por debajo de los reportados por países como España y Holanda (FAOstat, 2013).

**Tabla 1.1 – Producción de tomate en invernadero**

<b>País</b>	<b>Producción</b>
<b>México</b>	20 kg/m <sup>2</sup>
<b>España</b>	40 kg/m <sup>2</sup>
<b>Holanda</b>	90 kg/m <sup>2</sup>

Anteriormente las plataformas tecnológicas aplicadas en agricultura se limitaban al uso de instrumentación para el monitoreo de variables climáticas. Sin embargo, para adquirir información relacionada con el estado del cultivo es necesario complementar el monitoreo con la medición de aspectos morfológicos y fisiológicos de las plantas (Hashimoto, 1989; Mazanti Hansen y Ehler, 1995).

El fitomonitorio es la primera tecnología computarizada aplicable para la observación en tiempo real del estado de salud de la planta así como del desarrollo a largo plazo de los cultivos bajo invernadero. El fitomonitorio proporciona información esencial acerca de la condición fisiológica del cultivo. Esta tecnología combina sistemas de adquisición de datos basados con sensores muy específicos y software

para el procesamiento de señales, el cual presenta información cuantitativa en términos agronómicos. El objetivo principal del fitomonitorio es alertar oportunamente al agricultor sobre fallas en los equipos así como errores humanos en el manejo del cultivo. A su vez, el sistema ayuda al agricultor a reducir el daño o pérdidas en el cultivo bajo condiciones climáticas severas. También es una buena herramienta para examinar los efectos ocasionados por diferentes tratamientos o materiales (Ton *et al.*, 2001).

La mayoría de los controladores climáticos modernos para invernadero funcionan solo con los parámetros del clima. Una retroalimentación relacionada con el estado real del cultivo solo es proporcionada por el agricultor con base en su experiencia y en algunos análisis de laboratorio. Hace más de 30 años surgió el paradigma llamado la “planta parlante” (“*the speaking plant*”), donde los sistemas automáticos de control consideraban aspectos fisiológicos del cultivo para programar decisiones. Esto se basa en la suposición de que el conocimiento de factores externos por sí solos es insuficiente para trazar con precisión conclusiones acerca del cultivo. Solo la planta en sí puede proporcionar información de su estado fisiológico; sin embargo, a pesar de los esfuerzos realizados, su aplicación fue viable hasta principios del siglo XXI (Van Leeuwen *et al.*, 2009).

A pesar de todos los esfuerzos por controlar el sistema con la retroalimentación directa de la planta, la mayoría de las mediciones provenientes del fitomonitorio han sido utilizadas únicamente como información adicional para la toma de decisiones. Una aplicación tan ambiciosa requiere de un protocolo completo que estandarice todo el proceso de medición (muestreo, colocación y posicionamiento de sensores), técnicas para la interpretación de datos y procedimientos para la toma de decisiones (Ton y Kopyt, 2003).

Dado que la fotosíntesis es la función fisiológica que produce el 90% de la materia seca, ésta es la variable de mayor importancia en todo sistema de fitomonitorio (Biswas *et al.*, 2001; Tian *et al.*, 2005). Sin embargo, existen variables fisiológicas de gran interés como son transpiración, diámetro de tallos, tamaño de frutos, flujo de savia, temperatura de hoja, clorofila y área foliar por mencionar algunas.

## I.2 Planteamiento del problema

Hoy como nunca afrontamos grandes retos que no terminan con producir alimentos para más de 7 mil millones de personas. Además, se deben de combatir plagas y enfermedades que son cada vez más adaptables y resistentes a los actuales métodos agronómicos de control. Aunado a esto, el cambio climático presenta condiciones cada vez más adversas (veranos más calientes, inviernos más fríos y una acentuada escases de agua) que impactan directamente a la producción y en algunos casos provocan pérdidas totales (Aroca, 2012a).

Ante este panorama desalentador solo dos alternativas prometen ser soluciones contundentes: La generalización del uso de agricultura protegida y el mejoramiento de variedades de cultivos. La primera va enfocada a incrementar el uso de invernaderos tecnificados que controlen variables importantes para la planta (temperatura, humedad, CO<sub>2</sub>, etc.), la protejan del clima y propicien un ambiente libre de patógenos, plagas y malezas; además de proporcionar la cantidad justa de agua para garantizar el óptimo desarrollo del cultivo (van Straten *et al.*, 2010). La segunda opción implica el mejoramiento a través de cruzas selectivas, generando híbridos con mayor resistencia a plagas, enfermedades, sequía, etc. También se pueden mejorar las variedades mediante la manipulación específica de determinadas características de la planta, obteniendo organismos genéticamente modificados (OGM), y finalmente la aplicación exógena de reguladores de crecimiento (PGR), la cual ha demostrado mejorar la tolerancia de las plantas a ciertas condiciones de estrés (García-Mier *et al.*, 2013).

Ambas alternativas necesitan apoyarse en herramientas tecnológicas cada vez más sofisticadas, como los equipos para monitoreo fisiológico que permiten medir y estimar variables y procesos vitales en las plantas. Con estos equipos es posible diagnosticar la salud de la planta bajo condiciones de invernadero, predecir la producción al final del ciclo y caracterizar las nuevas variedades de plantas (Schmidt, 1998; Millan-Almaraz *et al.*, 2013).

En sistemas automatizados para invernaderos, tanto control de clima como de riego; los sistemas de control actuales no garantizan el uso apropiado de los recursos necesarios para la producción. Su principio de operación consiste en tratar de

mantener con una desviación mínima, las condiciones óptimas para el desarrollo de los cultivos (Bennis *et al.*, 2008). Finalmente, los sistemas de monitoreo y control climático para invernaderos no proporcionan ningún diagnóstico del estado de estrés o confort que experimenta el cultivo (Millan-Almaraz *et al.*, 2013).

### **I.3 Hipótesis y objetivos**

#### **I.3.1 Hipótesis general**

Un sistema de fitocontrol con capacidad de monitoreo en tiempo real de fotosíntesis y transpiración, permite detectar y corregir oportunamente condiciones de estrés en las plantas.

#### **I.3.2 Objetivo general**

Desarrollar un sistema que emplee fitomonitoreo en tiempo real para detectar, monitorear y corregir condiciones de estrés en las plantas.

#### **I.3.3 Objetivos específicos**

1. Diseñar y validar una red inalámbrica de sensores con capacidad para estimar procesos fisiológicos en plantas.
2. Detectar y monitorear un tipo de estrés en plantas (caso de estudio: *Solanum lycopersicum* L.).
3. Proponer un índice para cuantificar el impacto de un estrés en plantas.
4. Implementar un sistema de fitomonitoreo que emplee datos del estado fisiológico de la planta para controlar la calendarización de riego.

## II REVISIÓN DE LITERATURA

### II.1 Estrés en plantas

Los cultivos vegetales están expuestos a condiciones de estrés bióticos y abióticos que afectan el crecimiento y desarrollo de la planta e impactan la calidad y producción de los cultivos. Los causantes de estrés biótico son plagas y patógenos (virus, bacterias, hongos, etc.) mientras que una condición de estrés abiótico puede ser causada por deficiencia o exceso de nutrientes (lo cual produce toxicidad en la planta), un alto índice de metales pesados en el suelo, temperaturas extremas, contaminación del aire y lluvia acida, radiación solar excesiva o insuficiente y finalmente condiciones inadecuadas de humedad en el suelo. La sequía está considerada como el estrés ambiental más devastador para las plantas, ya que afecta la producción más rápidamente y con mayor magnitud que cualquier otro tipo de estrés (Aroca, 2012a).

### II.2 Estrés hídrico

Un continuo déficit de precipitaciones (sequía meteorológica) acoplado a altos índices de evapotranspiración provoca sequía del suelo. En términos agrícolas, se considera sequía a la ausencia de la humedad necesaria en el suelo para el crecimiento y desarrollo de la planta a lo largo de su ciclo. Las principales consecuencias de la sequía en plantas son: reducción de la tasa de división celular y tamaño de la hoja, elongación del tallo y proliferación de raíces, oscilación anormal de la actividad estomática y déficit de nutrientes. No obstante el panorama desalentador que atraviesa la agricultura debido a la sequía, los modelos climáticos actuales predicen un incremento en su frecuencia y severidad como respuesta al cambio climático (Walter *et al.*, 2011).

El déficit hídrico acelera la biosíntesis del ácido abscísico, lo que disminuye la conductancia estomática para minimizar las pérdidas por transpiración (Yamaguchi-Shinozaki y Shinozaki, 2006; Yamaguchi *et al.*, 2007). El déficit en el suministro de agua en cualquier etapa de crecimiento de la planta tiene efectos perjudiciales sobre el crecimiento y desarrollo del cultivo, pero varía dependiendo de la gravedad del estrés



(magnitud y frecuencia) y la etapa de crecimiento del cultivo. Los efectos se presentan a niveles morfológicos, fisiológicos y bioquímicos (Aroca, 2012a).

La resistencia de las plantas a la sequía se basa en estrategias de adaptación a niveles morfológico, fisiológico, bioquímico y molecular. Por ejemplo; la modificación de los tiempos de las fenofases y alteración de rasgos estructurales principalmente relacionados con el aumento de captación y almacenamiento de agua, la disminución de la pérdida de agua durante periodos de sequía, el reforzamiento mecánico de los tejidos para evitar marchitamiento que conlleva a un colapso y daño irreversible de las células, la regulación del crecimiento de la planta incrementando el desarrollo de raíces para explorar volúmenes más grandes de suelo en búsqueda de agua (limitando a su vez el desarrollo de la canopia), la reducción de la conductancia estomática para evitar perder agua por transpiración e incluso la reprogramación de la expresión de genes relacionados con el balance del crecimiento de la planta de acuerdo a la disponibilidad de agua (Faraloni *et al.*, 2011).

Debido a los problemas que genera el estrés hídrico en plantas es necesario desarrollar tecnología para monitorear y detectar oportunamente la respuesta de la planta ante una condición de estrés. Los métodos tradicionales se basan en el monitoreo de variables primarias que impactan el desarrollo del cultivo, tales como: temperatura y humedad del aire, radiación solar, contenido de agua en el suelo, y concentración de CO<sub>2</sub> en la atmósfera. Con base en la medición de estas variables y conociendo los rangos que favorecen en óptimo desarrollo del cultivo (ver Tabla 2.1) se determina si la planta está sometida a estrés hídrico (Baert *et al.*, 2013) .

**Tabla 2.1— Rangos óptimos para el desarrollo de los cultivos (Baert *et al.*, 2013).**

<b>Variable</b>	<b>Rango</b>
<b>Temperatura</b>	22 – 28 °C
<b>Humedad relativa</b>	60 – 80 %
<b>Radiación Solar</b>	30mil - 100mil Luxes
<b>Concentración de CO<sub>2</sub></b>	300 - 1300 ppm

<b>Humedad en el suelo</b>	10 - 30 kPa
----------------------------	-------------

Sin embargo, los modelos que utilizan información de estas variables para detectar estrés hídrico presentan limitaciones como: dificultad para utilizarse con diferentes especies de plantas, baja resolución en la detección del estrés y limitación para operar en tiempo real (Baert *et al.*, 2013). Debido a estos problemas en la detección de estrés fue necesario cambiar el esquema de monitoreo, pasando de medir las variables antes mencionadas a medir variables y estimar procesos fisiológicos de la planta. A este nuevo esquema se le conoce como fitomonitorio o monitoreo fisiológico del cultivo; busca estudiar cómo responde la planta a determinada condición de estrés, detectar diferentes tipos de estrés de manera oportuna y predecir la calidad y rendimiento de un cultivo sometido a determinadas condiciones de crecimiento (Ton, 1997).

El monitoreo fisiológico del cultivo es posible gracias al incremento en las capacidades computacionales y al desarrollo y/o reducción en los costos de nuevas tecnologías y sensores. Permite monitorear de manera continua variables morfológicas del cultivo como: diámetro de tallos y frutos, rugosidad, turgencia, coloración, flujo de savia y temperatura foliar. También se pueden estimar con alta resolución procesos fisiológicos importantes como fotosíntesis, respiración, transpiración y conductancia estomática entre otros (Schmidt, 2005). Finalmente, anomalías en las mediciones se logran asociar a diferentes tipos de estrés logrando cuantificar *in-situ* el tipo de estrés y la severidad del mismo en tiempo real (Millan-Almaraz *et al.*, 2013).

Las tecnologías que se usan para fitomonitorio comprenden el uso de dendrómetros, galgas extensiométricas, encoders lineales o transductores LVDT (por sus siglas en inglés "*linear variable distance transducer*") para monitorear el diámetro de tallos o frutos hasta procesamiento de imágenes térmicas de alta resolución adquiridas por satélites o por vehículos aéreos no tripulados (drones). Técnicas muy finas como espectroscopia y electroacústica, limitadas a aplicaciones industriales o para medición de sustancias químicas son aplicadas para estimar procesos fisiológicos (transpiración, fotosíntesis, etc.) y su variación ante determinado tipo de estrés.

En la siguiente sección se presenta un análisis de las ventajas y desventajas de los sistemas de fitomonitorio actuales y se discuten las tendencias con base en dichos resultados.

### **II.3 Fitomonitorio**

Solo las plantas pueden proporcionar un indicador de su estado de confort o estrés. Este índice se obtiene monitoreando variables como temperatura foliar o estimando procesos fisiológicos como transpiración o fotosíntesis. El esquema conocido como “planta parlante” trata de solucionar esta problemática (Ton, 1997). Sin embargo, la medición del desempeño de la planta presenta diversos problemas técnicos porque requiere el uso de un número prohibitivo de sensores y la relación señal-ruido podría ser insuficiente debido a la naturaleza del fenómeno. Además, monitorear un pequeño grupo de plantas permite estudiar la respuesta de cada una de manera precisa, pero podría no ser representativo para todo el cultivo, y realizar mediciones generalizadas reduce la resolución de las mismas y dificulta distinguir entre diversos tipos de estrés (Linker y Seginer, 2003).

Partiendo de estas limitaciones, diversas técnicas han sido implementadas con el objetivo de diagnosticar el estado de salud de la planta. Apoyándose de dispositivos de bajo costo para la medición de micro variaciones en diámetros de tallos y frutos, Song *et al.* (2004) lograron monitorear un conjunto grande de plantas de lichi (*Litchi chinensis*) encontrando que las variaciones en el crecimiento de los tallos se relacionan inversamente con el déficit de presión de vapor (*VPD*) y con el contenido de agua en el suelo, permitiendo de esta manera proponer un indicador de estrés hídrico en la planta. Posteriormente se determinó que este comportamiento es común sin importar el modo fotosintético de las plantas (C3, C4 o CAM), y se ha utilizado para predecir la producción del cultivo mediante la correlación con la fotosíntesis y para manejar el sistema de irrigación (Šimpraga *et al.*, 2011; Matimati *et al.*, 2012). Sin embargo no se ha logrado asociar las variaciones en el diámetro del tallo con otros tipos de estrés, por lo cual se han explorado técnicas que faciliten la adquisición de los datos y proporcionen más información del estado de la planta.

Otro método para monitorear el contenido de agua en las plantas y su correspondiente estrés hídrico es utilizando basculas o lisímetros. El método consiste en colocar celdas de carga debajo y sobre la planta para determinar los cambios de peso asociados a la transpiración de la misma. El hardware y los dispositivos para su instalación presentan muchas ventajas contra otros sistemas utilizados para estimar transpiración, permiten además estimar fácilmente parámetros como el desarrollo de cultivo, uso de agua y predecir la producción final (Helmer *et al.*, 2005; Ben-Gal *et al.*, 2010). La combinación de las lecturas de estos sensores con técnicas de procesamiento de datos más sofisticadas permite la estimación de variables como fotosíntesis y conductancia estomática (Dayan *et al.*, 2004). Ehret *et al.* (2011) utilizaron datos del sistema *CropAssist* que combina mediciones de lisímetros con monitoreo de variables climáticas y mediante el uso de una red neuronal encontraron una correlación múltiple que puede estimar la fotosíntesis y la producción del cultivo. La desventaja de este método es que otro tipo de efectos negativos sobre el cultivo (como plagas que limitan el desarrollo) podrían ser confundidos con estrés hídrico al crear fluctuaciones en el peso registrado por los lisímetros.

Un problema común de los métodos descritos anteriormente es considerar que monitorear el comportamiento de una planta o conjunto de plantas sea significativo para extrapolarse a toda la canopia. El uso del procesamiento de imágenes es una técnica que permite solucionar este problema ya que puede analizar todo el cultivo con imágenes de muy alta resolución. Se han realizado trabajos para detectar estrés hídrico en arbustos caducifolios como la *Forsythia* mediante análisis morfológico de toda la planta utilizando visión artificial y geometría fractal, encontrando que esta última técnica es muy apropiada para realizar discriminaciones de forma asociadas a estrés por sequía (Foucher *et al.*, 2004). A la par del experimento, se realizaron mediciones fisiológicas del contenido de agua en las plantas para validar los resultados obtenidos por visión artificial, encontrando correlaciones de 0.8 para los primeros días de estrés, pero estas correlaciones bajan drásticamente conforme incrementa el periodo de medición. Finalmente se concluye que para generalizar el método se requiere más experimentación bajo diferentes condiciones de estrés, tamaño de planta y especie.

Se han llevado a cabo análisis morfológicos a gran escala, basados en visión artificial utilizando aviones no tripulados, adquiriendo imágenes y relacionando el índice de reflexión fotoquímica y características morfológicas con el contenido de agua en la planta. Suárez *et al.* (2008) incluyeron índices de la relación vegetación-suelo y diferencia longitudinal de vegetación, encontrando que la correlación con el contenido de agua mejoraba ( $r^2 = 0.7$ ) incrementando así la capacidad de detectar estrés en el cultivo. Por su parte, Hilker *et al.* (2013) lograron correlaciones más altas ( $r^2 = 0.85$ ) al estimar la transpiración y el contenido de agua en cultivos utilizando imágenes de reflexión fotoquímica captadas en diferentes ángulos (no solamente imágenes aéreas como en los estudios anteriores). Zhao *et al.* (2012) utilizaron imágenes en 3D y análisis fractal sobre una sola planta para identificar más rápidamente síntomas de marchitamiento, que los métodos mencionados anteriormente. La desventaja de este método es la infraestructura para instalar y alinear el láser sobre el cultivo, razón que lo hace impráctico para aplicaciones en campo.

Hasta ahora solo se han discutido metodologías de visión artificial de imágenes adquiridas por dispositivos de carga acoplada (CCD por sus siglas en inglés "*charge-coupled device*"), sin embargo, diversos estudios han demostrado que las imágenes térmicas proporcionan más información sobre el fenómeno y son más sensibles a los cambios, permitiendo de esta manera una detección más temprana del estrés (Contreras-Medina *et al.*, 2012).

Lenthe *et al.* (2007) realizaron un experimento para determinar el contenido de agua en trigo analizando imágenes infrarrojas de campos estresados y no estresados. La termografía infrarroja arrojó resultados sensibles a la intensidad del estrés. En este mismo estudio se buscó identificar los efectos de hongos (*Septoria tritici* y *Puccinia triticina*) en el cultivo, sin embargo, no se pudo detectar ninguna correlación entre la presencia de los hongos con los cambios de temperatura del cultivo. Los resultados también demuestran que para poder interpretar correctamente las imágenes termográficas, se necesita mayor experimentación para entender el impacto del estrés abiótico sobre la temperatura del cultivo. Una combinación que permite realizar esta distinción fue propuesta por Ondimu y Murase (2008), quienes combinaron análisis de

imágenes infrarrojas y de espectro visible para cuantificar el estrés hídrico en un cultivo bajo invernadero. Las imágenes infrarrojas se utilizaron para monitorear patrones de transpiración relacionados a índices de estrés hídrico, imágenes de espectro visible en escala de grises sirvieron para detectar cambios en la textura y las imágenes en RGB (por sus siglas en inglés “*red, green and blue*”) se utilizaron para detectar cambios en la reflectividad de la luz sobre el cultivo. Sin embargo, antes de aplicar esta técnica es necesario incorporar mediciones de fotosíntesis para verificar las mediciones de reflectividad de acuerdo al nivel de estrés. Wang *et al.* (2010) a través de la combinación imágenes visibles y térmicas, encontraron que la eficiencia de la técnica se ve afectada si las cámaras ópticas e infrarrojas están desalineadas, situación usual en aplicaciones de campo.

No obstante los problemas que presentan las técnicas de procesamiento de imágenes –principalmente al intentar discriminar entre niveles o diferentes tipos estrés– tienen la gran ventaja de estimar el estado de un cultivo a gran escala a cielo abierto o bajo invernadero, sin embargo, adquirir las imágenes es complicado y costoso. Una solución presentara por diversos investigadores es usar vehículos aéreos no tripulados (UAV por sus siglas en inglés “*Unmanned Aerial Vehicle*”) para adquirir las imágenes (Suárez *et al.*, 2008; Suárez *et al.*, 2009; Suárez *et al.*, 2010; Zarco-Tejada *et al.*, 2013).

## **II.4 Fitocontrol**

Los sistemas de fitocontrol explotan el conocimiento relacionado con los cultivos y la relación de estos con el invernadero y el clima para proponer modelos dinámicos que maximicen las ganancias, a través de prácticas que minimicen los costos de producción y garanticen el bienestar del cultivo (van Straten *et al.*, 2000; van Straten *et al.*, 2010).

Un algoritmo en tiempo real fue presentado por Chalabi *et al.* (1996) para ajustar la temperatura del invernadero sobre un determinado periodo de tiempo, logrando así obtener ahorros energéticos. Este método se basa en resultados de estudios fisiológicos que demuestran que para una gran cantidad de plantas es suficiente con mantener una temperatura promedio a lo largo de su ciclo, que pueden tolerar desviaciones temporales de temperatura y recuperarse sin impactar en la producción.

Los procesos fisiológicos de la planta varían con su estado fenológico y en determinados momentos la planta no se desarrolla aunque las condiciones del microclima sean óptimas. Por lo tanto no es necesario gastar energía en proporcionarle todo el tiempo condiciones apropiadas para su crecimiento (Schmidt *et al.*, 2008; van Straten *et al.*, 2010). Con base en este supuesto Körner y van Straten (2008) implementaron un sistema de integración de temperatura que considera los procesos de la planta por su tiempo de respuesta (procesos lentos como desarrollo foliar y rápidos como fotosíntesis o estrés) y genera rangos dinámicos de temperatura, estos límites son flexibles y se ajustan a la respuesta de la planta promoviendo el desarrollo de la misma a través de prácticas que ahorran energía.

El estudio del comportamiento de la temperatura foliar de la planta y su correlación con procesos como la fotosíntesis, transpiración y estrés hídrico (bajo restricciones bióticas y del clima) ha facilitado la implementación de sistemas que obtengan de esta variable una retroalimentación del estado de confort del cultivo. Sin embargo, tomar una decisión correctiva con base en una medición es arriesgado, la relación señal-ruido de los sistemas de adquisición en campo no es buena porque la magnitud del ruido puede hacer que las mediciones sean ilegibles. El uso de algoritmos de procesamiento digital de señales en tiempo real han ayudado a solucionar este problema, algunos sistemas que utilizan wavelets para analizar las señales de la planta son capaces de detectar los momentos en que la planta se estresa (Cheng *et al.*, 2011). Sistemas de filtrado digital por sobre-muestreo combinado con filtro adaptivos discriminan el ruido de las señales permitiendo tomar decisiones con base en mediciones más puras (Jiaying *et al.*, 2010; Peng *et al.*, 2012).

A pesar de los avances en los sistemas de adquisición, el control en tiempo real del cultivo con base en la respuesta de la planta no se ha logrado, sin embargo, sistemas que promedian las lecturas de la planta sobre un par de horas han permitido detectar y corregir condiciones de estrés con retrasos aceptables y logran reajustar el régimen climático para la siguiente fase del cultivo (Schmidt *et al.*, 2008). Sistemas similares emplean estas técnicas de muestreo sobre un periodo de tiempo más grande, obteniendo una relación de la diferencia entre los promedios de temperatura durante el

día y la noche, y han logrado anticipar el comportamiento del cultivo y modificar el régimen de clima (Körner y van Straten, 2008).

La información relacionada con el estado de salud de la planta no solo es útil para detectar y corregir condiciones de estrés, Candogan *et al.* (2013) utilizaron índices del desarrollo de cultivo para diseñar estrategias de control que favorezcan la rentabilidad económica del sistema de producción. Esto se logró realizando un monitoreo y control independiente de procesos en la planta; procesos como fotosíntesis y transpiración son controlados por un sistema predictivo mientras que procesos no tan críticos se dejan al agricultor.

Es fácil observar la tendencia en los sistemas para administrar la producción en agricultura de precisión, el fitocontrol es el nuevo esquema que propone el uso de la respuestas fisiológica de la planta para realizar ajustes en el control de clima, irrigación, etc. Sin embargo, los sistemas antes descritos solo correlacionan los procesos de la planta con variables fáciles de medir. Esta metodología es útil en condiciones controladas, pero cuando se presenta más de un estrés, es difícil detectarlos y las predicciones se alejan de la realidad. Schmidt *et al.* (2007) utilizaron sistemas de bajo costo para monitoreo fisiológico logrando detectar condiciones de estrés y reajustar variables del microclima del invernadero como humedad y temperatura. Por su parte, Ballester *et al.* (2013) utilizaron equipos comerciales para estimación de fotosíntesis y transpiración para programar la irrigación de las plantas con base en el estrés hídrico que éstas presentan.

La tendencia en agricultura protegida es muy clara, monitorear la salud de la planta es la mejor opción si se busca alcanzar calidad y rentabilidad, pero es necesario resolver problemas relacionados con la correcta estimación de los procesos fisiológicos de la planta, la detección oportuna del estrés, el diseño de equipos robustos de medición de bajo costo que puedan operar de manera continua en condiciones de campo, y la investigación dirigida a determinar la teoría de control que mejor se ajusta a un esquema donde la planta es el eje central del lazo de control.



### III METODOLOGÍA

Los dos pasos generales del proyecto son monitorear variables primarias y procesos fisiológicos que sean útiles para determinar el momento en que la planta comienza a sufrir algún tipo de estrés; y con esta información ajustar procesos agrícolas como el riego o el control de clima para corregir oportunamente dicho estrés. Para lograrlo es necesario contar con dispositivos capaces de medir variables como temperatura, humedad relativa, radiación y concentración de CO<sub>2</sub>; y con base en estas mediciones estimar procesos fisiológicos como transpiración y fotosíntesis.

Los equipos de medición (fitomonitores) deben de tener la capacidad de operar en condiciones de invernadero, realizar los cálculos en tiempo real y tener capacidades de comunicación inalámbrica para transmitir los datos a un coordinador (computadora personal) que se encuentra fuera del invernadero. Posteriormente es necesario analizar los datos *off-line* y utilizar métodos de procesamiento digital de señales (DSP, por sus siglas en inglés "*digital signal processing*") para filtrar y extraer información de las señales monitoreadas. Una vez determinada la señal que es más sensible al estrés inducido en las plantas, se procedió a realizar modificaciones en el *firmware* de los fitomonitores para incluir el método DSP que funcionó mejor y poder detectar el estrés pero en esta ocasión *on-line*.

Finalmente se formuló una metodología para modificar el suministro de agua a las plantas utilizando los indicadores de estrés encontrados.

#### III.1 Estimación de procesos fisiológicos

Los fitomonitores tienen la capacidad de estimar procesos fisiológicos como fotosíntesis, transpiración, diferencia de temperatura aire-hoja, conductancia y resistencia estomática, déficit de presión de vapor, balance de carbono y las tasas de cambio de estos procesos.

### III.1.1 Estimación de fotosíntesis

El intercambio de CO<sub>2</sub> es el método más utilizado a nivel comercial o experimental para medir la fotosíntesis neta de las plantas. Esta técnica emplea analizadores infrarrojos de gas (IRGA, por sus siglas en inglés “*Infrared Gas Analyzer*”) para medir la concentración inicial de CO<sub>2</sub> en sistemas cerrados; que pueden describirse como una cámara de material transparente donde se aísla la planta y después de un periodo de tiempo se mide la concentración final de CO<sub>2</sub> (Phytech Ltd., 2013). En este trabajo se utilizaron sistemas abiertos, los cuales cuentan con una cámara foliar (también de material transparente) en la que se aísla momentáneamente una hoja de la planta, se mide la cantidad de CO<sub>2</sub> asimilado y se libera la hoja para evitar estresarla. A diferencia de los sistemas cerrados necesitan menos tiempo para llevar a cabo una medición, permitiendo monitorear el proceso a frecuencias más altas y estudiar en detalle la dinámica del proceso. Además, de que nos permite utilizar cámaras foliares de diferentes formas y tamaños para adaptarnos a distintos tipos de plantas (incluso cactáceas como nopales y cactus).

Para calcular la fotosíntesis en un sistema abierto es necesario medir la concentración de CO<sub>2</sub> en la atmósfera y en la cámara foliar donde se aísla la muestra después de un periodo de 60 segundos aproximadamente. También se debe convertir el flujo volumétrico del sistema neumático en flujo másico (expresado en mol/m<sup>2</sup>/s) utilizando el factor  $W$  que se calcula con la Ecuación 1 (Bittelli, 2010).

$$W = (2005.39) \frac{(V)(P)}{(T_a K)(A)} \quad (1)$$

Donde  $P$  es la presión atmosférica en bares,  $V$  es el flujo volumétrico de aire en litros por minuto (lpm),  $T_a K$  en la temperatura del aire en °K,  $A$  es el área de la hoja en cm<sup>2</sup> y la constante 2005.39 es un coeficiente de ajuste para convertir unidades de masa a moles, superficie de cm<sup>2</sup> a m<sup>2</sup> y tiempo de minutos a segundos.

Una vez calculado el factor  $W$  la estimación de fotosíntesis se realiza con la Ecuación 2, donde  $C_i$  corresponde a la medición de  $\text{CO}_2$  en la atmósfera próxima a la planta y  $C_o$  la concentración de  $\text{CO}_2$  en la cámara foliar tras el paso de unos segundos de haber aislado a la muestra, obteniendo así la cantidad de carbono asimilada por la hoja.  $P_n$  es expresada en  $\mu\text{mol}/\text{m}^2/\text{s}$ .

$$P_n = (W)(C_i - C_o) \quad (2)$$

### III.1.2 Estimación de transpiración

El cálculo de la transpiración es más sencillo a nivel de hardware ya que solo requiere sensores para medir humedad relativa, pero como se ve a continuación; requiere resolver ecuaciones más complejas que las utilizadas para estimar fotosíntesis. La transpiración  $E$ , expresada en  $\text{mmol}/\text{m}^2/\text{s}$  es una función fisiológica que depende de la diferencia entre el contenido de vapor de agua en la atmósfera ( $e_i$ ) y el contenido de vapor de agua de salida del sistema neumático  $e_o$ , este último se mide en el aire que quedo confinado junto con la hoja dentro de la cámara foliar unos segundos después del cierre de la cámara, permitiendo a la hoja modificar el contenido de humedad en el aire mediante transpiración o absorción de agua. Sin embargo, los sensores comerciales normalmente proporcionan valores de humedad relativa que necesitan convertirse en valores de humedad absoluta  $e_i$  y  $e_o$ . Para esto es necesario calcular la máxima cantidad de vapor de agua  $e_s$  que el aire puede contener a una temperatura  $T_a$  usando curvas del diagrama de Mollier o utilizando la Ecuación 3 como ha sido previamente reportado por Wu *et al.* (2013). De esta manera  $e_i$  y  $e_o$  pueden ser obtenidas fácilmente con las Ecuaciones 4 y 5, donde  $RH_i$  es la humedad relativa del aire de entrada al sistema neumático (humedad relativa de la atmósfera) y  $RH_o$  es la humedad relativa de salida de la cámara de intercambio de gases.

$$e_s = 6.13753 \times 10^{-3} \exp \left( T_a \frac{18.564 - \frac{T_a}{254.4}}{T_a + 255.57} \right) \quad (3)$$

$$e_i = \frac{(RH_i)(e_s)}{100} \quad (4)$$

$$e_o = \frac{(RH_o)(e_s)}{100} \quad (5)$$

Una vez calculados los valores de  $e_i$ ,  $e_o$  y  $W$ , la transpiración  $E$  puede calcularse con la Ecuación 6, donde  $P$  es la presión atmosférica y 18.02 es una constante para convertir de  $\text{mmol/m}^2/\text{s}$  a  $\text{mg/m}^2/\text{s}$ .

$$E = (W)(1000)(18.02) \frac{(e_o - e_i)}{(P - e_o)} \quad (6)$$

### III.1.3 Estimación de conductancia estomática

La conductancia estomática es una variable relacionada con la dinámica de transpiración de la planta que representa la conductividad de vapor de agua de las células guardianas. Ésta puede ser estimada a partir de sensores primarios de temperatura y humedad relativa. Primero es necesario calcular la presión de saturación de vapor  $e_{leaf}$  a la temperatura de la hoja  $T_{leaf}$ . Para esto se puede utilizar la misma Ecuación de  $e_s$  pero sustituyendo  $T_a$  por  $T_{leaf}$  (ver Ecuación 7). Calculando  $e_{leaf}$ , la conductancia estomática  $C_{leaf}$  expresada en  $\text{mmol/m}^2/\text{s}$  puede ser obtenida con la Ecuación 8, donde  $r_b$  es considerada una constante de  $0.3 \text{ m}^2/\text{s}/\text{mol}$ .

$$e_{leaf} = 6.13753 \times 10^{-3} \exp \left( T_{leaf} \frac{18.564 - \frac{T_{leaf}}{254.4}}{T_{leaf} + 255.57} \right) \quad (7)$$

$$C_{leaf} = \frac{W}{\left( \frac{e_{leaf} - e_o}{e_o - e_i} \right) \left( \frac{P - e_o}{P} - r_b(W) \right)} (1000) \quad (8)$$

### III.1.4 Estimación del déficit de presión de vapor

El déficit de presión de vapor (*VPD*) es la cantidad de vapor de agua que se necesita en un determinado momento para saturar la atmósfera, es decir, es la diferencia entre la cantidad de vapor de agua que puede retener la atmósfera dependiendo de la temperatura, y la cantidad de vapor de agua que contiene la atmósfera en ese momento. El *VPD* es de suma importancia para la transpiración de las plantas, porque un *VPD* elevado hace que las plantas transpiren más tratando de saturar la atmósfera, por lo tanto, al haber mayor transpiración habrá un incremento en la absorción de nutrientes, en la fotosíntesis y en el rendimiento. Sin embargo, un *VPD* muy elevado provocará que las plantas cierren las estomas para evitar la pérdida excesiva de agua o deshidratación por transpiración, afectando la fotosíntesis y el rendimiento.

Por otro lado con un *VPD* cercano a cero las plantas dejan de transpirar, debido a que la atmósfera se encuentra saturada y no existe un gradiente de concentración hacia donde se difunda el vapor de las estomas, afectando la fotosíntesis y el rendimiento. El cálculo de *VPD*, expresado en kPa consiste en realizar la resta entre  $e_s$  y  $e_i$  (ver Ecuación 9).

$$VPD = e_s - e_i \quad (9)$$

### III.1.5 Cálculo de la diferencia de temperatura aire-hoja

La diferencia de temperatura aire-hoja (*LADT*) expresada en grados Celsius (ver Ecuación 10), es un importante indicador del estado de estrés de la planta, ya que condiciones de estrés hídrico por sequía provocan que la hoja se caliente más que el aire durante el día y se enfríe en exceso durante la noche.

$$LADT = T_a - T_{leaf} \quad (10)$$

## III.2 Sensor inteligente para fitomonitorio

El desarrollo del sensor inteligente para fitomonitorio requiere la integración de varios subsistemas (Figura 3.1). Involucra un sistema de adquisición de datos (DAS) para la lectura de sensores primarios de temperatura, humedad, concentración de CO<sub>2</sub>, presión, flujo volumétrico y radiación. Un sistema neumático para intercambio de gases, un sistema mecánico para control de la cámara foliar donde se aísla la muestra de la hoja, una unidad para control y procesamiento digital de señales y finalmente un subsistema de comunicación inalámbrica. Todos estos componentes integran un nodo de monitoreo. El presente proyecto requirió tres de estos nodos durante la experimentación, además fue necesario un nodo extra que funcionó como coordinador de la red inalámbrica y una computadora para almacenar los datos provenientes de la red de sensores.

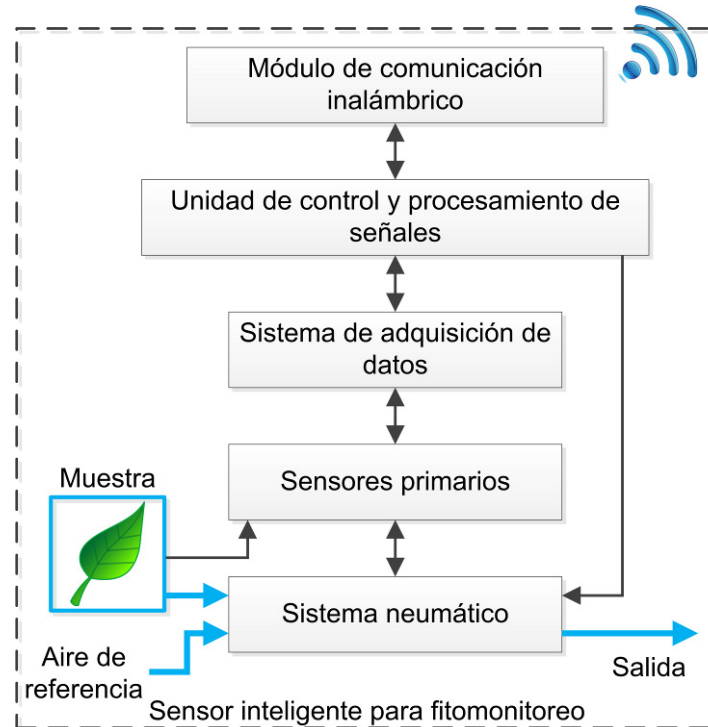


**Figura 3.1— Diagrama a bloques del fitomonitor. Los bloques en negro representan las etapas de hardware del sensor inteligente, la flechas nos indican el sentido de flujo de la información (uni o bidireccional). El bloque en azul representa la cámara foliar transparente donde se aísla la muestra a analizar.**

En las siguientes secciones se presenta una descripción detallada de cada subsistema que integra los sensores inteligentes.

### III.2.1 Sistema neumático

Debido a que la estimación de transpiración y fotosíntesis requieren la comparación entre el canal de aire de referencia y de la muestra, ambos procesos se pueden estimar simultáneamente. Como se puede observar en la Figura 3.2, los componentes del sistema neumático marcados con amarillo son los sensores, dos electroválvulas seleccionan la línea de aire que entra en el resto del sistema neumático. Finalmente, un filtro de aire, una bomba de vacío y una válvula mecánica para limitar el flujo de aire a 0.5 lpm componen el sistema. El ciclo comienza monitoreando la línea de

aire de referencia que viene de la atmosfera circundante a la planta; al pasar por el sistema neumático se miden alguna variables del aire como: temperatura del aire ( $T_a$ ), humedad relativa de entrada ( $RH_i$ ), flujo de aire de referencia ( $V_i$ ), presión de entrada ( $P_i$ ), y concentración de  $CO_2$  de entrada ( $C_i$ ). Una vez terminado este ciclo, un servomotor cierra la cámara foliar aislando una hoja de la planta y las electroválvulas cambian de posición permitiendo al aire del canal de medición entrar en el sistema neumático para estimar las propiedades siguientes: humedad relativa de salida ( $RH_o$ ), flujo de aire de salida ( $V_o$ ), presión de salida ( $P_o$ ), y concentración de  $CO_2$  de salida ( $C_o$ ). Simultáneamente, los sensores incorporados en la cámara foliar monitorean paralelamente al ciclo neumático, la temperatura de la hoja ( $T_{leaf}$ ) y la radiación solar ( $Rad$ ).

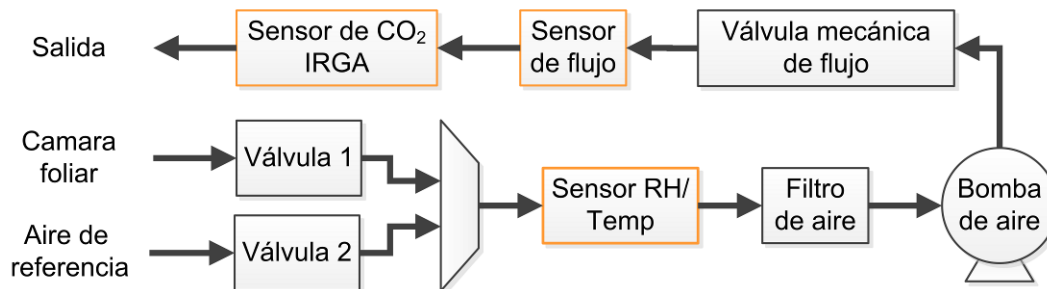


**Figura 3.2 – Diseño del sistema neumático para intercambio de  $CO_2$ . A lo largo de las líneas neumáticas se observa la disposición de los diferentes sensores.**

Cuando el ciclo termina, los procesos fisiológicos de la planta son estimados, los datos son transmitidos y almacenados, la cámara foliar se abre, las electroválvulas regresan a su posición original y la bomba de aire se apaga para ahorrar energía. A pesar de que la transpiración se puede monitorear a frecuencias altas, el sistema adquiere una medición cada 17 minutos y un total de 48 mediciones por día. Esto se debe a las limitaciones relacionadas con la estabilización de la línea neumática que presenta la estimación de fotosíntesis.



### III.2.2 Sistema de adquisición de datos (DAS)

El Sistema de adquisición de datos está integrado por 5 sensores, para medir las variables  $T_{leaf}$ ,  $T_a$ ,  $RH_i$ ,  $RH_o$ ,  $P_i$ ,  $P_o$ ,  $V_i$ ,  $V_o$ ,  $Rad$ ,  $C_i$ ,  $C_o$ . Cada uno con su etapa de instrumentación para acondicionar la señal de medición a un formato estándar de salida de 0-5 Volts. Para medir los flujos volumétricos ( $V_i$  y  $V_o$ ) en la línea neumática se utilizaron sensores del tipo sistema microelectromecánico (MEMS por sus siglas en inglés “microelectromechanical system”) D6F de la marca Omron, los cuales manejan un rango de medición de 0 a 5 lpm con una precisión de  $\pm 3\%$ , características apropiadas para nuestra aplicación ya que el sensor de  $CO_2$  utilizado requiere mantener flujos de aire en el rango de 0.1 a 1 lpm (a mayor flujo respuesta más rápida pero más inestable).

Es necesario medir la presión atmosférica para calibrar las mediciones del sensor de  $CO_2$  (las cuales varían con la altura y por eso no puede considerarse la presión a nivel del mar como constante) y para calcular algunos parámetros necesarios en las mediciones de fotosíntesis y transpiración (ver Ecuaciones 1 y 6). La medición de la presión atmosférica se realizó con un sensor de presión absoluta MPXAZ4115AC6U de la compañía Freescale Semiconductor, el cual tiene un rango de medición de 15 a 115 kPa y una precisión de  $\pm 1.5\%$ .

La temperatura de la hoja ( $T_{leaf}$ ) se midió utilizando sensores de temperatura tipo RTD (por sus siglas en inglés “*resistance temperature detector*”) de platino HEL-700 de la marca Honeywell que maneja un rango de medición de -200 a 540 °C con una precisión de  $\pm 2.0\%$ , sin embargo, la etapa de instrumentación está configurada para medir de 0 a 65 °C, un rango apropiado para medir la temperatura de la planta.

La medición de la temperatura y humedad relativa del aire ( $T_a$ ,  $RH_i$ ,  $RH_o$ ) se realizó con un sensor tipo MEMS SHT75 de la marca SENSIRION, el cual es un sensor digital auto-calibrado, sobre-muestreado, que maneja un protocolo de comunicación serial I<sup>2</sup>C (“*inter-integrated circuit*”) modificado y una frecuencia de operación de aproximadamente 3 Hz (para más detalles ver Tabla 3).

Tabla 3.1 – Características del sensor SHT75

Parámetro	Temperatura	Humedad
Resolución	14 bits	12 bits
Precisión	± 0.3 °C	± 1.8 % RH
Rango de medición	-40 a 123.8 °C	0 a 100 %

La radiación solar es uno de los factores más importantes para la planta, sin embargo la metodología de intercambio de gases no necesita medir la radiación para calcular la fotosíntesis neta. Aun así, esta variable fue monitoreada para obtener relaciones con otras variables y para determinar el momento del día en que inicia y termina el fotoperiodo. Su medición se llevó a cabo con un sensor cuántico de silicio OSRAM SFH711, con un rango de medición de 0 a 100,000 luxes y una precisión de ±0.4%. Como se puede observar en la Figura 3.3 éste sensor se ubica al igual que el sensor de la hoja en la cámara foliar donde se aísla la muestra de la planta.

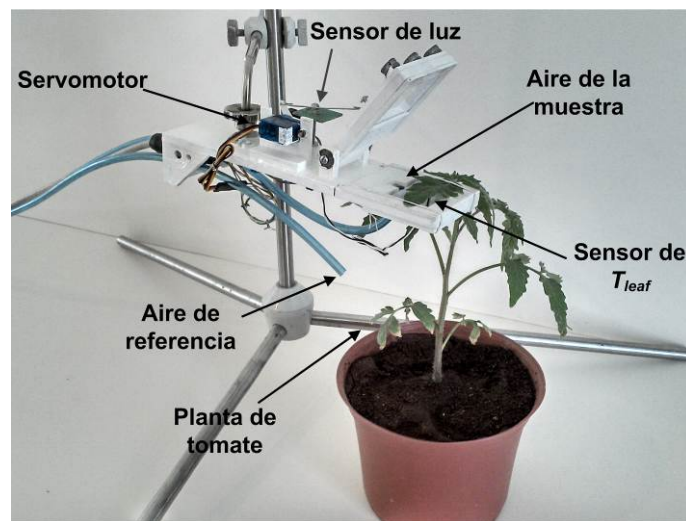


Figura 3.3 – Cámara foliar y disposición de sensores de temperatura y radiación.

La concentración de CO<sub>2</sub> en la atmósfera y la asimilada por la hoja en la cámara foliar se midió utilizando un sensor infrarrojo de gas (IRGA), Gascheck 2 de la

compañía Edinburgh Instruments, el cual tiene un rango de medición de 0 a 3000 ppm y una precisión de  $\pm 30$  ppm. El rango es apropiado para medir las concentraciones de CO<sub>2</sub> en un invernadero, las cuales oscilan de 300 ppm durante el día hasta 1000 ppm durante la noche. Sin embargo, la resolución presenta una limitante ya que el fenómeno a estudiar exige que se puedan detectar cambios de 1 a 50 ppm. Por lo tanto se requirió aplicar técnicas avanzadas de procesamiento digital de señales para reducir esta desviación a valores aceptables para esta aplicación.

Cada uno de los sensores se conecta a los canales de la tarjeta de adquisición de datos Hydra—Plant Monitoring Health V1.0 desarrollada por el cuerpo académico de Biosistemas de la Facultad de Ingeniería-UAQ. La tarjeta consta de una etapa de instrumentación con cinco canales de entrada, utiliza amplificadores operacionales Texas Instruments OPA4347 configurados como filtros analógicos Butterworth de orden 2, con respuesta de rechazo de banda 40 dB/dec y una frecuencia de corte de 20 Hz. La tarjeta utiliza un convertidor de analógico a digital ADS7844 de 12 bits, 8 canales y capaz de realizar 200 mil conversiones por segundo. Ambas características (resolución y tasa de muestreo) se ajustan a los requerimientos de los sensores que se están utilizando en el diseño del fitomonitor. El ADS7844 utiliza una interfaz serial SPI (por sus siglas en inglés "*Serial Peripheral Interface*") para comunicarse con un dispositivo FPGA por sus siglas en inglés "*Field Programmable Gate Array*"), modelo Altera Cyclone IV EP4CE22F17C6N que realiza las funciones de unidad de control y procesamiento de datos.

### **III.2.3 Unidad de procesamiento de señales**

Esta unidad es parte del procesador embebido incluido en el firmware del FPGA de cada nodo de la WSN. En la unidad de procesamiento de señales (ver Figura 3.4), se observan dos etapas de filtrado de señales y una etapa para calcular los procesos fisiológicos con base en la medición de las variables primarias.

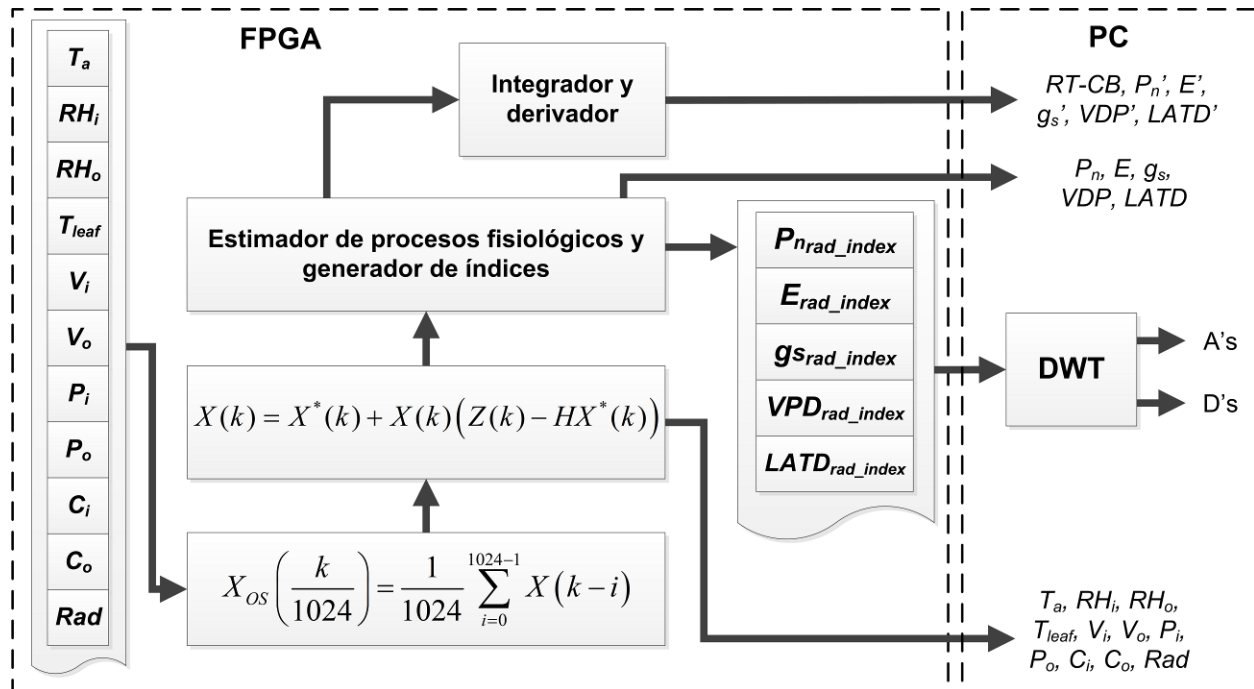


**Figura 3.4 – Unidad de procesamiento de señales embebida en FPGA.** En la memoria RAM de la izquierda se encuentran los datos de los sensores primarios que pasan por dos etapas de filtrado para obtener señales más puras y calcular los procesos fisiológicos que se almacenan en la RAM de la derecha. Los módulos integrador y derivador se incluyen en la unidad para obtener las tasas de cambio de los procesos fisiológicos y el balance de carbono en tiempo real (RTCB). Finalmente son transmitidos a una PC para su procesamiento junto con algunos índices.

Las señales de fotosíntesis estimadas mediante metodologías de intercambio de gases presentan una cantidad importante de ruido. Este ruido es introducido principalmente por los sensores de dióxido de carbono, donde, de acuerdo a la ley de los gases, las mediciones se ven afectadas por cambios de temperatura, presión, volumen del gas; y no solo por la concentración de  $\text{CO}_2$ . Es por esto que las señales obtenidas por el ADS7844 de los sensores primarios tales como  $T_{leaf}$ ,  $P_i$ ,  $P_o$ ,  $V_i$ ,  $V_o$ ,  $C_i$ , y  $C_o$  no se utilizan en bruto para calcular los procesos fisiológicos de la planta; antes pasan por filtros paralelos de diezmo por promedio, donde la señal es sobremuestreada y promediada 1024 veces por segundo, buscando con esto reducir errores de cuantización y ruido de las señales. A través de estos filtros se obtienen versiones nuevas de las señales obtenidas por los sensores primarios y se distinguen de sus versiones previas utilizando el sufijo “OS”, como se puede observar en la Ecuación 11,

donde  $X(k)$  representa la señal proveniente de cualquier sensor del sistema y  $X_{Os}(k)$  es la versión filtrada por diezmado de promedio de la señal  $X(k)$ .

$$X_{Os}\left(\frac{k}{1024}\right) = \frac{1}{1024} \sum_{i=0}^{1024-1} X(k-i) \quad (11)$$

La siguiente etapa es el filtro Kalman, el cual se encuentra embebido en el FPGA y su algoritmo ha sido previamente reportado por Rodriguez-Donate *et al.* (2011) quien a su vez se basó en las ecuaciones de Che *et al.* (2010). Este filtro se basa en un proceso estadístico y es similar a un controlador retroalimentado. Primero, el filtro estima el estado siguiente de la señal y entonces obtiene una retroalimentación de las mediciones ruidosas para modificar el estado estimado (ver Ecuaciones 12 y 13):

$$X^*(k) = SX(k-1) + Bu(k-1) \quad (12)$$

$$P^*(k) = SP(k-1)S^T + Q \quad (13)$$

Donde  $S$  es la matriz que relaciona los estados previos y el estado estimado actual,  $B$  relaciona una entrada óptima de control  $u$  con  $X^*(k)$ ,  $Q$  es la covarianza de la señal de interés y  $P^*(k)$  es la estimación de la varianza del error. La etapa de corrección se basa en las Ecuaciones 14, 15 y 16 donde  $R$  es la covarianza del ruido del fenómeno en estado estacionario,  $H$  relaciona las lecturas de los sensores  $Z(k)$  con el estado actual  $X(k)$ ,  $K(k)$  es el factor de ganancia que es empleado para minimizar la covarianza del error  $P(k)$ .

$$K(k) = P^*(k)H^T (HP^*(k)H^T + R)^{-1} \quad (14)$$

$$X(k) = X^*(k) + K(k)(Z(k) - HX^*(k)) \quad (15)$$

$$P(k) = (I - K(k)H)P^*(K) \quad (16)$$

Finalmente, las señales sobre-muestreadas  $X_{Os}(k)$  pasan a través del filtro Kalman para obtener las señales filtradas  $X_{OsK}(k)$ . Para lograr esto, se consideran a  $S$  y  $H$  como matrices identidad, los valores previos de las señales se cargan en  $X(k)$  y los

valores actuales en  $Z(k)$ , Q y R son matrices diagonales que contienen las covarianzas de señal y de ruido asociado para cada señal  $X_{OS}(k)$ . Una vez calculadas todas las señales  $X_{OSK}(k)$ , el estimador de procesos fisiológicos calcula la  $P_n$ , E,  $C_{leaf}$ , VPD y LATD. Además, el sensor inteligente propuesto proporciona una nueva versión de estas señales donde las variaciones espaciales del invernadero provocadas por la radiación no homogénea se ven mitigadas usando el índice expresado en la Ecuación 17. Aquí,  $X_{norm}(k)$  es la versión normalizada de las señales  $P_n$ , E,  $gs$ , VPD o LATD. Por su parte  $Rad_{norm}(k)$  representa la versión normalizada de la radiación considerando el valor máximo de Rad de los tres nodos. Finalmente,  $X_{rad\_index}(k)$  es el índice que relaciona el proceso fisiológico con la radiación neta recibida por la planta bajo análisis.

$$X_{rad\_index}(k) = \frac{X_{norm}(k)}{Rad_{norm}(k)} \quad (17)$$

La última etapa del módulo de procesamiento de señales consiste en dos módulos para obtener el balance de carbón en tiempo real (*RT-CB*) de la planta y la primera derivada de los procesos  $P_n$ , E,  $C_{leaf}$ , VPD y LATD. Es importante obtener el *RTCB* ya que proporciona información sobre las pérdidas de carbono a través de la respiración, la cantidad de biomasa que la planta genera y cómo esta acumulación se ve afectada por factores climáticos como la cantidad de radiación y concentración de CO<sub>2</sub> disponible en el aire, o por factores de estrés bióticos como plagas y microorganismos (Millan-Almaraz *et al.*, 2013). El cálculo del *RT-CB* se realiza integrando  $P_n$  a través de la Ecuación 18. Para su integración en FPGA se utilizó la Ecuación 19, donde la integral continua es cambiada por sumas acumulativas de  $P_n$  obteniendo la versión en tiempo discreto de *RT-CB*.

$$RTCB(t) = \int_a^b P_n(t) dt \quad (18)$$

$$RTCB(k) = T_s \sum_{k=0}^N P_n(k) \quad (19)$$

A diferencia del módulo integrador que solo obtiene la integral numérica para la fotosíntesis, el módulo que calcula la derivada lo hace para todos los procesos fisiológicos estimados. Este indicador se utilizó durante la experimentación para estudiar cambios en la actividad fotosintética y de transpiración de la planta como respuesta a diferentes tratamientos y prácticas agrícolas en el cultivo. En la Ecuación 20 podemos observar el cálculo de la primera derivada donde,  $X(k)$  puede ser cualquier proceso fisiológico estimado por el procesador embebido y  $X'(k)$  su primer derivada. Para poder calcular la derivada en un sistema digital (FPGA) es necesario implementar la versión discreta mostrada en la Ecuación 21.

$$X' = \frac{X(k)}{dt} \quad (20)$$

$$X'(k) = \frac{X(k) - X(k-1)}{T_s} \quad (21)$$

Finalmente, los procesos estimados  $P_n$ ,  $E$ ,  $C_{leaf}$ ,  $VPD$ ,  $LATD$ , sus respectivas derivadas ( $X'$ ) y el  $RTCB$  son transmitidos de manera remota al coordinador de la red junto con los señales en bruto  $X_{OS}(k)$  para su almacenamiento y procesamiento *off-line*.

### III.3 Sistema de comunicación inalámbrica

El desarrollo del sistema de comunicación inalámbrica implicó la evaluación de diferentes tecnologías de comunicación y la comparación de factores como ancho de banda, rango de transmisión, escalabilidad y consumo de potencia que deben tomarse en cuenta de acuerdo a las necesidades de la aplicación. Tras evaluar los estándares IEEE 802.15.1 BLUETOOTH, GSM-GPRS, IEEE 802.11 WIFI se optó por el estándar IEEE 802.15.4 ZigBee que teóricamente tiene una tasa de transferencia de datos de 250 kbps, un rango máximo de 1000 m y un bajo consumo de potencia. Este estándar trabaja en tres diferentes bandas de frecuencia y puede integrar una red de hasta 65,536 nodos administrados por un solo coordinador.

El punto final de la red (*end-point*), es el sensor inteligente los sistemas neumático, la macara foliar para aislar la muestra de la planta, el sistema de instrumentación necesario para medir variables de sensores primarios y a través de módulos de procesamiento de señales basados en FPGA, estimar los procesos fisiológicos  $P_n$ ,  $E$ ,  $VPD$ ,  $C_{leaf}$  y  $LATD$ . El coordinador de la red se implementó en una plataforma similar a los demás nodos de la WSN (FPGA—EP4CE22F17C6N), es responsable de enviar comandos de inicio de medición a los nodos que se encuentren dentro de su red de área personal (por sus siglas en inglés PAN, “*personal area network*”) y recibir de cada uno las lecturas de los sensores y procesos fisiológicos. Este nodo se comunica vía USB con una computadora personal para almacenar la información y graficar las mediciones de los nodos.

La WSN tiene una topología tipo estrella donde el coordinador se puede comunicar con cada nodo de la red pero los puntos finales (*end-point*) no pueden comunicarse entre ellos. La red descrita en este proyecto está integrada por tres puntos finales y un coordinador. Sin embargo, sensores inteligentes adicionales pueden añadirse a la red en futuras actualizaciones del sistema donde se requiera monitorear un mayor número de plantas.

Para entender con precisión la operación del protocolo de comunicación inalámbrico es necesario entender algunas especificaciones del proceso de medición. Una vez que un nodo recibe el comando de inicio de medición por parte del coordinador. El nodo debe tomar en un periodo de un segundo, 1024 mediciones de las variables  $T_a$ ,  $T_{leaf}$ ,  $RH_i$ ,  $RH_o$ ,  $C_i$ ,  $C_o$ ,  $V_i$ ,  $V_o$ ,  $P_i$ ,  $P_o$ ,  $Rad$ ; obtener los promedios de cada una de ellas y transmitir las al coordinador de la red. El ciclo completo de medición de cada fitomonitor dura 20 minutos durante los cuales se mantiene enviando datos de los sensores primarios cada segundo y en la última transmisión de datos se envían los datos de los procesos fisiológicos estimados por el procesador embebido en el FPGA. Si bien la información de los procesos fisiológicos es de mayor interés y suficiente para estudiar la fenomenología de la planta, los datos en bruto se transmiten para su procesamiento off-line, para estudiar su comportamiento dinámico y para proponer modificaciones a la metodología de estimación de los procesos fisiológicos de la planta.



El sistema de adquisición de datos adquiere mediciones de los sensores analógicos de temperatura de hoja ( $T_{leaf}$ ), radiación solar ( $Rad$ ), dióxido de carbono ( $CO_2$ ), presión ( $P$ ) y flujo volumétrico ( $V$ ) en un formato de 12 bits. Los valores de temperatura ( $T_a$ ) y humedad relativa del aire ( $RH$ ) son adquiridos por el FPGA—EP4CE22F17C6N en formatos de 14 y 12 bits respectivamente. Por cuestiones de estandarización las mediciones de todos los sensores se guardan en dos bytes, donde el byte más significativo almacena los 4 bits más significativos de la medición (los 4 bits restantes se llenan con ceros) y el byte menos significativo almacena los 8 bits restantes. Esta regla aplica para todos los sensores, excepto para el sensor de temperatura de aire MEMS SHT75 (que maneja lecturas de 14 bits), donde los seis bits más significativos se cargan en el byte más significativo (ver Figura 3.5).

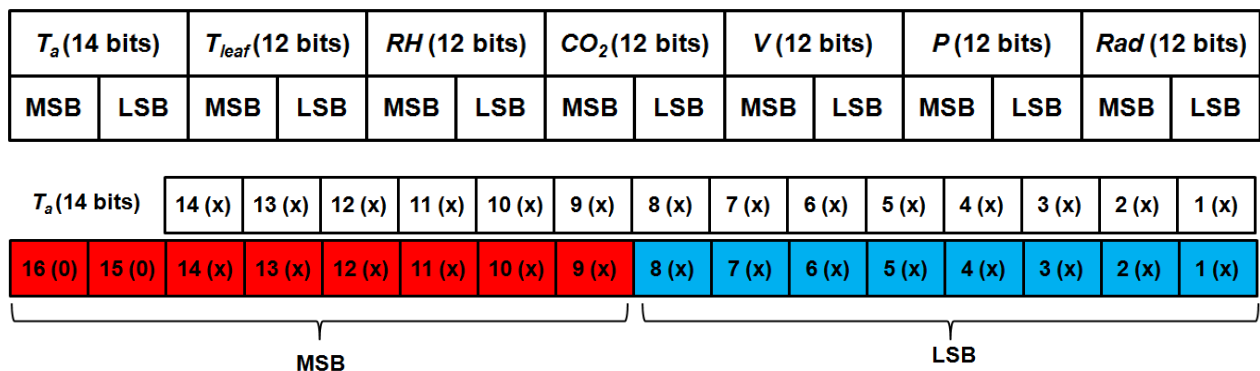


**Figura 3.5 – Estandarización de la transmisión de datos.** Las lecturas de los sensores se adquieren en un formato de 12 bits, excepto  $T_a$  que es de 14 bits. Para su transmisión de manera inalámbrica se dividen dos bytes, un byte más significativo (MSB) y un byte menos significativo (LSB), donde el LSB siempre contiene los primeros 8 bits de las mediciones. El resto de los bits (4 ó 6) se cargan en MSB, los bits sobrantes de MSB se llenan con ceros.

De esta manera, una vez recibido el comando de inicio de medición, cada fitomonitor ocupa la red para transmitir cada segundo 14 bytes de información más dos bytes que identifican de que nodo viene la trama de datos correspondiente. Al final del ciclo de medición las estimaciones de fotosíntesis ( $P_n$ ), transpiración ( $E$ ), déficit de presión de vapor ( $VPD$ ), conductancia estomática ( $C_{leaf}$ ) y diferencia de temperatura aire-hoja ( $LATD$ ) son transmitidas ocupando cada una dos bytes en la última trama de datos.

Finalmente, cuando el coordinador de la red recibe la trama de datos de un nodo, este manda el comando de inicio de medición al nodo siguiente y así consecutivamente hasta completar todos los nodos de la red. Una vez encendidos todos los nodos, estos se mantendrán enviando datos cada segundo hasta terminar su ciclo de medición (20 minutos), donde se detendrán y esperaran por un nuevo comando de inicio del coordinador de la red. Es importante señalar que dos nodos no pueden utilizar la red al mismo tiempo, lo hacen individualmente de manera sincronizada, y si por alguna razón se pierde una trama de datos o un nodo no responde a la petición del coordinador, los datos de este nodo se tomaran como ceros para esta medición.

### **III.4 Software para adquisición de datos**

Cuando el coordinador recibe datos de algún nodo de la red, este los transmite vía USB a una computadora personal que almacena y grafica las diferentes señales. El programa para recibir los datos del coordinador fue desarrollado utilizando el compilador Builder C++ versión 6.0. Al ser software libre se puede emplear a nivel comercial sin tener que pagar regalías a la empresa que lo desarrolló.

El programa basa su funcionamiento en un hilo informático que se mantiene a la escucha del puerto serie (RS-232 para esta aplicación). De manera que si llega algún dato este se encuentra listo para procesarlo y almacenarlo. El programa de adquisición recibe datos de tres nodos diferentes, y genera un archivo de texto (\*.TXT) para cada nodo, en estos archivos almacena las mediciones de los sensores primarios y tras transcurrir 1024 mediciones guarda también las estimaciones de los procesos fisiológicos realizadas por el FPGA. El algoritmo comienza reconociendo el byte identificador de cada nodo (0x0001, 0x0002 y 0x0003), posteriormente recibe en formato hexadecimal las mediciones de cada sensor y realiza las operaciones necesarias para convertirlas a formato entero con 4 decimales.

El software es portable y no requiere la instalación de ningún programa para su ejecución, basta ejecutar la aplicación Plant\_DataLogger\_V2.0.exe para que se despliegue la interfaz gráfica de usuario y tras comenzar a adquirir datos, generar los archivos de texto en la misma carpeta donde se encuentra la aplicación. Es importante

señalar que por estar compilado en una plataforma libre, el software diseñado puede ser usado a nivel comercial sin tener que pagar regalías a la empresa desarrolladora. En la figura 3.6 se observa la interfaz gráfica del software inquisidor de dato donde cada columna presenta la información de un nodo, permitiendo así ver en tiempo real las mediciones de los sensores primarios, la muestra actual, el ciclo de medición y el identificador de cada nodo. Esto facilita la detección de fallas en sensores o en el nodo completo.



Figura 3.6 – Software para adquisición de datos. Se diseñó utilizando Builder C++ V6.0, muestra de manera simultánea las lecturas de los sensores de los tres nodos que integran la red, además de la muestra actual para cada ciclo y el byte identificador de cada fitomonitor.

### III.5 Calibración y validación de sensores de sensores

Debido a que la confiabilidad de las estimaciones realizadas por el sensor inteligente depende en gran medida de la integridad de las lecturas de los sensores primarios, fue necesario realizar una validación de los sensores de CO<sub>2</sub> con una referencia, en este caso de 1100 ppm. Esta prueba fue necesaria porque los sensores

de CO<sub>2</sub> son los que presentan la mayor componente de ruido. Como se puede observar en la Figura 3.7a, las primeras 512 muestras corresponden a la referencia de CO<sub>2</sub> mientras que las siguientes 512 muestras corresponden al aire al interior de un invernadero cerrado y sin plantas. Esta prueba se repitió en 16 ocasiones durante el mismo día. Finalmente se realizó un Análisis de Varianza (ANOVA) con los promedios de cada ciclo de medición. Esto con el propósito de evaluar la respuesta de cada sensor ante una referencia común. El valor de  $\alpha$  para esta y las demás pruebas en este trabajo fue de 0.05 (ó 95% de confianza). El valor resultante de  $p$  fue de 0.2205, este valor es mucho mayor que el umbral 0.05 que representa el límite superior para considerar diferencias estadísticas entre tratamientos (Goodman, 1999). De esta manera, el valor resultante de  $p$  significa que las lecturas de cada nodo ante una referencia no presentan diferencias estadísticas significantes, además, como puede observarse en la Figura 3.7b, solo existen dos valores fuera del intervalo de confianza. Las medias del análisis fueron de 1098.4, 1098.3 y 1098.3 ppm con desviaciones estándar de 4.49, 4.31 y 4.67 ppm para los nodos 1, 2 y 3 respectivamente.

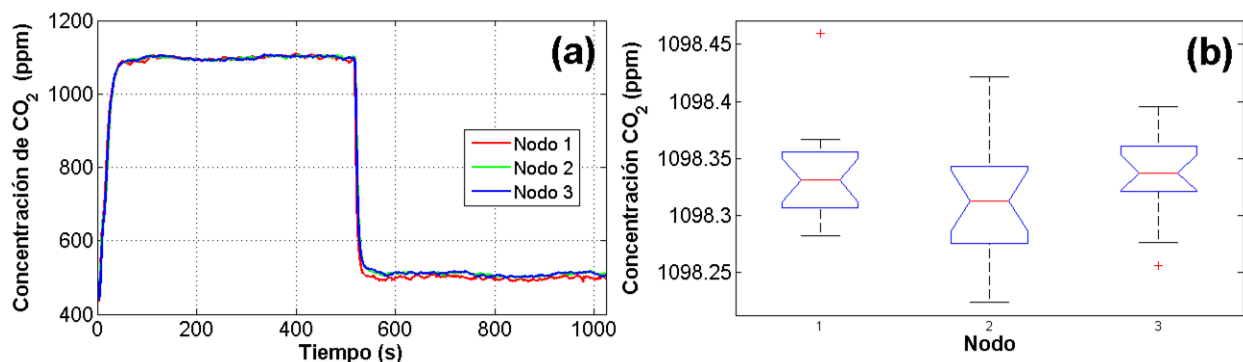


Figura 3.7 — Prueba de validación de los sensores de CO<sub>2</sub>. (a) Un ciclo de monitoreo con referencia de 1100 ppm de CO<sub>2</sub>. (b) Resultados del Análisis de Varianza.

### III.6 Calibración por estrés químico

La última prueba realizada para validar el correcto funcionamiento de los dispositivos se realizó utilizando un herbicida funcional que dañe el fotosistema II de las plantas inhibiendo de esta manera la asimilación de CO<sub>2</sub> y por tanto la fotosíntesis neta.

El herbicida utilizado fue Sencor 480 SC (compuesto activo METRIBUZIN) de la compañía Bayer Crop-Science. La dosis utilizada fue 1 ml de herbicida disuelto en 1 litro de agua. Las plantas del tratamiento fueron asperjadas con 100 ml cada una. El monitoreo se llevó a cabo 10 minutos después de la aplicación.

Los resultados ilustrados en la Figura 3.8 muestran como las plantas estresadas por el herbicida (PS1 y PS2) detuvieron su actividad fotosintética, mientras que la planta de referencia PR muestra una actividad fotosintética normal y coherente con la radiación monitoreada y expresada con la señal amarilla (Rad). Finalmente es importante aclarar que las señales han sido normalizadas para graficarlas bajo la misma escala. Estos resultados comprueban el correcto funcionamiento de los equipos de fitomonitorio ya que las estimaciones para las plantas PS1 y PS2 son muy similares, a pesar de ser en diferentes plantas y con diferentes equipos de monitoreo. Por su lado la señal de la planta de referencia PR se mantuvo coherente de acuerdo a la radiación incidente.

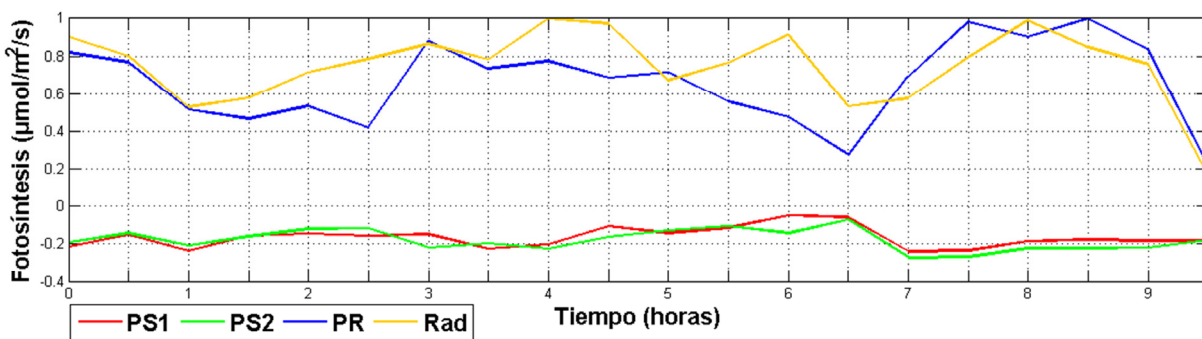
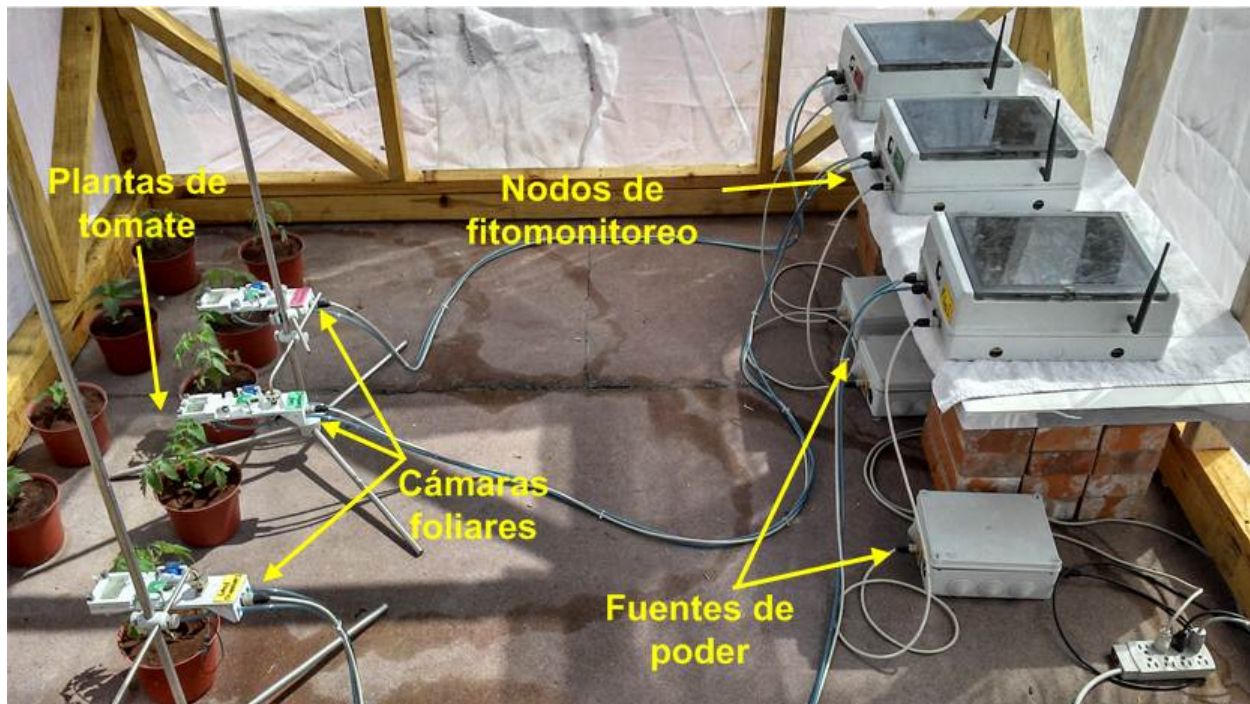


Figura 3.8 – Resultados de estimación de fotosíntesis en plantas con herbicida. Las señales en verde y rojo corresponden a plantas con herbicida, la señal azul es la planta de referencia y la amarilla representa la radiación. Todas las señales han sido normalizadas.

### III.7 Diseño del experimento

El experimento se llevó a cabo durante el 2013 en un invernadero de investigación localizado a una altitud de 54 msnm en la Universidad Autónoma de Sinaloa, Escuela de Biología. Culiacán Rosales, Sinaloa, México (24°48'0" N, 107° 23'0" W). El invernadero utilizado es del tipo Quonset y tiene una superficie de 50 m<sup>2</sup>,

está equipado con un control de temperatura comercial y un sistema de riego (ver Figura 3.9). Para la experimentación se emplearon plantas de tomate del mismo genotipo, variedad Raffaello (*Solanum lycopersicum* L.), el cual es una variedad indeterminada, resistente a enfermedades y plagas y apropiada para su cultivo bajo invernadero.



**Figura 3.9** – Instalación del sistema de detección de sequía en un experimento bajo condiciones reales de operación.

El diseño del experimento fue del tipo unifactorial con dos niveles. El factor de variación fue el contenido de agua en el sustrato. Los niveles fueron capacidad de campo (CC) y sequía. Se emplearon cinco unidades experimentales por tratamiento. Se emplearon tres fitomonitores para medir la respuesta de las plantas a los diferentes niveles de estrés hídrico (dos para sequía y uno para la planta de referencia). Variables primarias como temperatura y humedad relativa del aire, temperatura de la hoja, radiación y déficit de presión de vapor fueron monitoreadas durante un mes. También,

respuestas fisiológicas como fotosíntesis, transpiración, conductancia estomática, diferencia de temperatura aire-hoja fueron estimadas on-line, *in-situ* durante el mismo periodo.

El trasplante de la plantas se llevó a cabo 30 días después de la germinación cuando las plantas tenían 6 hojas verdaderas. Se trasplantaron en macetas de 1.5 litros llenas de tezontle, el tezontle se cribó para homogenizar su granulometría a aproximadamente  $605 \text{ kgm}^{-3}$  de densidad aparente y así evitar variaciones por diferentes tamaños de grano de sustrato. Para el riego se utilizó solución nutritiva Steiner inyectada por el sistema de riego.

Las plantas se mantuvieron bajo estas condiciones durante 10 días mientras alcanzaban un tamaño de hoja apropiado para las mediciones. Posteriormente se adquirieron señales con los fitomonitores durante 3 días (periodo de referencia) y a partir del sexto día comenzó la inducción del estrés hídrico.

## IV RESULTADOS Y DISCUSIÓN

### IV.1 Resultados del filtrado digital

La Figura 4.1 muestra las mejoras en la calidad de las señales después de las etapas de filtrado. En la figura 4.1a se puede apreciar fácilmente la cantidad de ruido presente en la señal de  $\text{CO}_2$ , consecuentemente la estimación de fotosíntesis es demasiado ruidosa (Figura 4.1b). Sin embargo, se observa como las etapas de filtrado mejoraron la calidad de las señales de concentración de  $\text{CO}_2$  en la Figura 4.1c y la fotosíntesis estimada en la Figura 4.1d.

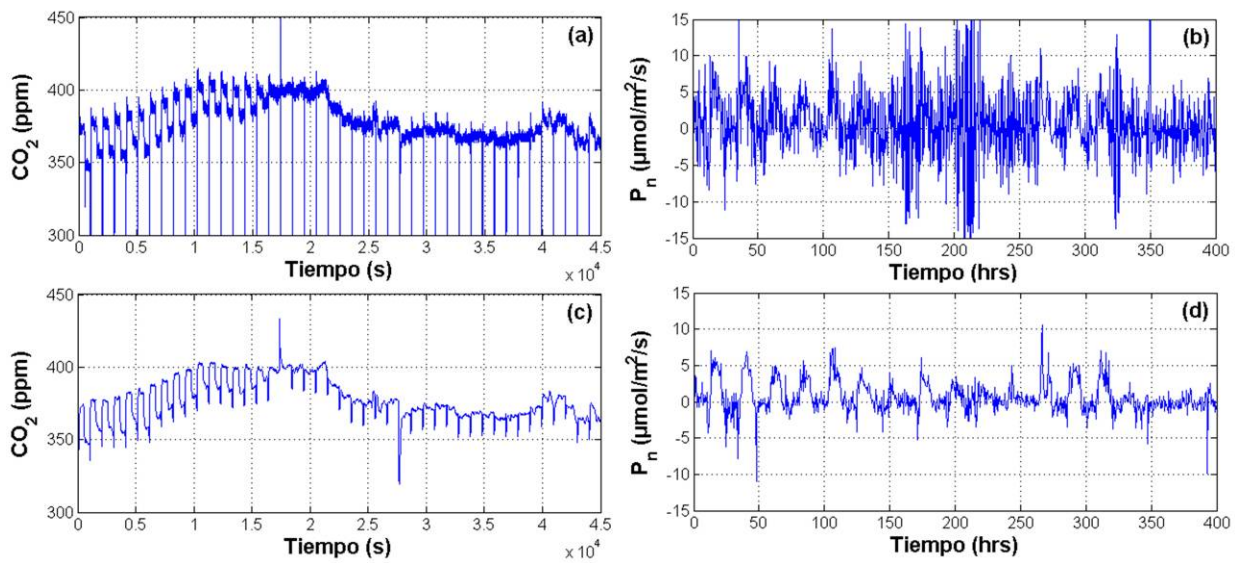


**Figura 4.1 – Resultados del filtrado digital en la estimación de fotosíntesis. a) Señal de  $\text{CO}_2$  sin filtrar, (b) estimación de  $P_n$  basada en señales en bruto, (c) señal de  $\text{CO}_2$  filtrada y (d) estimación de  $P_n$  basada en señales filtradas.**

La Figura 4.1 muestra los resultados de uno de los tres nodos, sin embargo, se obtuvieron resultados muy similares para demás nodos de la red de sensores. Posteriormente se procedió a realizar una correlación de Pearson entre las señales de fotosíntesis contra la radiación solar recibida por la planta, este análisis se realizó para cuantificar cuanto mejoraba la estimación de procesos una vez que las señales primarias habían sido filtradas de manera digital. Los resultados del análisis presentado en la Tabla 4 sugieren que el comportamiento de  $P_n$  estimada con señales no filtradas no corresponde con el patrón de radiación percibida. En contraste, se encontró una



mejor correlación entre la señal de  $Rad$  y la señal de  $P_n$  estimada con base en señales primarias filtradas digitalmente (diezmado por promedio y filtro Kalman). En la Tabla 4, la variable fotosíntesis con el subíndice  $osk$  es la señal estimada con señales primarias previamente filtradas. Los valores de correlación corresponden a la columna de  $R$ , mientras que los valores  $p$  por debajo de 0.05 confirman la existencia de correlación entre las señales.

**Tabla 4.1 – Resultados del análisis de correlación de radiación contra fotosíntesis. La fotosíntesis con el subíndice  $osk$  corresponde a la estimación con base en señales primarias filtradas digitalmente.**

Variables	Fotosíntesis – Radiación		Fotosíntesis <sub>osk</sub> – Radiación	
	$R$	$p$	$R$	$p$
<b>Nodo 1</b>	0.0672	0.0515	0.5146	<0.0001
<b>Nodo 2</b>	0.2023	<0.0001	0.5307	<0.0001
<b>Nodo 3</b>	0.1027	0.0028	0.6557	<0.0001

## IV.2 Señales ambientales

Debido a que el experimento se llevó a un invernadero comercial, las variaciones espaciales del microclima provocan cambios en los procesos fisiológicos, incluso para plantas bajo un mismo tratamiento de estrés hídrico. Por lo tanto fue necesario monitorear las variables relacionadas con el microclima del invernadero para entender los cambios en los procesos fisiológicos de la plantas. La Figura 4.2 ilustra las variables ambientales más importantes dentro del invernadero en tres posiciones diferentes (posiciones que corresponden con la ubicación de las plantas monitoreadas). La Figura 4.2a muestra las lecturas obtenidas para la radiación durante el experimento. Esta variable es de especial interés porque modifica las variables temperatura (4.2b),  $VPD$  (4.2c) y humedad relativa (4.2d) del aire dentro del invernadero y por lo tanto la transpiración de las plantas. Además, la fotosíntesis es más sensible a esta variable que a cualquier otro factor.

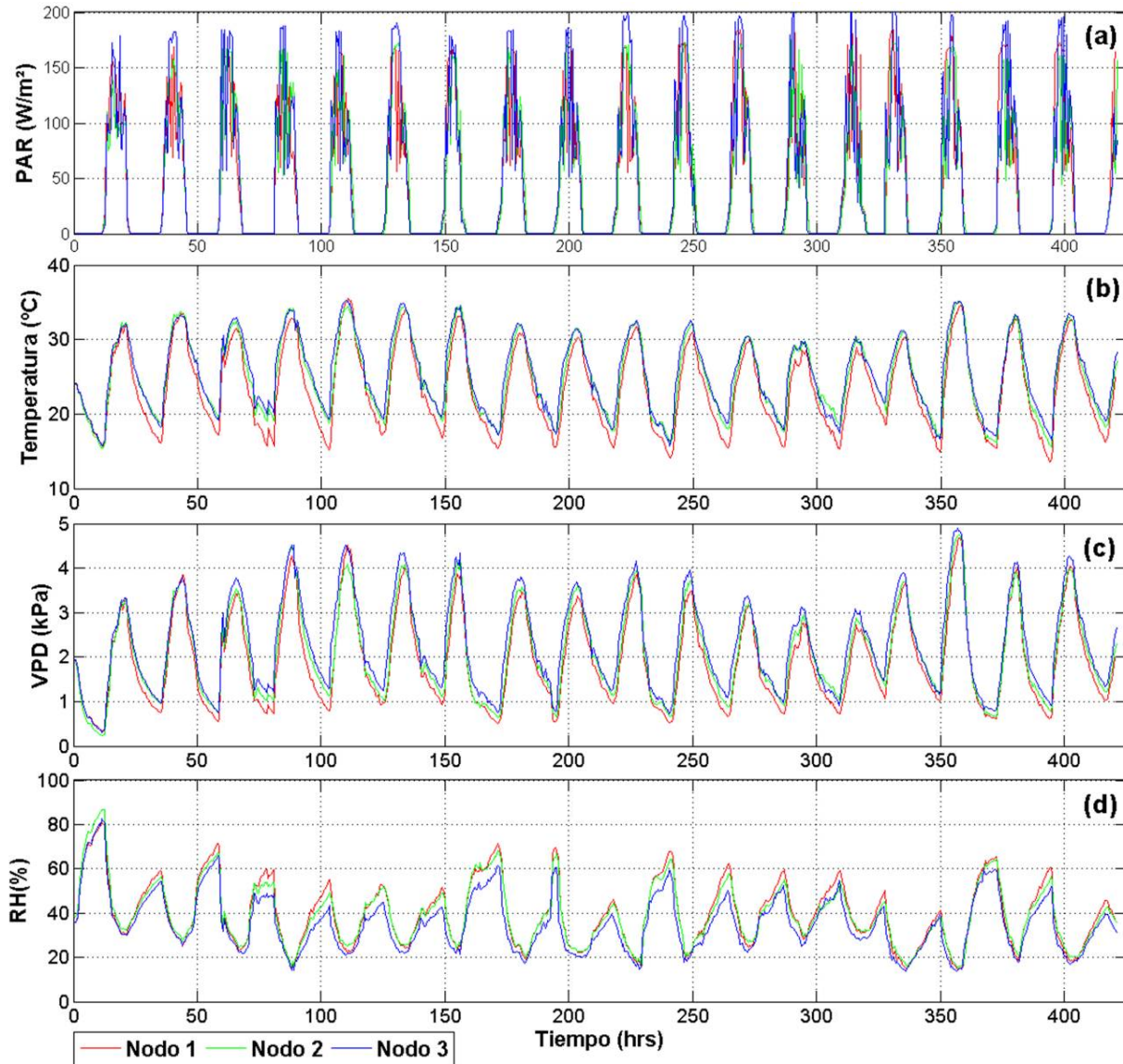


Figura 4.2 – Lecturas del clima dentro del invernadero en las posiciones de los Nodos 1, 2 y 3 de la WSN. (a) Radiación solar, (b) temperatura del aire, (c) déficit de presión de vapor y (d) humedad relativa.

Las diferencias entre las mediciones de cada no varían durante el día, pero mantienen un patrón regular donde el nodo 3 registra una temperatura más alta y condiciones de aire más secas. Como se observa en la Figura 4.3, este fenómeno está relacionado con la cantidad total de radiación recibida en este punto del invernadero. Esta figura ilustra como el invernadero presenta diferencias espaciales provocadas principalmente por su propia geometría y ubicación. Este aspecto es importante porque ayuda a entender cambios súbitos en las señales de transpiración y fotosíntesis

adquiridas por el sistema. Finalmente es importante aclarar que la radiación recibida de aproximadamente  $175 \text{ W/m}^2$  es apropiada para el cultivo de tomates de la variedad Rafaello (Vazquez-Cruz *et al.*, 2012).

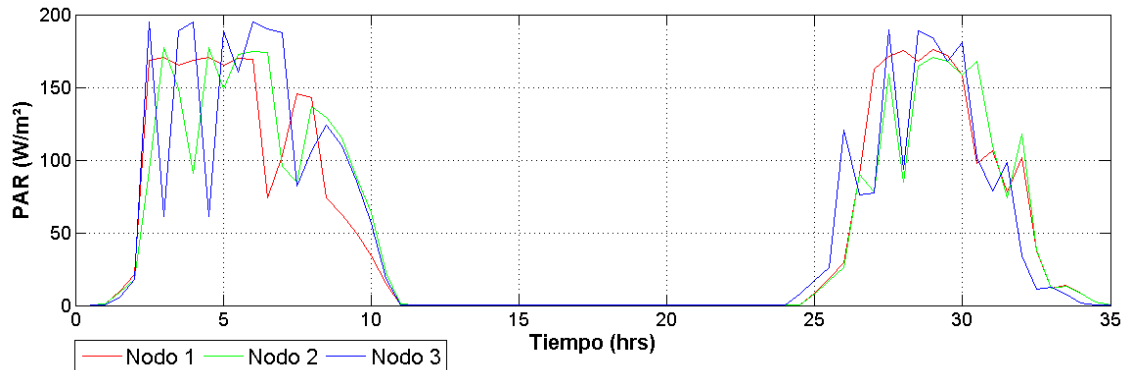


Figura 4.3 – Imagen ampliada de dos días de radiación.

### IV.3 Señales de procesos fisiológicos

La metodología para inducir el estrés fue la siguiente: Los primeros dos días corresponden a un periodo de estabilización del monitoreo donde las plantas fueron regadas a capacidad de campo (10 kPa); en el tercer día, la irrigación fue suspendida para que dos plantas alcanzaran condiciones de sequía de suelo de 30-40 kPa. Entonces, el día siguiente estas plantas se rehidrataron para evitar alcanzar el punto de marchitez permanente (PMP). El tratamiento de sequía se reanuda después de un día de rehidratación para las planta bajo estrés. El experimento duró 19 días. Como se observa en la Figura 4.4, las señales en colores rojo y verde corresponden con las plantas bajo tratamiento de estrés por sequía (PS1 y PS2 respectivamente). La señal de color azul representa la planta de referencia que se mantuvo irrigada a capacidad de campo o 10 kPa. El fondo color azul claro corresponde con los días de irrigación mientras que el fondo color naranja corresponde a los días donde las plantas bajo estrés dejan de recibir agua. Finalmente, las flechas de la figura sirven para indicar cuando se suspendió y reanudo para la planta de referencia al final del experimento. La flecha café indica interrupción del riego, y la flecha azul ubicada dos días después indica reanudación del riego.

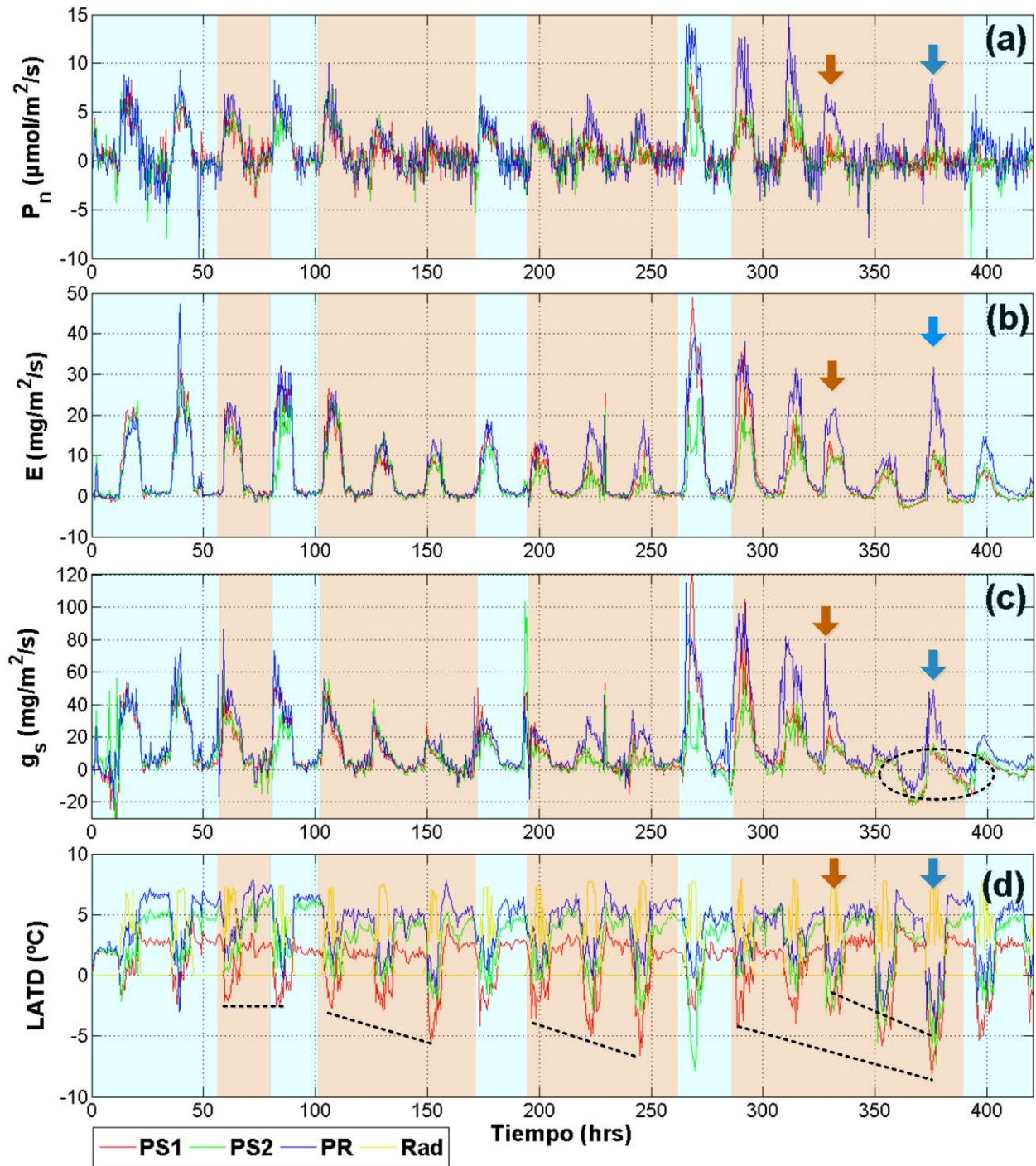


Figura 4.4 – Señales de procesos fisiológicos. (a) Fotosíntesis, (b) transpiración, (c) conductancia estomática y (d) diferencia de temperatura aire-hoja.

La figura 4.4 contiene las señales fisiológicas que proporcionan información más relacionada con el estado de la planta ( $P_n$ ,  $E$ ,  $g_s$ , and  $LATD$ ). Como se esperaba, la fotosíntesis no fue sensible a estadios tempranos de sequía. En la Figura 4.4a, las

diferencias de fotosíntesis entre la planta de referencia RP y los tratamientos PS1 y PS2 son observables hasta el tercer periodo de sequía alrededor de la hora 225. Sin embargo, después del cuarto periodo de sequía alrededor de la hora 400, la actividad fotosintética de las plantas PS1 y PS2 no se recupera incluso después de ser rehidratadas. Este comportamiento se puede explicar debido a que los periodos de sequía generan estrés oxidativo acumulativo en las hojas dañando el Fotosistema II de manera permanente con especies reactivas del oxígeno (Aroca, 2012a; Sharma *et al.*, 2012).

Los señales de la Figura 4.4b muestran respuesta temprana de la transpiración a los tratamientos de sequía. Sin embargo, el comportamiento más interesante aparece al final del experimento encerrado en la elipse de color negro. Aquí se muestra una tasa de transpiración negativa de baja amplitud. Esto indica que la planta está tomando vapor de agua del aire en lugar de expulsarlo a través de la hoja hacia la atmosfera. Éste mecanismo de defensa se observa en plantas bajo condiciones severas de estrés por sequía (Beebe *et al.*, 2013). Por otro lado, las señales de conductancia estomática (Figura 4.4c) presentan diferencias más notables entre tratamientos comparadas con  $P_n$ . Incluso en el primer día de sequía, las plantas PS1 y PS2 presentan una caída repentina en  $g_s$ . Este comportamiento concuerda con la teoría que establece que el cierre estomático y la reducción de  $g_s$  son las primeras líneas de defensa que las plantas usan para reducir la pérdida de agua. También está establecido que este comportamiento está más relacionado con las sequía en raíces que con el contenido de agua en las hojas (Aroca, 2012b). El decremento mayor de  $g_s$  en el tercer periodo de sequía puede estar relacionado con un decremento en la conductancia mesofilica  $g_m$  por que las hojas se están preparando para condiciones de sequía más severas.

La Figura 4.4d ilustra las diferencias de temperatura entre el aire y la hoja de la plantas. En esta figura, la señal amarilla representa el día durante el cual la variable  $LATD$  debe ligeramente positiva o igual a cero. Éste es un comportamiento normal en plantas sanas bien regadas por que la temperatura de la hoja  $T_{leaf}$  debe ser menor a la temperatura del aire  $T_a$ . Sin embargo, si las plantas están bajo condiciones de sequía, la  $T_{leaf}$  es mayor que  $T_a$ . Esta tendencia es claramente observable en la Figura 4.4d, ya

que una vez que se suspende el riego las señales presentan lecturas negativas. Esta tendencia está marcada con las líneas punteadas de color negro. Sin embargo, a pesar de estar sometidas al mismo tratamiento, PS2 siempre presentó una mejor tolerancia al estrés por sequía que PS1. Esto se puede observar en la Figura 4.4d porque la línea roja siempre presentó cambios negativos mayores en el *LATD*. Por otro lado, la planta de referencia PR siempre mostro un comportamiento estable con lectura cero o positivas hasta que el riego se suspendió alrededor de la hora 330. Después de este punto, una clara caída en el *LATD* se observa los siguientes dos días en que la planta no fue regada. Después de la rehidratación en la hora 375, el *LATD* de la planta PR regreso lentamente a cero y a tener valores positivos.

Finalmente, es importante mencionar que las plantas del tratamiento de sequía PS1 y PS2 presentaron una reducción en altura comparadas con la planta de referencia. Al final del experimento las plantas bajo estrés hídrico mantuvieron una altura del 80% de las plantas no estresadas.

#### **IV.4 Análisis con Transformada Wavelet Discreta (DWT)**

A pesar que la Figura 4.4 proporciona información importante sobre los efectos de la sequía en plantas, el análisis requiere información de al menos dos días para observar un patrón de comportamiento útil para tomar decisiones. El problema con realizar una comparación para un solo día está limitado por la cantidad de ruido presente en la señales (principalmente para  $P_n$  y  $g_s$ ), esto incluso después de filtrar las señales primarias con los filtros digitales antes descritos. Otro problema importante es que las variaciones en las condiciones del cultivo, principalmente de radiación a lo largo del invernadero pueden provocar que plantas bajo un mismo tratamiento respondan diferente. Este problema se atendió utilizando la Ecuación 17 descrita anteriormente. De esta manera, si plantas bajo un mismo tratamiento reciben diferente radiación solar, las diferencias en las variables en respuesta se reducirán permitiendo realizar una comparación más confiable. Esta metodología fue útil en las señales de  $P_n$ ,  $E$  y  $g_s$  ya

que presentaban una componente de ruido mayor comparadas con las señales *VPD* o *LATD*.

Como se puede observar en la Figura 3.4, después del proceso de normalización las señales fueron analizadas utilizando la Transformada Discreta Wavelet (DWT). En un experimento preliminar, varias DWT se ejecutaron con varias configuraciones para explorar cual era la que extraía la información de las señales. Finalmente, la DWT utilizada para filtrar las señales de la Figura 4.5 utiliza una ondeleta madre tipo Daubechies db40 en nivel A2 el cual rechaza señales fuera del ancho de banda de 0 a 0.27 mHz. Este criterio se seleccionó porque ondeletas madre de nivel más bajo rechazaban información relacionada con cambios súbitos (generados por cambios en radiación). Además, la ondeleta db40 requiere menos recursos computacionales que otras ondeletas como las Symmlets. El análisis en alta frecuencia (niveles D) no es reportado en este manuscrito ya que no se encontró patrón alguno que pueda usarse para analizar el fenómeno de sequía. Esto puede ser consecuencia de la baja frecuencia de muestreo del sistema propuesto. Finalmente, las versiones nuevas de  $P_n$  correspondientes a la Figura 4.5a presenta un reducción en la componente de ruido de alta frecuencia comparado con la Figura 4.4a, señal que incluso después de las etapas de filtrado digital mantiene un relación señal ruido muy alta. Esta componente puede ser un alias de la frecuencia generada por el mismo sensor de CO<sub>2</sub>. Sin embargo, después de utilizar la DWT como un etapa extra de filtrado, esta componente de ruido se redujo permitiendo realizar una análisis comparativo a lo largo de un solo día.

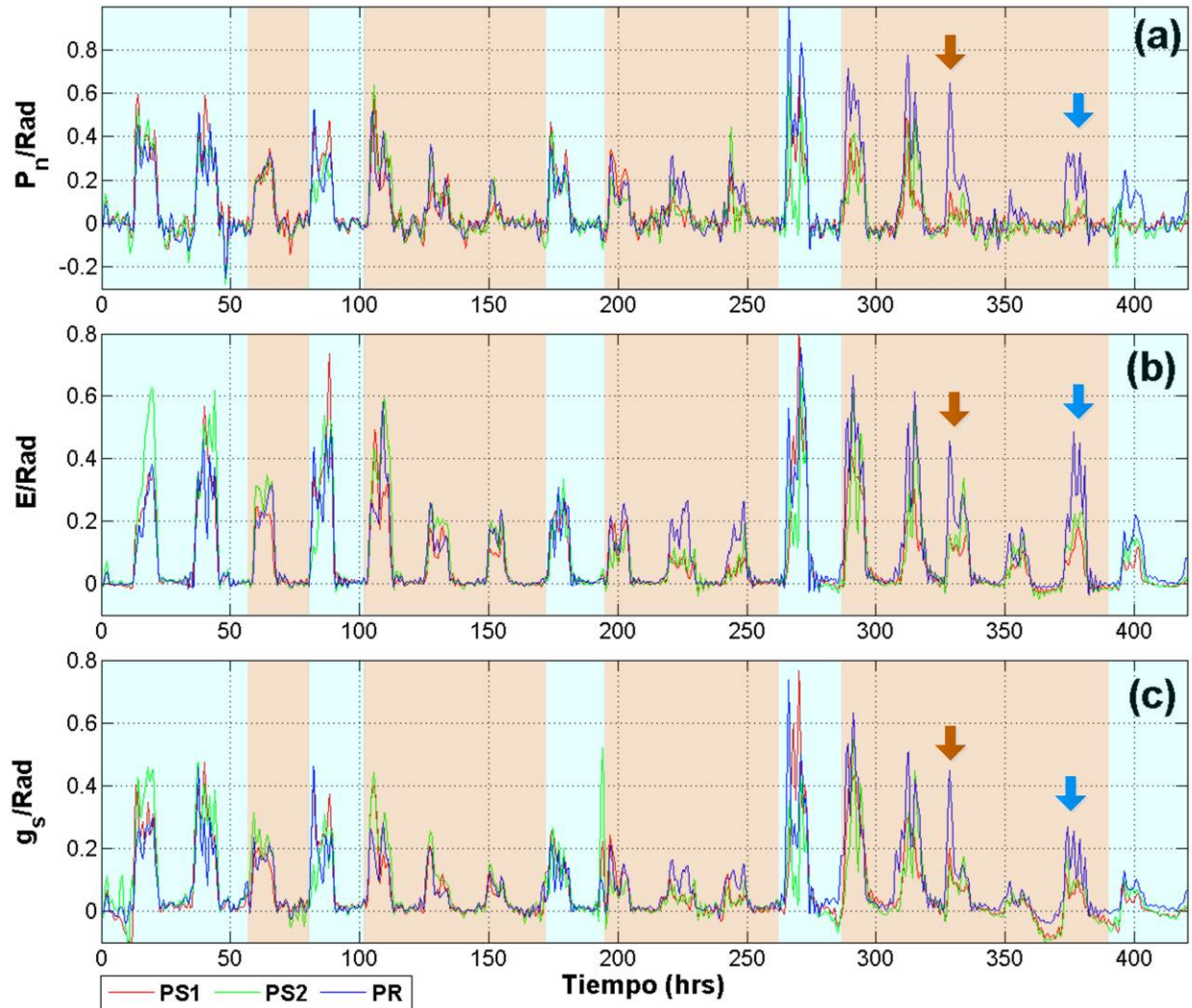


Figura 4.5 – Wavelets de los índices Procesos/Radiación. (a) Fotosíntesis, (b) transpiración, and (c) conductancia estomática.

Además, con el objetivo de evitar eliminar información relacionada con la respuesta de la planta y tomando en cuenta que fotosíntesis está más fuertemente relacionada con la radiación que con cualquier otra variable, una correlación de Pearson se realizó para comparar estas variables antes y después del procesamiento con la DWT. Los resultados de correlación presentados en la Tabla 4.2 apoyan la idea de que la DWT elimina el ruido presente en la señal de fotosíntesis pero mantiene la información relacionada con el proceso fisiológico en sí. Como se puede observar en ésta Tabla, la correlación entre  $P_n$  y Rad incremento cuando la  $P_n$  es filtrada con la DWT. Solo en el nodo 3 no se repitió este patrón. Sin embargo, el decremento en este



caso no es significativo. Esta tabla también presenta los resultados de la hipótesis de no correlación donde los valores  $p$  sugieren que la hipótesis de nulidad es rechazada.

**Tabla 4.2 – Resultados de las correlaciones de Fotosíntesis contra Radiación con y sin filtrado Wavelet (DWT).**

Variables	Fotosíntesis <sub>osk</sub> – Radiación		Fotosíntesis <sub>DWT</sub> – Radiación	
	$R$	$p$	$R$	$p$
<b>Nodo1</b>	0.5146	<0.0001	0.5600	<0.0001
<b>Nodo 2</b>	0.5307	<0.0001	0.5574	<0.0001
<b>Nodo 3</b>	0.6557	<0.0001	0.6308	<0.0001

Finalmente, con el objetivo de entender el impacto de la sequía sobre el desarrollo de las plantas a largo plazo, se propuso el índice llamado en este trabajo Balance de Carbono en Tiempo Real (*RT-CB*), el cual está basado en la integral de  $P_n$ . Como se puede observar en la Figura 4.6, durante el día el *RT-CB* se incrementa pero se detiene o decrece un poco durante las noches. Este comportamiento es resultado de las actividades fotosintéticas y de respiración de la planta; pero como es indicado por las elipses, cuando las plantas son somitas a sequía el *RT-CB* se mantiene constante hasta el día de rehidratación de la planta. Es importante aclarar que el primer periodo de sequía no afectó significativamente las respuestas de las plantas y que los resultados aparecen hasta el día dos de la sequía. Durante los días de rehidratación correspondiente a las horas 75, 175 y 275, las plantas recuperaron su actividad fotosintética. Sin embargo, las plantas PS1 y PS2 no se recuperaron después del cuarto periodo de sequía, incluso cuando las plantas se regaron nuevamente aproximadamente en la hora 380. En este punto el índice *RT-CB* mantiene una tendencia negativa que significa que la actividad fotosintética se detuvo y que la respiración se incrementa produciendo pérdida de material seco. La Figura 4.6 también muestra el comportamiento exponencial de la fotosíntesis conforme la planta crece. Porque alrededor de la hora 275 de la experimentación, el *RT-CB* registró un incremento importante para la planta de referencia PR. Sin embargo esta tendencia

cambio cuando se suspendió el riego a esta planta. El primer día de escasez de agua indicado por la flecha café no hubo cambios en la respuesta de la planta. Sin embargo, el día siguiente se presentó una caída abrupta en la asimilación de Carbono. Ésta tendencia continuo hasta que la irrigación se reanudo el día marcado por la flecha azul.

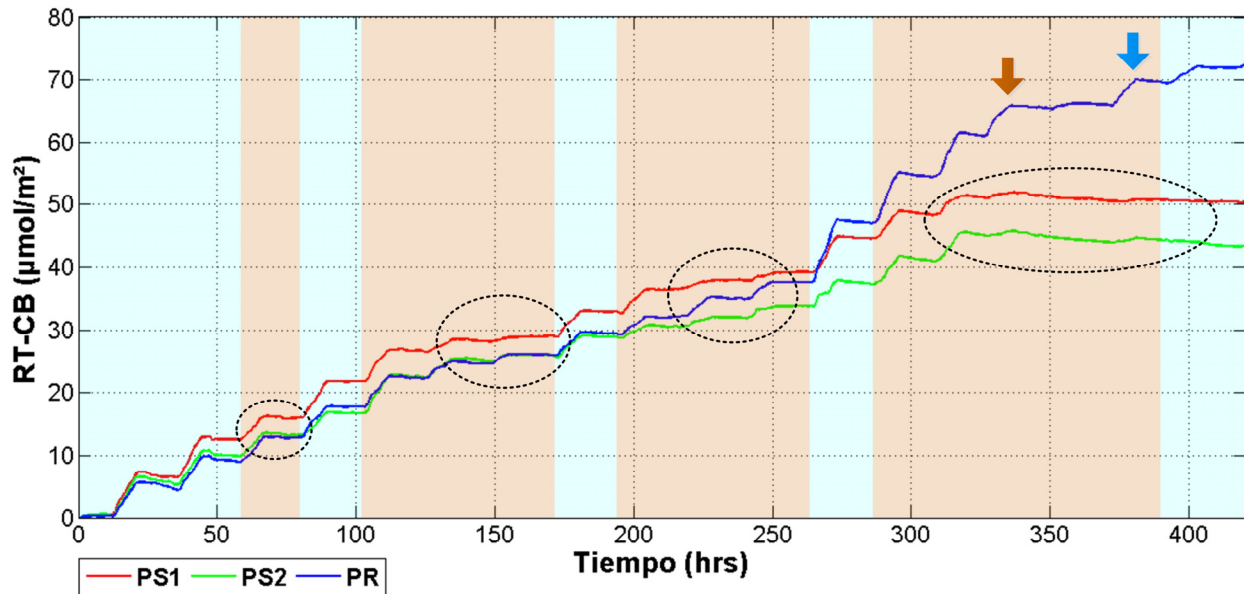


Figura 4.6 – Balance de Carbono en Tiempo Real (*RT-CB*).

## IV.5 Conclusiones y perspectivas

En la presente investigación se desarrolló un sensor inteligente para monitorear variables primarias en plantas y con base en estas mediciones estimar procesos fisiológicos como fotosíntesis, transpiración y conductancia estomática. El experimento realizado demostró las capacidades del sistema para detectar estrés inducido por sequía en plantas de tomate. Además se comprobó que el sistema puede operar bajo condiciones operativas reales (condiciones de invernadero). Sin embargo, si el sistema se quiere utilizar en campo abierto se tienen que realizar algunas consideraciones, principalmente por la radiación solar directa y la lluvia que pueden dañar el equipo. No obstante, es importante aclarar que este es un primer prototipo que puede mejorarse a futuro. Otra consideración importante es el diseño de la cámara foliar y el estrés mecánico y térmico que genera en las hojas que son aisladas para la medición.

Durante el experimento fue necesario cambiar las hojas de manera periódica, sin embargo, los periodos fueron de tres días durante los cuales no se apreció daño en las hojas, esto se debe a que la cámara foliar está construida con una combinación de acrílico y Nylamid, estos materiales no se sobrecalientan bajo la radiación solar como lo hacen las cámaras foliares de aluminio utilizadas en equipos comerciales.

Además, se utilizó la Transformada Wavelet Discreta en conjunto con un índice que ajusta las estimaciones de acuerdo a las condiciones del microclima particulares para cada planta dentro del invernadero. Esta metodología resultó útil ya que permitió realizar comparaciones entre tratamiento para datos de un solo día, esto es importante ya que el análisis convencional requiere lecturas de varios días para poder encontrar patrones de comportamiento asociados al estrés por sequía. También, el índice *RT-CB* proporciona una alternativa para monitorear el desarrollo del cultivo sin necesidad de utilizar análisis de laboratorios invasivos donde la muestra de la planta se tiene que destruir. Asimismo, el índice *RT-CB* proporciona información sobre condiciones de crecimiento irregular en los cultivos como las ocasionadas por la sequía. Finalmente, la metodología de procesamiento digital de señales implementada con el sistema de intercambio de gases es una alternativa para detectar y monitorear condiciones de sequía en plantas bajo condiciones operativas reales. Además, esta metodología se puede utilizar para propósitos de filtrado en aplicaciones de agricultura de precisión donde la relación señal-ruido es alta (aplicaciones como fluorescencia de clorofila o sensores de impedancia). Finalmente, esta metodología se podría utilizar para explorar propiedades de una gran variedad de señales en el dominio del tiempo-frecuencia.

**BIBLIOGRAFÍA**

- Agrios, G. 2005. Plant Pathology. 5th. New York: Elsevier.
- Aroca, R. 2012a. Plant Responses to Drought Stress.
- Aroca, R. 2012b. Plant Responses to Drought Stress: From Morphological to Molecular Features. Springer.
- Baert, A., K. Villez, y K. Steppe. 2013. Automatic drought stress detection in grapevines without using conventional threshold values. *Plant Soil* 369: 439-452.
- Ballester, C., J. Castel, M. A. Jiménez-Bello, J. R. Castel, y D. S. Intrigliolo. 2013. Thermographic measurement of canopy temperature is a useful tool for predicting water deficit effects on fruit weight in citrus trees. *Agricultural Water Management* 122: 1-6.
- Baptista, F., B. Bailey, J. Meneses, y L. Navas. 2010. Greenhouses climate modelling. Tests, adaptation and validation of a dynamic climate model. *Spanish Journal of Agricultural Research* 8: 285-298.
- Beebe, S. E., I. M. Rao, M. W. Blair, y J. A. Acosta-Gallegos. 2013. Phenotyping common beans for adaptation to drought. *Frontiers in physiology* 4.
- Ben-Gal, A. *et al.* 2010. Whole-tree water balance and indicators for short-term drought stress in non-bearing 'Barnea' olives. *Agricultural Water Management* 98: 124-133.
- Bennis, N., J. Duplaix, G. Enéa, M. Haloua, y H. Youlal. 2008. Greenhouse climate modelling and robust control. *Computers and Electronics in Agriculture* 61: 96-107.
- Biswas, D., M. Haque, A. Hamid, y M. Rahman. 2001. Photosynthetic gas exchange characteristics, leaf area and dry matter accumulation of two blackgram cultivars. *J. Biol. Sci* 1: 951-954.
- Bittelli, M. 2010. Measuring soil water potential for water management in agriculture: A review. *Sustainability* 2: 1226-1251.
- Candogan, B. N. *et al.* 2013. Yield, quality and crop water stress index relationships for deficit-irrigated soybean [*Glycine max* (L.) Merr.] in sub-humid climatic conditions. *Agricultural Water Management* 118: 113-121.
- CONAGUA. 2013. Comisión Nacional del Agua. <http://www.cna.gob.mx/Contenido.aspx?n1=3&n2=60&n3=87&n4=34>.

- Contreras-Medina, L. M. *et al.* 2012. Smart sensor for real-time quantification of common symptoms present in unhealthy plants. *Sensors* 12: 784-805.
- Chalabi, Z., B. Bailey, y D. Wilkinson. 1996. A real-time optimal control algorithm for greenhouse heating. *Computers and Electronics in Agriculture* 15: 1-13.
- Che, J. *et al.* 2010. Plant stem diameter measuring device based on computer vision and embedded system. In: *World Automation Congress (WAC)*, 2010. p 51-55.
- Cheng, T., B. Rivard, y A. Sánchez-Azofeifa. 2011. Spectroscopic determination of leaf water content using continuous wavelet analysis. *Remote Sensing of Environment* 115: 659-670.
- Dayan, E., E. Presnov, J. Dayan, y A. Shavit. 2004. A system for measurement of transpiration, air movement and photosynthesis in the greenhouse. *654*: 123-132.
- Ehret, D. L., B. D. Hill, T. Helmer, y D. R. Edwards. 2011. Neural network modeling of greenhouse tomato yield, growth and water use from automated crop monitoring data. *Computers and Electronics in Agriculture* 79: 82-89.
- FAOstat. 2013. Food and Agriculture Organization of the United Nations. <http://faostat.fao.org/> 2013.
- Faraloni, C. *et al.* 2011. Chlorophyll fluorescence technique as a rapid tool for in vitro screening of olive cultivars (*Olea europaea* L.) tolerant to drought stress. *Environmental and Experimental Botany* 73: 49-56.
- Foucher, P., P. Revollon, B. Vigouroux, y G. Chassériaux. 2004. Morphological Image Analysis for the Detection of Water Stress in Potted Forsythia. *Biosystems Engineering* 89: 131-138.
- García-Mier, L., R. G. Guevara-González, V. M. Mondragón-Olguín, B. del Rocío Verduzco-Cuellar, y I. Torres-Pacheco. 2013. Agriculture and bioactives: achieving both crop yield and phytochemicals. *International journal of molecular sciences* 14: 4203-4222.
- Goodman, S. N. 1999. Toward evidence-based medical statistics. 1: The P value fallacy. *Annals of internal medicine* 130: 995-1004.
- Hashimoto, Y. 1989. Recent strategies of optimal growth regulation by the speaking plant concept. In: *International Symposium on Growth and Yield Control in Vegetable Production* 260. p 115-122.

- Helmer, T., D. L. Ehret, y S. Bittman. 2005. CropAssist, an automated system for direct measurement of greenhouse tomato growth and water use. *Computers and Electronics in Agriculture* 48: 198-215.
- Hilker, T. *et al.* 2013. Remote sensing of transpiration and heat fluxes using multi-angle observations. *Remote Sensing of Environment* 137: 31-42.
- INEGI. 2013. Censo Agrícola, Ganadero y Forestal 2007. <http://www3.inegi.org.mx/sistemas/tabuladosbasicos/default.aspx?c=17177&s=est> 2013.
- Jiaying, C. *et al.* 2010. Plant stem diameter measuring device based on computer vision and embedded system. In: *World Automation Congress (WAC)*, 2010. p 51-55.
- Körner, O., y G. van Straten. 2008. Decision support for dynamic greenhouse climate control strategies. *Computers and Electronics in Agriculture* 60: 18-30.
- Lenthe, J.-H., E.-C. Oerke, y H.-W. Dehne. 2007. Digital infrared thermography for monitoring canopy health of wheat. *Precision Agric* 8: 15-26.
- Linker, R., y I. Seginer. 2003. Water Stress Detection in a Greenhouse by a Step Change of Ventilation. *Biosystems Engineering* 84: 79-89.
- Matimati, I., C. F. Musil, L. Raitt, y E. C. February. 2012. Diurnal stem diameter variations show CAM and C3 photosynthetic modes and CAM–C3 switches in arid South African succulent shrubs. *Agricultural and Forest Meteorology* 161: 72-79.
- Mazanti Hansen, J., y N. Ehler. 1995. The Plants-on-line-box: A Tool for Future Greenhouse Crop Management: System Concepts, Design, and User Interface. In: *II International Symposium On Sensors in Horticulture* 421. p 137-144.
- Millan-Almaraz, J. R. *et al.* 2013. FPGA-based wireless smart sensor for real-time photosynthesis monitoring. *Computers and Electronics in Agriculture* 95: 58-69.
- Ondimu, S., y H. Murase. 2008. Water stress detection in Sunagoke moss (*Rhacomitrium canescens*) using combined thermal infrared and visible light imaging techniques. *Biosystems Engineering* 100: 4-13.
- Peng, S., L. Xiaoli, L. Fei, y H. R. Karimi. 2012. Kalman filtering on greenhouse climate control. In: *Control Conference (CCC)*, 2012 31st Chinese. p 779-784.
- Phytech Ltd. 2013. [www.phytech.com](http://www.phytech.com) 2013.
- Rodriguez-Donate, C., R. A. Osornio-Rios, J. R. Rivera-Guillen, y R. d. J. Romero-Troncoso. 2011. Fused smart sensor network for multi-axis forward kinematics estimation in industrial robots. *Sensors* 11: 4335-4357.

- Schmidt, U. 1998. Low-cost system for on-line measurement of plant transpiration and photosynthesis in greenhouse production. *Acta Horticulturae* 421.
- Schmidt, U. 2005. MICROCLIMATE CONTROL IN GREENHOUSES BASED ON PHYTOMONITORING DATA AND MOLLIER PHASE DIAGRAM. *Acta Horticulturae* 691: 125-132.
- Schmidt, U., C. Huber, y T. Rocks. 2007. Evaluation of combined application of fog system and CO<sub>2</sub> enrichment in greenhouses by using phytomonitoring data. In: International Symposium on High Technology for Greenhouse System Management: Greensys2007 801. p 1301-1308.
- Schmidt, U., C. Huber, T. Rocks, R. Salazar Moreno, y A. Rojano Aguilar. 2008. Greenhouse cooling and carbon dioxide fixation by using high pressure fog systems and phytocontrol strategy. *Acta Horticulturae* 797: 279-284.
- Sharma, P., A. B. Jha, R. S. Dubey, y M. Pessarakli. 2012. Reactive oxygen species, oxidative damage, and antioxidative defense mechanism in plants under stressful conditions. *Journal of Botany* 2012.
- Šimpraga, M. *et al.* 2011. Clear link between drought stress, photosynthesis and biogenic volatile organic compounds in *Fagus sylvatica* L. *Atmospheric Environment* 45: 5254-5259.
- Song, S., M. Kopyt, Y. Ton, y S. Xie. 2004. A Trial Application of the Phytomonitoring Technique for Litchi in Shenzhen Area of China. In: GGIR International Conference—Beijing. p 11-24.
- Suárez, L., P. J. Zarco-Tejada, J. A. J. Berni, V. González-Dugo, y E. Fereres. 2009. Modelling PRI for water stress detection using radiative transfer models. *Remote Sensing of Environment* 113: 730-744.
- Suárez, L. *et al.* 2010. Detecting water stress effects on fruit quality in orchards with time-series PRI airborne imagery. *Remote Sensing of Environment* 114: 286-298.
- Suárez, L. *et al.* 2008. Assessing canopy PRI for water stress detection with diurnal airborne imagery. *Remote Sensing of Environment* 112: 560-575.
- Tian, Y., Y. Zhu, y W. Cao. 2005. Monitoring leaf photosynthesis with canopy spectral reflectance in rice. *Photosynthetica* 43: 481-489.
- Ton, Y. 1997. Phytomonitoring system. In: IV International congress on new agricultural technologies. Puerto Vallarta. Jalisco. Mexico. p 89-95.

- Ton, Y., y M. Kopyt. 2003. Phytomonitoring information and decision-support system for crop growing. Proceedings of the 2nd IS on Intelligent Information Technology in Agriculture. Zhao Chunjiang (ed.). Beijing, China.
- Ton, Y., N. Nilov, y M. Kopyt. 2001. Phytomonitoring: The new information technology for improving crop production. *Acta Horticulturae* 562: 257-262.
- Van Leeuwen, C. *et al.* 2009. Vine water status is a key factor in grape ripening and vintage quality for red Bordeaux wine. How can it be assessed for vineyard management purposes. *J. Int. Sci. Vigne Vin* 43: 121-134.
- van Straten, G., H. Challa, y F. Buwalda. 2000. Towards user accepted optimal control of greenhouse climate. *Computers and Electronics in Agriculture* 26: 221-238.
- van Straten, G., E. van Henten, L. van Willigenburg, y R. van Ooteghem. 2010. Optimal control of greenhouse cultivation. CRC Press.
- Vazquez-Cruz, M., R. Luna-Rubio, L. Contreras-Medina, I. Torres-Pacheco, y R. Guevara-Gonzalez. 2012. Estimating the response of tomato (*Solanum lycopersicum*) leaf area to changes in climate and salicylic acid applications by means of artificial neural networks. *Biosystems Engineering* 112: 319-327.
- Walter, J. *et al.* 2011. Do plants remember drought? Hints towards a drought-memory in grasses. *Environmental and Experimental Botany* 71: 34-40.
- Wang, X., W. Yang, A. Wheaton, N. Cooley, y B. Moran. 2010. Automated canopy temperature estimation via infrared thermography: A first step towards automated plant water stress monitoring. *Computers and Electronics in Agriculture* 73: 74-83.
- Wu, Q. *et al.* 2013. CO<sub>2</sub> response process and its simulation of *Prunus sibirica* photosynthesis under different soil moisture conditions. *Ying yong sheng tai xue bao*= The journal of applied ecology/*Zhongguo sheng tai xue xue hui, Zhongguo ke xue yuan Shenyang ying yong sheng tai yan jiu suo zhu ban* 24: 1517-1524.
- Yamaguchi-Shinozaki, K., y K. Shinozaki. 2006. Transcriptional regulatory networks in cellular responses and tolerance to dehydration and cold stresses. *Annu. Rev. Plant Biol.* 57: 781-803.
- Yamaguchi, K. *et al.* 2007. A protective role for the polyamine spermine against drought stress in *Arabidopsis*. *Biochemical and biophysical research communications* 352: 486-490.
- Zarco-Tejada, P. J. *et al.* 2013. A PRI-based water stress index combining structural and chlorophyll effects: Assessment using diurnal narrow-band airborne imagery and the CWSI thermal index. *Remote Sensing of Environment* 138: 38-50.



Zhao, Y.-d., Y.-r. Sun, X. Cai, H. Liu, y P. S. Lammers. 2012. Identify Plant Drought Stress by 3D-Based Image. *Journal of Integrative Agriculture* 11: 1207-1211.

# **APÉNDICE A**

## **ARTÍCULOS INTERNACIONALES PUBLICADOS**

## Review. Advantages and disadvantages of control theories applied in greenhouse climate control systems

C. Duarte-Galvan<sup>1</sup>, I. Torres-Pacheco<sup>1</sup>, R. G. Guevara-Gonzalez<sup>1</sup>, R. J. Romero-Troncoso<sup>2</sup>,  
L. M. Contreras-Medina<sup>1</sup>, M. A. Rios-Alcaraz<sup>1</sup> and J. R. Millan-Almaraz<sup>3</sup>, \*

<sup>1</sup> *CA Ingeniería de Biosistemas, División de Investigación y Posgrado, Facultad de Ingeniería, Universidad Autónoma de Querétaro, Cerro de las Campanas s/n, 76010, Querétaro, Qro., Mexico*

<sup>2</sup> *HSPdigital-CA Telemática, DICIS, Universidad de Guanajuato, Carr. Salamanca-Valle km 3.5+1.8, Palo Blanco, 36885 Salamanca, Gto., Mexico*

<sup>3</sup> *Facultad de Ciencias Físico-Matemáticas, Universidad Autónoma de Sinaloa, Av. de las Américas y Blvd. Universitarios, Cd. Universitaria, CP 80000, Culiacán, Sinaloa, Mexico*

---

### Abstract

Today agriculture is changing in response to the requirements of modern society, where ensuring food supply through practices such as water conservation, reduction of agrochemicals and the required planted surface, which guarantees high quality crops are in demand. Greenhouses have proven to be a reliable solution to achieve these goals; however, a greenhouse as a means for protected agriculture has the potential to lead to serious problems. The most of these are related to the inside greenhouse climate conditions where controlling the temperature and relative humidity (RH) are the main objectives of engineering. Achieving appropriate climate conditions to ensure high yield and quality crops reducing energy consumption have been the objective of investigations for some time. Different schemes in control theories have been applied in this field to solve the aforementioned problems. Therefore, the objective of this paper is to present a review of different control techniques applied in protected agriculture to manage greenhouse climate conditions, presenting advantages and disadvantages of developed control platforms in order to suggest a design methodology according to results obtained from different investigations.

**Additional key words:** controller; conventional control; optimal control; precision agriculture; protected agriculture.

### Resumen

#### Revisión. Ventajas y desventajas de los sistemas de control climático aplicados en agricultura de precisión

Hoy en día la agricultura está cambiando de acuerdo a las necesidades de la nueva sociedad. Las nuevas tendencias son asegurar la producción de alimentos a través de prácticas tales como ahorro de agua, reducción en el uso de agroquímicos y el espacio requerido para sembrar los cultivos mientras se garantiza la alta calidad de los cultivos. Los invernaderos han demostrado ser una solución viable para garantizar estos objetivos. Sin embargo, el uso de un invernadero conlleva serios problemas. Los más importantes están relacionados con las condiciones del microclima dentro del invernadero, donde el objetivo de la ingeniería es controlar la temperatura y humedad relativa (RH). Alcanzar las condiciones adecuadas del microclima para garantizar la alta productividad y calidad de los cultivos mientras se reducen los consumos de energía ha sido el objetivo de diversos investigadores a través del tiempo. Diversos esquemas de teoría de control han sido aplicados con el objetivo de resolver los problemas antes mencionados. Por lo tanto, el objetivo de este artículo es presentar una revisión de las diferentes técnicas de control aplicadas en agricultura de precisión para manejar las condiciones del microclima del invernadero, presentando las ventajas y desventajas de los sistemas desarrollados con la finalidad de proponer una metodología de diseño de acuerdo a los resultados obtenidos de las diferentes investigaciones.

**Palabras clave adicionales:** agricultura de precisión; agricultura protegida; control óptimo; controlador; control convencional.

## Introduction

A greenhouse is an enclosed space that creates a different environment to that found outside due to the confinement of the air and to the absorption of short-wave solar radiation through a plastic or glass covers (El Ghomari *et al.*, 2005). This generates a new environment inside the greenhouse which is better known as microclimate. The greenhouse microclimate can be manipulated by control actions, such as heating, ventilation, CO<sub>2</sub> enrichment to name a few; in order to provide appropriate environmental conditions (Bennis *et al.*, 2008). These modifications imply additional use of energy in the production process. Furthermore, it requires a control system that minimizes the energy consumption while keeping the state variables as close as possible to the optimum crop physiological reference (Coelho *et al.*, 2005). Horticulture in greenhouse conditions is a rapidly expanding interest and is consequently increasing in its economic and social importance.

Many efforts have been made to develop advanced computerized greenhouse climate control systems. In particular, interesting and important optimal control approaches have been proposed (Ioslovich *et al.*, 2009). As was previously reported, crop production using controlled environments has several advantages over conventional crop production such as greater productivity, better product quality, and low water and fertilizer consumption. Nevertheless, environmental requirements for living systems are very complex and nonlinear. Furthermore, the biological system likely has a significant and multiple effects on its physical surroundings (Pasgianos *et al.*, 2003). Researchers have used many control techniques in different fields. From the conventional or sometimes referred to as classic

control theory such as: proportional, integral and derivative (PID) controllers, artificial intelligence (AI) such as fuzzy logic systems (FLS), artificial neural networks (ANNs) and genetic algorithms (GAs) to advanced techniques like predictive, adaptive, robust and non-linear control (Castañeda-Miranda *et al.*, 2006). The aforementioned control techniques have been widely utilized on research (Trabelsi *et al.*, 2007; Bennis *et al.*, 2008).

In this review, updated information is provided about modern methods to control the greenhouse environments which can be taken into account as criteria to design new greenhouse microclimate control systems. The paper is divided in four sections, the first focuses on the different control theories applied to design climate control systems for protected agriculture. The second section is an overview of the technology platforms where the controllers were implemented. The third section discusses new tendencies in the development of environmental controllers for protected agriculture. Finally, in the last section the conclusions are presented.

## Control theories applied in greenhouse climate control systems: An analysis of advantages and disadvantages

Different research has been conducted regarding climate control for protected agriculture applications. The primary objective of these investigations is to find an accurate model that represents the greenhouse environmental dynamics and an efficient and flexible controller that adjusts the microclimate variables of

---

Abbreviations used: AGA (annealing genetic algorithm); AI (artificial intelligence); ANN (artificial neural network); DIF (difference between average day temperature and average night temperature); DSP (digital signal processor); FL (feedback linearization); FLS (fuzzy logic system); FPGA (field programmable gate array); GA (genetic algorithm); MIMO (multiple-input-multiple-output); MPC (model predictive control); PC (personal computer); PD (proportional derivative control); PDF (pseudo-derivative-feedback); PI (proportional integral control); PID (proportional integral and derivative control); PMP (pontryagin's maximum principle); PSO (particle swarm optimization); RH (relative humidity); SCS (sequential control search). Nomenclature:  $A_g$  (covered ground surface, m<sup>2</sup>);  $A_r$  (roof to soil rate, m<sup>2</sup> m<sup>-2</sup>);  $C$  (greenhouse heat capacity, J K<sup>-1</sup> m<sup>-2</sup>);  $C_p$  (air specific heat, J K<sup>-1</sup> kg<sup>-1</sup>);  $e_i$  (internal mean vapour pressure, Pa);  $e(t)$  (error);  $E(s)$  (Laplace error representation);  $G$  (outside short-wave radiation, W m<sup>-2</sup>);  $I_{LA}$  (leaf area index, m<sup>2</sup> m<sup>-2</sup>);  $K_i$  (integral gain);  $K_d$  (derivative gain);  $K_{out,air}$  (heat loss coefficient from greenhouse air to outside air);  $K_p$  (proportional gain);  $q_h$  (heat input, W m<sup>-2</sup>);  $r_s$  (stomatic resistance, s m<sup>-1</sup>);  $r_a$  (aerodynamic resistance, s m<sup>-1</sup>);  $s$  (Laplace transform parameter);  $t$  (time, s);  $T_c$  (crop temperature, K);  $T_a$  (adjustment coefficient);  $T_G$  (internal air temperature, K);  $T_g$  (ground temperature, K);  $T_i$  (adjustment coefficient);  $T_o$  (external air temperature, K);  $T_r$  (roof temperature, K);  $u(t)$  (process input);  $U(s)$  (Laplace input representation);  $V_i$  (greenhouse air to soil area rate, m<sup>3</sup> m<sup>-2</sup>);  $x_i$  (internal absolute humidity, kg m<sup>-3</sup>);  $x_g$  (soil absolute humidity, kg m<sup>-3</sup>);  $x_o$  (external absolute humidity, kg m<sup>-3</sup>);  $y(t)$  (process output);  $y_d(t)$  (setpoint or desired process output);  $\alpha_{ci}$  (convection heat transfer coefficient, W m<sup>-2</sup>). Greek letters:  $\gamma$  (thermodynamic constant, Pa K);  $\delta$  (leaf slope, Pa K);  $\phi_v$  (ventilation rate, m<sup>3</sup> s<sup>-1</sup>);  $\eta$  (radiation conversion factor);  $\lambda$  (water vaporization energy);  $\rho_a$  (air density, kg m<sup>-3</sup>). Superscripts: \* indicates that considered quantity is saturated at vapour pressure.

interest. This problem has been the focus of many researchers worldwide who have analyzed, experimented and proposed many climate control systems in order to manipulate variables such as temperature, relative humidity (RH), CO<sub>2</sub> enrichment, radiation and many others that are necessary to generate the fundamental conditions for successful protected agriculture.

Since most control theories require the mathematical model of the system for tuning and simulating the proposed algorithms, different greenhouse models have developed. It includes simple models that only describe air temperature to detailed models that even involve crop response. The traditional greenhouse climate models are based on energy and mass balances (Setiawan *et al.*, 2000).

A model based on aforementioned balances over an elementary volume of greenhouse air was proposed by Arvanitis *et al.* (2000). Here, air temperature is represented by a differential Eq. [1]:

$$\frac{dT_G}{dt} = \frac{1}{C} [K_{out, air}(T_o - T_G) + q_h] \quad [1]$$

where the  $T_G$  is the greenhouse internal air temperature,  $C$  the greenhouse thermal capacity,  $K_{out, air}$  is the heat loss coefficient from greenhouse air to outside air.  $T_o$  is the external air temperature and  $q_h$  is the heating power.

Recently, more detail models have been used for control proposes (Castañeda-Miranda *et al.*, 2006). Those models involve almost all variables that influence the greenhouse behavior.

$$C \frac{dT_G}{dt} = \eta G + \alpha_{ci} [A_r(T_r - T_G) + 2I_{La}(T_c - T_G) + (T_g - T_G)] - \rho_a C_p (T_G - T_o) + q_h \quad [2]$$

$$V_l \rho_a \frac{dx_i}{dt} = \frac{1}{\lambda} \left( \frac{2I_{La} \rho_a C_p}{\gamma(rs + ra)} \left[ \delta^* (T_c - T_G) + (e_i^* - e_i) \right] + \alpha_{ci} \frac{\lambda}{C_p} (x_g^* - x_i) \right) - \frac{\phi_v}{A_g} \rho_a (x_i - x_o) \quad [3]$$

In Eqs. [2] and [3],  $T_c$  is the crop temperature,  $T_g$  is the ground temperature,  $T_r$  is the roof temperature,  $x_i$  is the internal absolute humidity,  $x_o$  is the external absolute humidity,  $x_g$  is the soil absolute humidity,  $e_i$  is the internal mean vapour pressure,  $C_p$  is the air specific heat,  $V_l$  is the greenhouse air to soil area rate,  $A_g$  is the covered ground surface,  $A_r$  is the roof to soil rate,  $r_s$  is

the stomatic resistance,  $r_a$  is the aerodynamic resistance,  $G$  is the outside short-wave radiation,  $I_{La}$  is the leaf area index,  $\alpha_{ci}$  is the convection heat transfer coefficient,  $\delta$  is the leaf slope,  $\rho_a$  is the air density,  $\lambda$  is the water vaporization energy,  $\eta$  is the radiation conversion factor,  $\gamma$  is the thermodynamic constant,  $\phi_v$  is the ventilation rate and  $t$  is the time in  $s$ . The superscript \* indicates that consider quantity is at saturated vapour pressure.

Finally, models that consider greenhouse-crop interaction and complex processes such as photosynthesis or transpiration have been developed (Van Straten *et al.*, 2000). By this way, the greenhouse system can be represented concisely in a space state form as:

$$\dot{x}_g = f_g \{ q_{gm} \{ x_g, u_m, u_a \}, q_{ga} \{ x_g, u_m, u_a \}, q_{gb} \{ x_g, x_b, u_m \}, q_{gc} \{ x_g, x_c, u_a \} \} \quad [4]$$

$$\dot{x}_b = f_b \{ q_{gb} \{ x_g, x_b, u_m \} \} \quad [5]$$

$$\dot{x}_c = f_c \{ q_{gc} \{ x_g, x_c, u_a \}, q_{cc} \{ x_g, x_c \} \} \quad [6]$$

Here,  $f\{\}$ s represent vector functions of the argument between brackets;  $x_g, x_b, x_c$  are the state vector of the greenhouse ( $g$ ), the storage buffers (non-structural biomass) ( $b$ ) and the crop ( $c$ ), respectively;  $u_m, u_a$ , the vectors of the manipulated control ( $m$ ) and ambient ( $a$ ) inputs, respectively;  $q_{ga}, q_{gm}$ , flux vectors representing fluxes between the greenhouse and the ambient environment ( $ga$ ) and the operating equipment ( $gm$ ), respectively;  $q_{gb}, q_{gc}$ , fluxes between greenhouse and buffer ( $gb$ ) and between greenhouse environment and crop ( $gc$ ), respectively;  $q_{cc}$ , flux vectors related to the internal greenhouse conditions  $x_g$  and the crop states  $x_c$ , but not directly on the ambient conditions outside the greenhouse. The state list typically consist of temperature, moisture content and carbon dioxide for greenhouse atmosphere, temperatures for the storage buffers, and various crop biomass states for the plans in the greenhouse.

It is easy to find how models have been improved in response to production schemes that require more precisely methods to control the environment greenhouse.

In this section, an analysis and classification of the different control theories is presented. Establishing a division between the controllers presented in current literature is complicated, due to the variety and integration of diverse techniques used to solve the same problem. Fig. 1 shows a classification proposed dividing

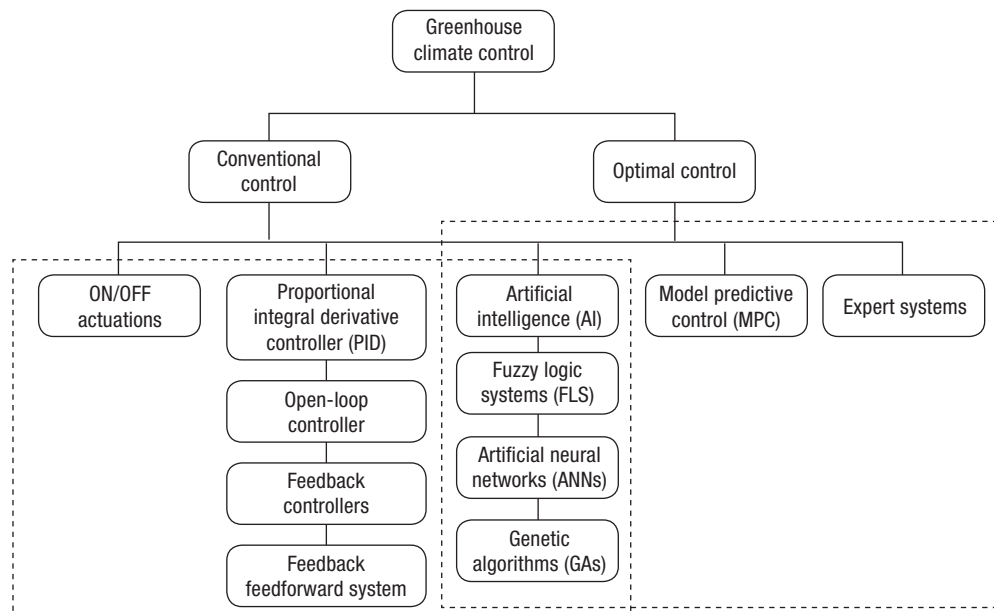


Figure 1. Greenhouse control theories classification.

greenhouse climate control task in two main fields. The first one is usually called conventional control which consists on control theories which try to control the greenhouse environment just by reducing the deviation between set points of the interest variables and measured values to zero. As examples of conventional control there are ON/OFF, PID, other classical controllers and also paradigms of AI such as ANNs, FLS, GAs, among others. The other field is optimal control, in which the requirement is to consider aspects such as greenhouse behavior, actuator capabilities, energy consumption and mainly crop response as input parameters of the control process. Here, Expert systems and Model Predictive Control (MPC) are the most common techniques. However, aforementioned AI-based techniques can be also considered as optimal control when they consider input parameters such as crop responses among others.

### Conventional greenhouse climate control

The most representative component of this theory is the PID (Ang *et al.*, 2005); which is a feedback mechanism commonly used in industrial control systems (Fig. 2). Therefore, it is necessary to explain each component and action of the PID controller.

— Proportional (P) control: In certain cases having a smooth control and an error that is almost zero in the

steady state is desired, where the proportional controller is suitable for this type of plant since that a proportional controller provides a control signal that is proportional to the error, that is, it returns its input multiplied by the proportional gain ( $K_p$ ), thus, the control signal is given as:

$$u(t) = K_p e(t) \quad [7]$$

$$e(t) = y_d(t) - y(t) \quad [8]$$

and the transfer function is obtained by means of the Laplace transform as:

$$\frac{U(s)}{E(s)} = K_p \quad [9]$$

— Integral action: When an integral action is implemented, the integral of the error is added to the control signal. If the error signal is large, then the control signal increases quickly, but if the error signal is small then the control signal increases slowly. It is remarkable that if the error approaches zero then the controller output would remain constant. Due to this feature, integral action can be used when a constant load is present in the plant; even when no error is present, the controller will keep on providing an output signal for compensation.

— Proportional integral (PI) control: Since a proportional control is not capable of compensating a load in the plant without error, the integral action is neces-

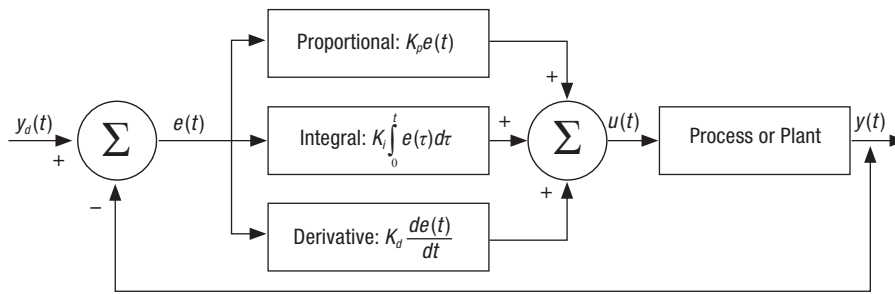


Figure 2. Block diagram of general PID controller.

sary. Integral action can compensate and provide a zero error; the PI controller is given as:

$$u(t) = K_p e(t) + K_i \int e(t) dt = K_p \left[ e(t) + \frac{1}{T_i} \int e(t) dt \right] \quad [10]$$

where  $T_i$  adjusts the integral action and  $K_p$  adjusts both the integral and proportional actions. Its transfer function is given as:

$$\frac{U(s)}{E(s)} = K_p + \frac{K_i}{s} = \frac{K_p s + K_i}{s} = \frac{K_p (T_i s + 1)}{T_i s} \quad [11]$$

$$T_i = \frac{K_p}{K_i} \quad [12]$$

— Proportional derivative (PD) control: The goal of a derivative controller is to provide a signal proportional to the signal error change rate, causing derivative action to be present only when there is a change in the error signal. In other words, the derivative action introduces damping to the system. The PD controller is given as:

$$u(t) = K_p e(t) + K_d \frac{de(t)}{dt} = K_p \left[ e(t) + T_d \frac{de(t)}{dt} \right] \quad [13]$$

and whose transfer function is:

$$\frac{U(s)}{E(s)} = K_p + K_d s = K_p (T_d s + 1) \quad [14]$$

$$T_d = \frac{K_d}{K_p} \quad [15]$$

— Proportional integral derivative (PID) control. By combining the three different control actions a PID controller is obtained by:

$$u(t) = K_p e(t) + K_i \int e(t) dt + K_d \frac{de(t)}{dt} \quad [16]$$

and whose transfer function is:

$$\frac{U(s)}{E(s)} = K_p \left( 1 + \frac{1}{T_i s} + T_d s \right) = K_p \left( \frac{T_i T_d s^2 + T_i s + 1}{T_i s} \right) \quad [17]$$

The PID controller is the most complete controller available and the most resorted to since it provides a quick response, a control signal that tends to provide stability to the system and a minimum steady state error. The PID controller is an important control tool for industrial processes and only three gains have to be tuned (Ogata, 2003; Dorf & Bishop, 2005).

Although the PID is the most utilized controller in industry and it is widely accepted for agricultural applications, it is not the only solution for agricultural problems. Occasionally it is not a good choice due to the absence of a reliable mathematical model within the system. Taking this into account, a climate control system based in ON/OFF operation has been proposed when the mathematical model is unknown, and this complicates the tuning of the controllers. It manages the times when actuators are turned on, and prevents external climatic changes issues based on recorded data (Ali & Abdalla, 1993). The aforementioned technique was studied by Hooper & Davis (1988), who implemented a controller based in an algorithm that modifies the greenhouse heating setpoints depending on previously achieved temperatures. This technique has shown good performance managing deviations in the setpoints through soft changes. Hooper (1988) also presented an integral greenhouse climate control by applying a mixture of controllers, a PI controller applied in heating and ventilation, and ON/OFF control applied for irrigation, pH, electrical conductivity and nutrients management. However, Setiawan *et al.* (2000) reported that a Pseudo-Derivative-Feedback (PDF) control presents better performance than a PI for agricultural application, due to the fact that PDF controls have better load handling capability than PI controls. PDF control was

better than PI for systems without time delay and significantly better for systems with time delay.

It is easy to find current investigative work regarding the field of greenhouse microclimate control; however, reported results reveal that aforementioned techniques are not the most adequate to solve the problems inherent in greenhouses. The reason lies in the fact that the model of a greenhouse is very complex and it has many non-linearities; consequently, this has encouraged the development of new control techniques that do not require the greenhouse mathematical model (Sigrimis *et al.*, 2002).

In the past, the application of new and advanced techniques for control was limited because of the limited computational power that was then available. Controllers based on FLS, ANNs or GAs could not be implemented in the former technological platforms due to their high complexity. These unconventional techniques based on soft computing and computational intelligence are now gaining popularity in the field of agriculture. Several soft-computing, such as ANNs and knowledge-based systems have been implemented with significant success (Soto-Zarazua *et al.*, 2010).

FLS controllers are conceptually very simple; they consist of an input stage, a processing stage and an output stage. The first stage maps sensors and other inputs to the appropriate membership functions and truth values. The processing stage invokes the appropriate rules and generates a result for each. Finally, the output stage converts the combined results into a specific control output value. Furthermore, ANNs is a knowledge paradigm and automatic processing system that attempts to imitate how the nervous system of animals works. The principal advantage of this technique is that it does not require a model of the system. The system is composed of neurons with propagation, activation, and transfer functions that are interconnected among them in an effort to reduce the error to zero. GAs is a heuristic research that mimics the process of natural evolution. This heuristic is routinely utilized to generate solutions to optimization and search problems. GAs generate solutions to optimize problems using techniques inspired by natural evolution such as inheritance, mutation, selection and crossover.

The relatively new field of evolutionary computing has become increasingly popular in recent years due to the development of powerful and low-cost computational systems. Because AI based systems have been updated and improved, these techniques solve the main problem of classic controls that being the identification

of the system which is commonly nonlinear (Caponetto *et al.*, 2002).

The classical solutions proposed are generally based on the linearization of the process behavior regarding the operating points. Other research has been carried out on this technique of linearization, not only dealing with the operating points, but also by taking into consideration all the input-output space to obtain several local linear models. The major difficulty with this technique is the model transition. Indeed, many techniques of modeling and identification based on FLS are often used for these types of systems (Trabelsi *et al.*, 2007). Some controllers base their operation on the aforementioned paradigm, as proposed by Castañeda-Miranda *et al.* (2006) who implemented a FLS on a field programmable gate array (FPGA) to control the temperature of the greenhouse microclimate or Kurata & Eguchi (1990) who applied this theory in crop management for protected agriculture.

Other systems which are classified in AI techniques are knowledge-based systems, as the one proposed by Gauthier & Guay (1990) which manages the climate control and production. This system supports dynamic optimization and continuous greenhouse monitoring. The proposed prototype was designed using object-oriented programming, obtaining good performance in the problem area. These expert-systems have proven to be a reliable alternative in greenhouse control applications. Jacobson *et al.* (1989) reported an expert system to control misting. This system was based on a strategy of an experienced grower. Gauthier (1992) reported changes to this scheme in a system that supports various types of digital process controllers as well as the creation and deployment of knowledge based control strategies with the goal of being able to intervene in a wide number of areas such as crop protection, climate control, crop nutrition, operational and strategic planning. This scheme received additional improvements such as changing the heuristic knowledge of the growers for data routinely collected in a commercial greenhouse (Seginer *et al.*, 1996).

Fuzzy systems achieved important results in the field of climate control for protected agriculture. Moreover, it is necessary to have reliable information of the system behavior, and that is not sufficient with this requirement a correct abstraction to create rules based in heuristic and empiric knowledge of the grower's experience is also necessary.

ANNs have proven their strengths and flexibility to adapt to non-linearities and unexpected parameters of



the system. Their main disadvantage is that their proper training requires large multi-dimensional sets of data to reduce the risk of extrapolation and the uncertainty about their response to inputs which differ in relation to the training information. Therefore, minimizing the dimensionality of the problem, both input and state vectors become of paramount importance (Seginer, 1997).

GAs as FLS and ANNs offer the ability to control the system with a good performance without the requirement to base their operation on plant identification of the system. Although GAs represents a solution in the control of nonlinear systems, the computational requirements have limited its use *in situ* applications until recently. The final conclusion is that the use of AI based systems is justified in control problems where the system plant is highly nonlinear or when the model is not reliable or has not been identified.

Each control technique offers solutions for specific problems. Unfortunately, a specific controller that deals with the different characteristics and limitations presented in highly non-linear and complex systems of greenhouse microclimate has not yet been found. Consequently, hybrid models which combine different control schemes have begun to appear.

Combinations of classical control theory with AI and considerations of crop process have been demonstrated as promising. A demonstration of this was reported by Pinon *et al.* (2005); he proposed a scheme for greenhouse temperature control using the advantages of combining Feedback Linearization (FL) and standard linear MPC. The discussed hybrid control structure, MPC + FL, offers a reliable solution of nonlinear control problems, transforming a non-linear greenhouse system subject to input constraints, to an optimized problem for a linear greenhouse system.

## Optimal control

The advantages of using optimal instead of conventional greenhouse climate control can be summarized as follows. An optimal control approach to greenhouse climate control fully exploits scientific quantitative knowledge concerning the greenhouse, the greenhouse equipment and the crop, captured all in a mathematical dynamic model that deals with the problem of maximizing the profit, achieving welfare of the crop through practices that minimizes production costs (Van Straten *et al.*, 2011).

In this section, climate controllers based on complex algorithms are discussed. An analysis of MPC, real time controllers, robust and non-linear control, feed-forward and systems that take into consideration decision support tools to gain efficient temperature integration are presented. Also, a survey of reported methods that considers morphological and physiological characteristics of the crops is presented.

The need of guarantee yield and quality of greenhouse crops has demanded stricter control of plant climate; previously, controllers were utilized for the sole purpose of adjusting the microclimate variables, but with recently increasing costs of energy, an appropriate controller that also considers the energy consumptions is necessary. One example of this was reported by Nielsen (1995) who presented a computer algorithm design to distribute the energy demands of greenhouses, reducing the peaks presented in the actuator in the day-to-night and night-to-day transitions. Other authors, proposed more complex systems (Arvanitis *et al.*, 2000; Davis & Hooper, 2002). These methods operate by considering that greenhouse parameters vary with operating conditions and applied a new pole-placement scheme. It estimates the unknown parameters of the greenhouse on-line from sequential data of the greenhouse temperature and the heating power which is recursively updated to obtain a slightly soft control.

Sigrimis & Rerras (1996) reported a controller based on a linear model structure to track and predict greenhouse behavior as a Multiple-Input-Multiple-Output (MIMO) system. This method takes into consideration disturbances like uncontrollable inputs. Climate controllers systems have been improved in order to consider external disturbances and have the ability to compensate for them; even they take into account plant responses such as crop growth. Reports regarding feed-forward controllers indicate that they are reliable and achieve good performance for greenhouse heating (Jewett & Short, 1992; Takakura *et al.*, 1994). On the other hand, real time systems have also been utilized in greenhouse applications, improving the systems to the point where operator intervention is only required to define the constraints of the heating setpoints.

Another real-time control algorithm for generating optimal heating setpoints was presented by Chalabi *et al.* (1996). This method adjusts greenhouse temperature setpoints over a period of time to achieve energy savings for a tomato crop, justifying these control actions by using the results of physiological stud-

ies showing that for some crops it is sufficient to maintain an average temperature in a greenhouse over a given period (Hurd & Graves, 1983; De Koning, 1990). The algorithm is based on a model of greenhouse energy requirements and on a numerical method for optimization, where the optimal control problem is converted into a non-linear programming problem solved by sequential quadratic programming.

AI was also applied combined with crop process knowledge to generate paradigms applied in protected agriculture. Fitz-Rodríguez & Giacomelli (2009) made use of FLS combined with ANNs to propose a better control strategy for agriculture under greenhouse conditions taking into account models of crop growth. However, one disadvantage of ANNs is that, it requires getting a considerable set of data to train the net. This problem was addressed by Linker *et al.* (1998) using previously acquired data over a two-month period in a commercial greenhouse to train the net. The resulting model not only fit with data, it also seemed qualitatively correct and produced reasonable optimization results in a scheme of CO<sub>2</sub> enrichment control.

Hybrid controllers which fuse FLS and GAs were presented by Goggos & King (2000) in a research project that applies qualitative reasoning and evolutionary computing in the design of optimal set points and control strategies for greenhouses. This fusion of different intelligent control techniques was also applied in an intelligent environment control for plant production systems. The author used a decision-marking system based on ANNs and GAs in order to optimize plant growth under hydroponics conditions and also identified the response of plant growth to the nutrient concentration (Hashimoto *et al.*, 2002).

One of the main problems with climate control is the greenhouse dynamic model which is highly non-linear. Consequently, many researchers have applied simplified models for the non-linear problem, such as Ioslovich *et al.* (1996), who designed a controller based on a simplified model of the crop growth with constraints on the control signals. The objective of this optimization was to take into account the cost of energy used by heating and ventilation systems.

When it is necessary to control non-linear systems where the plant model is unknown, the use of feedback-feedforward control is an alternative. In this configuration, unexpected events are considered in the control model and the controller attempts to reduce the error to zero no matter the disturbances. These system characteristics were used to design a non-linear controller

for coupled air temperature and humidity (Albright *et al.*, 2002). A feedback-feedforward combination was also used by Pasgianos *et al.* (2003) in a system linearization and decoupling of a greenhouse, maintaining control of ventilation/cooling and moisture. This technique also served to compensate for external disturbances. Finally, the controller was designed to consider the actuators capabilities and saturation setpoints.

In this section, applied strategies in climate controller systems with the objective of saving energy are considered. Nevertheless control techniques that consider physiological plant processes are also studied and described in this section.

Horticultural research has indicated that for the majority of plants, crop growth responds to long-term average temperatures rather than specific day and night temperature profiles (Langhans *et al.*, 1980; Miller *et al.*, 1985). Based on this research it has been suggested that the heating set-point can be adjusted to ensure that a desired average temperature over a given period can be achieved and thereby energy savings obtained. This knowledge was applied by Sigrimis & King (2000) in the design of a tool available to exploit the interaction between photosynthesis and growth according to the intuition of the grower because this interaction is not well known for most plants. The method is based on varying heating set-points using previously recorded information in order to achieve the desired average for any user-defined period. The proposed system does not require weather information and the grower can also set safety limits as the ultimate minimum and maximum temperatures permitted.

These control schemes were exploited by authors like Gauthier *et al.* (1995), who presented control strategies applied in heat, cool and dry greenhouse air, and also in the regulation of CO<sub>2</sub>, light and irrigation. Considering that plant processes vary with the day and vegetative state of the plant, they do not require strict control of the microclimate all the time. With this in mind, temperature integration systems for greenhouse cultivation were developed by Körner & Challa (2003a). The concept considers different crop processes, and a decoupled process with fast temperature response (*e.g.* photosynthesis or stress) from a process with a slow response time. The objective was to improve the temperature integration concept by introducing dynamic temperature constraints; these flexible boundaries depend on the underlying crop process while increasing the potential for energy saving in greenhouses.

A different approach was proposed with a decision support tool that assists in choosing the most appropriate climate according to the week of the year in order to obtain the optimal gains of sustainability and plant quality. The greenhouse climate and crop model are studied separately and jointly considering the effects of six different regimes with increasing degrees of freedom for various climate variables (Körner & Van Straten, 2008) which include: crop model, temperature integration, dynamic humidity control and negative DIF regimes (DIF = the difference between average day temperature and average night temperature, and therefore reduces the use of chemical growth regulators).

MPC is an advanced control technique applied in the field of protected agriculture. The objective was to predict the greenhouse variables behavior. Developments in MPC algorithms for greenhouse operation which takes into account weather predictions to generate new optimal control problems for each update of forecasted weather information as solved numerically by linear programming were also developed (Gutman *et al.*, 1993). A contribution to this scheme was offered by Van Straten *et al.* (2000) where information about crop growth simplifies the design of greenhouse control strategies to obtain a truly economical control strategy. This approach leads to the concept of selecting processes by time response where the short-term effects like photosynthesis and evapo-transpiration are dealt with by an automated model-predictive optimal controller, while the long-term effects are left to the grower.

Aiming energy saving proposes, MPC algorithm has seen advances that take into account constraints in both manipulated and controlled variables, using on-line linearization for a real-time application. This proposal was applied in greenhouse temperature regulation, achieving good performance and energy savings. The results were compared with a PID solution. MPC based controllers solve the problems commonly presented in PID systems (El Ghoumari *et al.*, 2005). Due to the advantages presented by MPC, different strategies have been applied to design optimal MPC controllers. The Particle Swarm Optimization (PSO) was applied to design a model-based predictive greenhouse air temperature controller subject to restrictions; the model employs data from the climate inside and outside the greenhouse, as well as the control inputs and controller outputs. The operation principle ensures set-point tracking and minimizes control efforts. The conclusions presented show better efficiency over GAs and sequential quadratic programming methods (Coelho *et al.*, 2005).

MPC with GAs facilitating the incorporation of energy and water consumption to adjust non-linear models parameters have been suggested. The combination of MPC and GAs permits the control of the greenhouse microclimate while achieving energy and water savings (Blasco *et al.*, 2007). GAs in annealing form (AGAs) has also been applied for calibrating classical controllers such as PID, where the AGAs play a role in the parameter identification, demonstrating advantages over traditional GAs like premature convergence and low computing efficiency that are required to implement these (Fan & Zuo-hua, 2006). Feed-forward neural networks have been applied in conjunction with simple neural models to drive the system outputs to desired values (Fourati & Chtourou, 2007).

Robust control also contributed to systems in protected agriculture because of its ability to deal with uncertain parameters, disturbances or modeling errors. It was applied focusing on managing the high correlations between air temperature and hygrometry (Bennis *et al.*, 2008). Different methods have been applied attempting to find a reliable optimal control solution for greenhouse environment, utilizing concepts from advance sequential control search (SCS) or Pontryagin's maximum principle (PMP)(Seginer & McClendon, 1992), to systems that consider the crop model and its effects on greenhouse behavior (Jones *et al.*, 1990). The objective of these approaches was to include weather and greenhouse-crop characteristics such as ventilation and stomatal resistance in the control actions (Baptista *et al.*, 2010). Humidity control regimes were also proposed by using information about the vegetative state of the plant (Körner & Challa, 2003b).

Authors worldwide have dedicated time and substantial effort to develop not only control systems, but they have also been working to create strategies to ensure reliable measurements through the use of filters and signal processing techniques to guarantee good performance of controller systems (Ibrahim & Sørensen, 2010).

One of the main objectives of the aforementioned developments is energy savings; however, all require knowledge of plant processes which is limited and usually empiric or heuristic. Consequently, advanced smart sensors are being developed in order to measure crop specific characteristics such as plant transpiration dynamics and photosynthesis in order to understand how physiological processes occur in the plants and how they affect and modify their surroundings (Millan-Almaraz *et al.*, 2010).

Throughout this review, special attention has been directed to demonstrate that not only the controller is necessary to guarantee appropriate microclimate conditions, but a fundamental part of the design is the use of reliable systems which take into consideration the importance of failure detection tools. By applying a hybrid of physical/neural network models with robust failure detection, failures are correctly detected and identified, leading to a significant reduction of losses caused by failures (Linker *et al.*, 2000).

## Technological platforms applied on climate control theories implementation

Technological platforms are also important when a system is being developed to solve specific problems; protected agriculture is not an exception to this rule. Agronomy field imposed hard operating conditions and found it is necessary to strictly consider these restrictions. Despite the fact that greenhouse climate is not a fast response system, robust platforms that guarantee uninterrupted operation are required, flexibility is crucial to improve changes in the system in order to solve emerging needs and lower cost is also necessary to ensure success of a newly emerging crop production industry (Fang & Zhen-xiao, 2008).

The first and most popular platform chosen for greenhouse control applications has been the personal computer (PC). The use of PCs in greenhouse operations has created possibilities to implement complex algorithms that were impossible to apply in the past (Fang & Zhen-xiao, 2008). Consequently, the integration of new task modules, sensor and communication devices becomes easier (Ali & Abdalla, 1993). Different configurations of PCs and networks have been proposed to achieve more efficient greenhouse management (Hooper, 1988).

Commercial climate control computers and proprietary data-logger were also applied (Nielsen, 1995; Linker *et al.*, 1998). These systems offer solutions for protected agriculture problems. However, PCs are not the most appropriate platforms for heavy duty field applications, and are characterized to be a noisy and harsh environment with high humidity rates that are subject to constant temperature changes. Consequently, PCs are susceptible to failures and damage caused by the greenhouse harsh environment. Another consideration when discussing the use of PCs is the high cost

to integrate PC networks or property systems. Other technological platforms should be proposed to ensure reliable sustainability. Microcontroller and Digital Signal Processors (DSP) based systems have attempted to solve the aforementioned problems with promising results; however, their limited capacities have proven to be difficult in the application of advanced algorithms with considerable computational demands (Coelho *et al.*, 2005).

The development of embedded systems for a particular application has been demonstrated to be the best choice for industrial applications. This idea was translated into precision agriculture field, designing platforms that consider hardware requirements and the conditions where the system will be placed to ensure robustness in the operation and low cost for the developed embedded platform. Field Programmable Gate Arrays (FPGAs) have been demonstrated to be a solution with a high performance, flexibility and robustness for greenhouse embedded applications (Castañeda-Miranda *et al.*, 2006).

## New tendencies on greenhouse climate control systems

This review clearly shows that there is a tendency to utilize climate controllers for protected agriculture applications where these are based on very simple control theories, like ON/OFF, PID controllers or some variation thereof. This tendency has been caused by the low computational power availability in the past. Consequently, the control was limited to basic operations and real-time processing was unreachable because of the absence of adequate processing devices. Because of this, recent mathematical algorithms and control theories evolved faster than computing technologies. Consequently, complex algorithms were not available to be implemented in any technological platforms at affordable cost a few years ago.

This scenario changed when computers cost decreased and the processing capabilities became considerably higher, at least to the point to make it possible to implement complex algorithms. Soon thereafter, modern control theories based on real-time control process, adaptive schemes or intelligent techniques were applied in order to achieve a more accurate, efficient and strict manipulation of the interest greenhouse variables. Considerations regarding quality, yield, water and energy savings were also studied and

integrated in the control models (Vazquez-Cruz *et al.*, 2010). These low cost platforms also make it possible to design and implement sensor networks, mobile robots for agricultural proposes, image processing for early diseases and pest detection as well as many other contributions to agriculture (Sigrimis *et al.*, 2000; Contreras-Medina *et al.*, 2009).

Despite the excellent results obtained with the high performances low cost computers, and advanced algorithms, tendencies are changing again; recently investigations and reports lead to the development of controllers which also consider plant physiology and morphology. Phenomena such as transpiration and photosynthesis have been studied for better understanding of plant behaviors in order to control climatic and nutritional requirements, according with real plant needs. New energy savings strategies have been proposed considering the available information regarding plant processes, manipulating climatic conditions when it is necessary for plant growth and the establishment of adaptive operating ranges for actuators with more degrees of freedom where strategies are helpful and when the reduction of energy consumption is essential. Nevertheless, the information about plant processes is limited. More investigation is necessary to establish correlations between physiological processes and plant growth in regards to temperature, humidity, nutrition and others controllable variables of the greenhouse, with the objective of reaching a sustainable protected agriculture industry (Millan-Almaraz *et al.*, 2009).

## Conclusions

Greenhouse climate control is currently one of the main objectives of engineering in precision agriculture. Temperature and humidity are variables which have a direct relationship with the plant production. Moreover, recent investigations have shown that is not enough to adjust temperature and humidity ratings to maximum and minimum setpoints which are affordable for plant needs. Because of this, many control theories have emerged along the years such as conventional control techniques and optimal control. Conventional control is based mainly on the proportional-integral-derivative controller and some variants. Furthermore, optimal control techniques relies mainly on AI algorithms and adaptive control theory which proposes an alternative way to solve the climate control problem when green-

house mathematical model is unknown or often very complex. Another important fact which has limited the development of more advanced climate control system was the technological limitations a few years ago. However, the relatively new computational technologies such as microprocessors, digital signal processors and field programmable gate arrays are allowing continuing the implementation of more sophisticated control systems. According to some authors, the application of advanced controllers capable of following specific variable setpoints has not yet proven to be an optimal solution. Because of this, new tendencies are appearing in greenhouse climate control based on gathering extra information about physiological and morphological processes on the plant such and transpiration, stomata conductance and photosynthesis. These new control theories report that it is not necessary to have strict temperature and humidity set points. Instead of this, more flexible thresholds are proposed to save unnecessary energy consumption which is consumed when controller tries to follow the set point in a strict way. Phytocontrol is the new theory which proposes the use of the plant physiological responses as input sensor to establish the set point in the climate controller. Also, this has not proved to be a stable and reliable method, because it is necessary to gather a lot of information to prove the reliability of this. Nevertheless, different types of controllers have emerged demonstrating advantages and disadvantages between them, better performance for some actions among other characteristics. Researchers need to analyze different control theories to determine which one is the most proper for their projects according to their specific requirements of greenhouse climate control systems.

## Acknowledgement

This project was partially supported by CONACYT scholarship 231946. The author wish to thank Silvia C. Stroet of the Engineering Faculty at Universidad Autónoma de Querétaro for reviewing the English content of this article.

## References

- Albright LD, Arvanitis KG, Drysdale AE, 2002. Environmental control for plants on earth and in space. Control Systems Magazine IEEE 21(5): 28-47.

- Ali IA, Abdalla AM, 1993. A microcomputer-based system for all-year-round temperature control in greenhouses in dry arid lands. *Comput Electron Agr* 8(3): 195-210.
- Ang KH, Chong G, Li Y, 2005. PID control system analysis, design, and technology. *IEEE T Contr Syst T* 13(4): 559-576.
- Arvanitis KG, Paraskevopoulos PN, Vernardos AA, 2000. Multirate adaptive temperature control of greenhouses. *Comput Electron Agr* 26(3): 303-320.
- Baptista FJ, Bailey BJ, Meneses JF, Navas LM, 2010. Greenhouses climate modelling. Tests, adaptation and validation of a dynamic climate model. *Span J Agric Res* 8(2): 285-298.
- Bennis N, Duplax J, Enéa G, Haloua M, Youlal H, 2008. Greenhouse climate modeling and robust control. *Comput Electron Agr* 61(2): 96-107.
- Blasco X, Martínez M, Herrero JM, Ramos C, Sanchis J, 2007. Model-based predictive control of greenhouse climate for reducing energy and water consumption. *Comput Electron Agr* 55(1): 49-70.
- Caponetto R, Fortuna L, Nunnari G, Occhipinti L, Xibilia MG, 2002. Soft computing for greenhouse climate control. *IEEE T Fuzzy Syst* 8(6): 753-760.
- Castañeda-Miranda R, Ventura-Ramos E, Peniche-Vera RR, Herrera-Ruiz G, 2006. Fuzzy greenhouse climate control system based on a field programmable gate array. *Biosyst Eng* 94(2): 165-177.
- Chalabi ZS, Bailey BJ, Wilkinson DJ, 1996. A real-time optimal control algorithm for greenhouse heating. *Comput Electron Agr* 15(1): 1-13.
- Coelho JP, De Moura Oliveira PB, Boaventura Cunha J, 2005. Greenhouse air temperature predictive control using the particle swarm optimisation algorithm. *Comput Electron Agr* 49(3): 330-344.
- Contreras-Medina LM, Torres-Pacheco I, Guevara-Gonzalez RG, Romero-Troncoso RJ, Terol-Villalobos IR, Osornio-Rios RA, 2009. Mathematical modeling tendencies in plant pathology. *Afr J Biotechnol* 8(25): 7391-7400.
- Davis PF, Hooper AW, 2002. Improvement of greenhouse heating control. In: *Control theory and applications, IEE Proceedings D* 138, IET: 249-255.
- De Baerdemaeker J, Munack A, Ramon H, Speckmann H, 2002. Mechatronic systems, communication, and control in precision agriculture. *Control Systems Magazine, IEEE*, 21(5): 48-70.
- De Koning ANM, 1990. Long-term temperature integration of tomato. Growth and development under alternating temperature regimes. *Sci Hortic* 45(1-2): 117-127.
- Dorf RC, Bishop RH, 2005. *Sistemas de control moderno*. Pearson Education, Madrid, 882 pp.
- El Ghomari MY, Tantau HJ, Serrano J, 2005. Non-linear constrained MPC: Real-time implementation of greenhouse air temperature control. *Comput Electron Agr* 49(3): 345-356.
- Fan X, Zuo-Hua T, 2006. Application of a genetic simulated annealing algorithm in the greenhouse system. *Computer Simulation* 12: 045.
- Fang L, Zhen-Xiao L, 2008. Research on the control mode of agriculture greenhouse control system in China. *J Agr Mechaniz Res* 10: 223-226.
- Fitz-Rodríguez E, Giacomelli GA, 2009. Yield prediction and growth mode characterization of greenhouse tomatoes with neural networks and fuzzy logic. *T ASABE* 52(6): 2115-2128.
- Fourati F, Chtourou M, 2007. A greenhouse control with feed-forward and recurrent neural networks. *Simul Model Pract Th* 15(8): 1016-1028.
- Gauthier L, 1992. A smalltalk-based platform for greenhouse environment control. Part I. Modeling and managing the physical system. *T ASABE* 35(6): 2003-2009.
- Gauthier L, Guay R, 1990. An object-oriented design for a greenhouse climate control system. *T ASABE* 33(3): 999-1004.
- Gauthier L, De Halleux D, Boisvert A, Trigui M, Zehrouni A, 1995. A control strategy for the operation of a reversible heat-pump in greenhouses. *Appl Eng Agr* 11(6): 873-879.
- Goggos V, King RE, 2000. Qualitative-evolutionary design of greenhouse environment control agents. *Comput Electron Agr* 26(3): 271-282.
- Gutman PO, Lindberg PO, Ioslovich I, Seginer I, 1993. A non-linear optimal greenhouse control problem solved by linear programming. *J Agr Eng Res* 55(4): 335-351.
- Hashimoto Y, Murase H, Morimoto T, Torii T, 2002. Intelligent systems for agriculture in Japan. *IEEE Contr Syst Mag* 21(5): 71-85.
- Hooper AW, 1988. Computer control of the environment in greenhouses. *Comput Electron Agr* 3(1): 11-27.
- Hooper AW, Davis PF, 1988. An algorithm for temperature compensation in a heated greenhouse. *Comput Electron Agr* 2(4): 251-262.
- Hurd RG, Graves CJ, 1983. The influence of different temperature patterns having the same integral on the earliness and yield of tomatoes. III *Int Symp on Energy in Protected Cultivation (ISHS)* 148: 547-554.
- Ibrahim IA, Sørensen CG, 2010. A more energy efficient controller for the greenhouses climate control system. *Appl Eng Agr* 25(3): 491-498.
- Ioslovich I, Gutman P, Linker R, 2009. Hamilton-Jacobi-Bellman formalism for optimal climate control of greenhouse crop. *Automatica* 45(5): 1227-1231.
- Ioslovich I, Gutman P, Seginer I, 1996. A non-linear optimal greenhouse control problem with heating and ventilation. *Optim Contr Appl Met* 17(3): 157-169.
- Jacobson BK, Jones PH, Jones JW, Paramore JA, 1989. Real-time greenhouse monitoring and control with an expert system. *Comput Electron Agr* 3(4): 273-285.
- Jewett TJ, Short TH, 1992. Computer control of a five-stage greenhouse shading system. *T ASABE* 35(2): 651-658.

- Jones P, Jones JW, Hwang Y, 1990. Simulation for determining greenhouse temperature setpoints. *T ASABE* 33(5): 1722-1728.
- Körner O, Challa H, 2003a. Design for an improved temperature integration concept in greenhouse cultivation. *Comput Electron Agr* 39(1): 39-59.
- Körner O, Challa H, 2003b. Process-based humidity control regime for greenhouse crops. *Comput Electron Agr* 39(3): 173-192.
- Körner O, Van Straten G, 2008. Decision support for dynamic greenhouse climate control strategies. *Comput Electron Agr* 60(1): 18-30.
- Kurata K, Eguchi N, 1990. Machine learning of fuzzy rules for crop management in protected cultivation. *T ASAE* 33(4): 1360-1368.
- Langhans RW, Wolfe M, Albright LD, 1980. Use of average night temperatures for plant growth for potential energy savings. *Symposium on More Profitable Use of Energy in Protected Cultivation (ISHS)* 115: 31-38.
- Linker R, Seginer I, Gutman P, 1998. Optimal CO<sub>2</sub> control in a greenhouse modeled with neural networks. *Comput Electron Agr* 19(3): 289-310.
- Linker R, Gutman PO, Seginer I, 2000. Robust model-based failure detection and identification in greenhouses. *Comput Electron Agr* 26(3): 255-270.
- Millan-Almaraz J, Guevara-Gonzalez R, Romero-Troncoso R, Osornio-Rios R, Torres-Pacheco I, 2009. Advantages and disadvantages on photosynthesis measurement techniques: A review. *Afr J Biotechnol* 8(25): 8316-8331.
- Millan-Almaraz J, Romero-Troncoso R, Guevara-Gonzalez R, Contreras-Medina L, Carrillo-Serrano R, Osornio-Rios R, Duarte-Galvan C, Rios-Alcaraz M, Torres-Pacheco I, 2010. FPGA-based fused smart sensor for real-time plant-transpiration dynamic estimation. *Sensors* 10(9): 7340-7349.
- Miller WB, Albright LD, Langhans RW, 1985. Plant growth under averaged day/night temperatures. *Symposium Greenhouse Climate and its Control (ISHS)* 174: 313-320.
- Nielsen OF, 1995. Climate computer algorithms for peak shaving of greenhouse heating demand. *Comput Electron Agr* 13(4): 315-335.
- Ogata K, 2003. *Ingenieria de control moderna*. Pearson Education. Madrid, 894 pp.
- Pasgianos GD, Arvanitis KG, Polycarpou P, Sigrimis N, 2003. A nonlinear feedback technique for greenhouse environmental control. *Comput Electron Agr* 40(1-3): 153-177.
- Pinon S, Camacho EF, Kuchen B, Peña M, 2005. Constrained predictive control of a greenhouse. *Comput Electron Agr* 49(3): 317-329.
- Seginer I, 1997. Some artificial neural network applications to greenhouse environmental control. *Comput Electron Agr* 18(2-3): 167-186.
- Seginer I, McClendon RW, 1992. Methods for optimal control of the greenhouse environment. *T ASAE* 35(4): 1299-1307.
- Seginer I, Hwang Y, Boulard T, Jones JW, 1996. Mimicking and expert greenhouse grower with a neural-net policy. *T ASAE* 39(1): 299-306.
- Setiawan A, Albright LD, Phelan RM, 2000. Application of pseudo-derivative-feedback algorithm in greenhouse air temperature control. *Comput Electron Agr* 26(3): 283-302.
- Sigrimis N, Rerras N, 1996. A linear model for greenhouse control. *T ASABE* 39(1): 253-261.
- Sigrimis N, Anastasiou A, Rerras N, 2000. Energy saving in greenhouses using temperature integration: A simulation survey. *Comput Electron Agr* 26(3): 321-341.
- Sigrimis N, Antsaklis P, Groumpos PP, 2002. Advances in control of agriculture and the environment. *IEEE Contr Syst Mag* 21(5): 8-12.
- Sigrimis N, King RE, 2000. Advances in greenhouse environment control. *Comput Electron Agr* 26(3): 217-219.
- Soto-Zarazua GM, Rico-Garcia E, Ocampo R, Guevara-Gonzalez RG, Herrera-Ruiz G, 2010. Fuzzy-logic-based feeder system for intensive tilapia production (*Oreochromis niloticus*). *Aquacult Int* 18(3): 379-391.
- Takakura T, Manning TO, Giacomelli GA, Roberts WJ, 1994. Feedforward control for a floor heat greenhouse. *T ASABE* 37(3): 939-945.
- Trabelsi A, Lafont F, Kamoun M, Enea G, 2007. Fuzzy identification of a greenhouse. *Appl Soft Comput* 7(3): 1092-1101.
- Van Straten G, Challa H, Buwalda F, 2000. Towards user accepted optimal control of greenhouse climate. *Comput Electron Agr* 26(3): 221-238.
- Van Straten G, Van Willigenburg LG, Van Henten EJ, Van Ooteghem RJC, 2011. *Optimal control of greenhouse cultivation*. CRC Press, NY, USA.
- Vazquez-Cruz M, Torres-Pacheco I, Miranda-Lopez R, Cornejo-Perez O, Osornio-Rios AR, Guevara-Gonzalez R, 2010. Potential of mathematical modeling in fruit quality. *Afr J Biotechnol* 9(3): 260-267.

Article

## FPGA-Based Smart Sensor for Drought Stress Detection in Tomato Plants Using Novel Physiological Variables and Discrete Wavelet Transform

Carlos Duarte-Galvan <sup>1</sup>, Rene de J. Romero-Troncoso <sup>2</sup>, Irineo Torres-Pacheco <sup>1</sup>, Ramon G. Guevara-Gonzalez <sup>1</sup>, Arturo A. Fernandez-Jaramillo <sup>1</sup>, Luis M. Contreras-Medina <sup>1,2</sup>, Roberto V. Carrillo-Serrano <sup>3</sup> and Jesus R. Millan-Almaraz <sup>4,\*</sup>

<sup>1</sup> CA Ingeniería de Biosistemas, División de Investigación y Posgrado, Facultad de Ingeniería, Universidad Autónoma de Querétaro, Cerro de las Campanas s/n, Querétaro 76010, Qro., Mexico; E-Mails: cduarte20@alumnos.uaq.mx (C.D.-G.); irineo.torres@uaq.mx (I.T.-P.); ramon.guevara@uaq.mx (R.G.G.-G.); aafernandez@hspdigital.org (A.A.F.-J.); mcontreras@hspdigital.org (L.M.C.-M.)

<sup>2</sup> HSPdigital-CA Telemática, DICIS, Universidad de Guanajuato, Carr. Salamanca-Valle km 3.5+1.8, Palo Blanco, Salamanca 36885, Gto, Mexico; E-Mail: troncoso@hspdigital.org

<sup>3</sup> División de Investigación y Posgrado, Facultad de Ingeniería, Universidad Autónoma de Querétaro, Cerro de las Campanas s/n, Querétaro 76010, Qro., Mexico; E-Mail: roberto.carrillo@uaq.mx

<sup>4</sup> Facultad de Ciencias Físico-Matemáticas, Universidad Autónoma de Sinaloa, Av. De las Américas y Blvd. Universitario, Cd. Universitaria, Culiacán 80000, Sinaloa, Mexico

\* Author to whom correspondence should be addressed; E-Mail: jrmillan@uas.edu.mx; Tel.: +52-667-716-1154 (ext. 117).

External Editor: Gonzalo Pajares Martinsanz

Received: 18 June 2014; in revised form: 9 September 2014 / Accepted: 10 September 2014 /

Published: 9 October 2014

---

**Abstract:** Soil drought represents one of the most dangerous stresses for plants. It impacts the yield and quality of crops, and if it remains undetected for a long time, the entire crop could be lost. However, for some plants a certain amount of drought stress improves specific characteristics. In such cases, a device capable of detecting and quantifying the impact of drought stress in plants is desirable. This article focuses on testing if the monitoring of physiological process through a gas exchange methodology provides enough information to detect drought stress conditions in plants. The experiment consists of using a set of smart sensors based on Field Programmable Gate Arrays (FPGAs) to monitor a



group of plants under controlled drought conditions. The main objective was to use different digital signal processing techniques such as the Discrete Wavelet Transform (DWT) to explore the response of plant physiological processes to drought. Also, an index-based methodology was utilized to compensate the spatial variation inside the greenhouse. As a result, differences between treatments were determined to be independent of climate variations inside the greenhouse. Finally, after using the DWT as digital filter, results demonstrated that the proposed system is capable to reject high frequency noise and to detect drought conditions.

**Keywords:** drought detection; smart sensor; transpiration dynamic; photosynthesis measurement; plant water stress monitoring

---

## 1. Introduction

Plant stress is any factor that promotes unfavorable growing conditions on plants. Soil drought is an environmental stress that affects crop productivity more than any other factor. Current monitoring devices for precision agriculture usually take into account climatic variables. However, it is desirable to have tools that provide information about plant health in order to explore responses under unfavorable conditions.

The main responses of plants under drought are photosynthetic dysfunction and overproduction of Reactive Oxygen Species (ROS) that are highly reactive and deteriorate the normal plant metabolism through oxidative damage of plant macromolecules [1]. These effects are cumulative; depend on the crop growth stage and the severity and frequency of the drought event. Fortunately, plants have several resistance mechanisms to survive under drought conditions; these range going from morphological to biochemical adaptations at subcellular, cellular, and organ level [2]. The disadvantage of such survival strategies is that they rely on limited plant development and low yield. However, the study of those mechanisms allows the development of strategies to increase drought tolerance without losing productivity, for example: crop varieties associated with high yield can be targeted in breeding programs to induce drought tolerance. Biotechnology research has made it possible to identify and change drought-responsive genes inducing some desired qualitative and quantitative traits. Finally, the exogenous application of plant growth regulators (PGR) have proven to enhance drought tolerance in plants [3]. Concluding, the impact of drought on agricultural practices and the requirements to maintain a constant improvement of drought resistant varieties makes the development of technological tools to detect and monitor drought in plants imperative.

Different methodologies have been proposed for early detection of drought stress in plants. The predominant tendency is to use thermography and hyperspectral vision [4]. Other methods use impedance, thermal or gas exchange principles. The thermography utilizes infrared thermometer sensors or thermal cameras to measure the canopy temperature ( $T_c$ ) and to define crop water stress indexes [5,6]. However,  $T_c$  measurement presents low resolution and it is susceptible to meteorological conditions and foliage geometric structure such as leaf angles [7]. On the other hand, hyperspectral analysis consists of monitoring changes in the chlorophyll fluorescence or in photochemical

reflectance. The problem with chlorophyll fluorescence analysis is that it requires a dark chamber to isolate a plant sample [8,9]. In this manner, the chlorophyll fluorescence response may occur as variations in magnitude or phase [4,10]. Monitoring reflectance has been applied to study entire crops; several wavelengths have been explored to find better responses and relations with current state of the crops. 705–750 nm was determined to be a suitable wavelength range to be used to explore plant response to water stress [11]. The aforementioned results have been supported by many researchers who have proposed different indexes to detect and even measure the effects of drought [12,13]. Though, the performance of hyperspectral imaging is critically affected by ambient illumination changes [11], it requires successive monitoring of plants [14], the image acquisition is complicated where drones or satellites are required [15,16].

Limitations to identify small variations in water stress could be solved using plant-based sensors. In this manner a simple sensor mounted on the leaf could measure variations in the temperature gradient according to the water content of the plant [17]. Electrical impedance spectroscopy is robust to environmental noise and has higher sensitivity than hyperspectral imaging; it has been proven to detect water stress, even environmental changes and nutrient deficit. However, additional studies are necessary to understand the environmental effects on plant impedance [18,19].

Gas exchange systems constitute the basis of most photosynthesis measurement tools. This consists of using Infrared Gas Analyzer (IRGA)-based carbon dioxide (CO<sub>2</sub>) sensors to measure the difference between ambient CO<sub>2</sub> concentration and the concentration in a transparent chamber where a plant leaf is isolated [20]. These tools also estimate important phenomena such as transpiration and stomatal conductance [21,22]. Despite the fact that CO<sub>2</sub> exchange method is more sensitive than fluorescence techniques to environmental changes; a higher amount of information related to plant physiology can be obtained [23].

The objective of this article is the development of a novel smart sensor that performs a new signal processing methodology to minimize the noise in a photosynthesis measurement system which is based on CO<sub>2</sub> exchange method. Furthermore, the proposed system is utilized to detect and monitor the effects of soil drought in tomato plants. The signal processing methodology combines average decimation and Kalman filters to improve signal quality, and an additional filtering stage based on Discrete Wavelet Transform (DWT) to explore plants signal response. Therefore, short and long-term novel indexes were proposed to provide a set of information regarding the response of plants to drought.

The smart sensor was implemented in a FPGA due to its parallel computation capabilities and flexible configurability. It made possible to implement the aforementioned algorithms to calculate *in-situ* and in *real-time* the physiological processes of plants for decision making, data storing and off-line processing purposes. In order to validate the drought detection capabilities of the developed smart sensor, an experimental setup was carried out using tomato plants in a greenhouse. Because of this, three smart sensors controlled by a coordinator were installed to monitor specific groups of plants subjected to induced drought conditions. Finally, interesting relations between drought and plant physiological responses were obtained.

## 2. Background

### 2.1. Plant Transpiration, Photosynthesis Dynamics and Drought

Photosynthesis and transpiration are two of main physiological processes in plants. Photosynthesis is a process performed by plants and other organisms to convert light into chemical energy that can later be released to fuel the organism activities. More specifically, light energy drives the synthesis of carbohydrates from carbon dioxide and water with the generation of oxygen ( $O_2$ ). On the other hand, transpiration is an important component of temperature regulation because plants can dissipate the heat input from sunlight through phase exchange of water that escape into the atmosphere. This process controls the water movement through the plant and the evaporation from aerial parts, especially from the leaves [24]. Leaf surfaces contain pores called stomata; the aperture of these pores is conducted by guard cells. Through the stomata, plants exchange moisture with the atmosphere and permit the diffusion of  $CO_2$ ; transpiration also changes osmotic pressure of cells and enables the flow of mineral nutrients and water from roots to shoots. Since both processes share the same pathways, carbon assimilation carries a loss of water to the atmosphere through the stomata. Consequently, effects of drought over both physiological processes are closely related with parameters that have been previously stated [25].

Plant responses to soil drought can change according to the severity and frequency of the stress and the effects over physiological process does not occur immediately and linearly. Therefore, the severity of the stress and plant responses to drought can be summarized in three phases. Phase 1: Mild water stress. A reduction in transpiration is caused by a decline of stomatal conductance ( $g_s$ ) is presented [26]. However, the rate of net  $CO_2$  assimilation remains constant because stomatal closure inhibits transpiration more than it decreases intercellular  $CO_2$  concentrations. Even during early stages of drought stress, the plant increases its water-use efficiency. Phase 2: Moderate water stress. Here, a further decrease of  $g_s$  is accompanied by large decrease of mesophyll conductance ( $g_m$ ), and a small but significant decrease in photosynthetic activity appears [27]. Finally, in phase 3: Severe water stress. Stomatal conductance drops below its threshold value, the photosynthetic capacity is impaired, and a permanent damage of photosystems suggests that the leaves are enduring oxidative stress, senescence and remobilization of leaf nutrients [28]. At this point, the effects of drought are irreversible and are reflected in the net  $CO_2$  assimilation of the plant [29].

Plants response is often affected by different stress conditions. Because of this, monitoring of multiple plant related variables promises to be a more accurate tool to assess the real plant state. Furthermore, changes on stomatal conductance and transpiration are more specifically related to soil water content than leaf water content. Consequently, stomata related changes are far more significant than changes in net photosynthesis; that could be considered for early detection. However, drought stress eventually provokes irreversible damage in photosystems and plant efficiency which allows utilizing this variable as a long-term indicator, principally after water recovery.

### 2.2. Estimation of Plant Physiological Processes

As aforementioned, the basis of the gas exchange method for photosynthesis ( $P_n$ ) estimation involves a comparison between  $CO_2$  concentration in the atmosphere ( $C_i$ ) and  $CO_2$  concentration in the

leaf chamber ( $C_o$ ) where the plant sample is isolated. Additionally, it is necessary to estimate the mass flow rate per leaf area ( $W$ ) as stated in its equation in Table 1 [30]. Here,  $P$  is the atmospheric pressure in Bar,  $V$  is the volumetric air flow in liters per minute (lpm),  $T_aK$  is air temperature in Kelvin (K) and  $A$  is leaf area in  $\text{cm}^2$ . The 2005.39 constant is an adjusted coefficient to change mass units to mol, surface to  $\text{m}^2$  and time from minutes to seconds. In a similar manner, estimation of transpiration ( $E$ ) is performed, but in this case by measuring the  $\text{H}_2\text{O}$  vapor exchange. Other important processes such as stomatal conductance, vapor pressure deficit ( $VPD$ ) and leaf to air temperature difference ( $LATD$ ) can be estimated by using equations that have been previously stated by many authors and are summarized in Table 1 [22,25,31].

**Table 1.** Equations for the estimation of physiological processes of plants.

Variable	Equation	Unit of Measurement
Mass flow rate per area	$W = (2005.39) \frac{(V)(P)}{(T_aK)(A)}$	$\text{mmol}/\text{m}^2/\text{s}$
Photosynthesis	$P_n = (W)(C_i - C_o)$	$\mu\text{mol}/\text{m}^2/\text{s}$
Transpiration	$E = (W)(1000)(18.02) \frac{(e_o - e_i)}{(P - e_o)}$	$\text{mg}/\text{m}^2/\text{s}$
Stomatal conductance	$g_s = \frac{W}{\left( \frac{e_{leaf} - e_o}{e_o - e_i} \right) \left( \frac{P - e_o}{P} - r_b(W) \right)} (1000)$	$\text{mmol}/\text{m}^2/\text{s}$
Vapor pressure deficit	$VPD = e_s - e_i$	kPa
Leaf to air temperature difference	$LATD = T_a - T_{leaf}$	$^{\circ}\text{C}$

### 3. Smart Sensor

The proposed smart sensor fuses a water vapor and a  $\text{CO}_2$  gas exchange system into the same pneumatic line in order to estimate  $P_n$  and  $E$ . The system also estimates other phenomena such as  $g_s$ ,  $VPD$ , and  $LATD$ . Climatic variables such as solar radiation, temperature and relative humidity can also be monitored with the same hardware. As can be seen in Figure 1, five stages (black blocks) integrate the smart-sensor.

First, the pneumatic system uses a transparent acrylic chamber to isolate the plant sample; a set of electrovalves switching between the environment air reference or leaf chamber, and an air pump applies negative pressure in order to move air through the pneumatic system where the sensors are attached. The set of primary sensors are located in two places as can be seen in Figure 2. A Honeywell Pt1000 Resistance Temperature Detector (RTD) configured to measure in a range from 0 to  $65^{\circ}\text{C}$  with a measurement error of  $\pm 0.3^{\circ}\text{C}$  is located in the leaf chamber, which has a suitable range to monitor leaf temperature of the plant on contact. Also, an OSRAM SFH5711 ambient solar radiation sensor with a 0 to 100,000 lux range and measurement error of  $\pm 0.04\%$  of its measured value is located near the plant sample, which is isolated in the leaf chamber. In the rest of the pneumatic system are attached a Sensirion SHT75 digital Micro Electro Mechanical System (MEMS)-based sensor that measures temperature and relative humidity ( $RH$ ) of air with a resolution of 14-bits for temperature and 12-bits for  $RH$  and measurement error of  $\pm 0.4^{\circ}\text{C}$  and  $\pm 1.8\%$ , respectively. An OMRON DF6 MEMS-based flow sensor is used to monitor the volumetric flow of the pneumatic line; this sensor has a

measurement range of 0 to 5 lpm with measurement error of  $\pm 0.4\%$ . To monitor the atmospheric pressure, a Freescale Semiconductor MPX4115A absolute pressure sensor with a range of 15 to 115 kPa and a measurement error of  $\pm 1.5\%$  was utilized. Finally, in order to monitor the CO<sub>2</sub> concentration an Edinburgh Instruments Gascheck 2 IRGA based CO<sub>2</sub> sensor is required. The sensor has a measurement range of 0–3000 ppm with measurement error of  $\pm 30$  ppm.

**Figure 1.** Block diagram of the phytomonitoring smart-sensor.

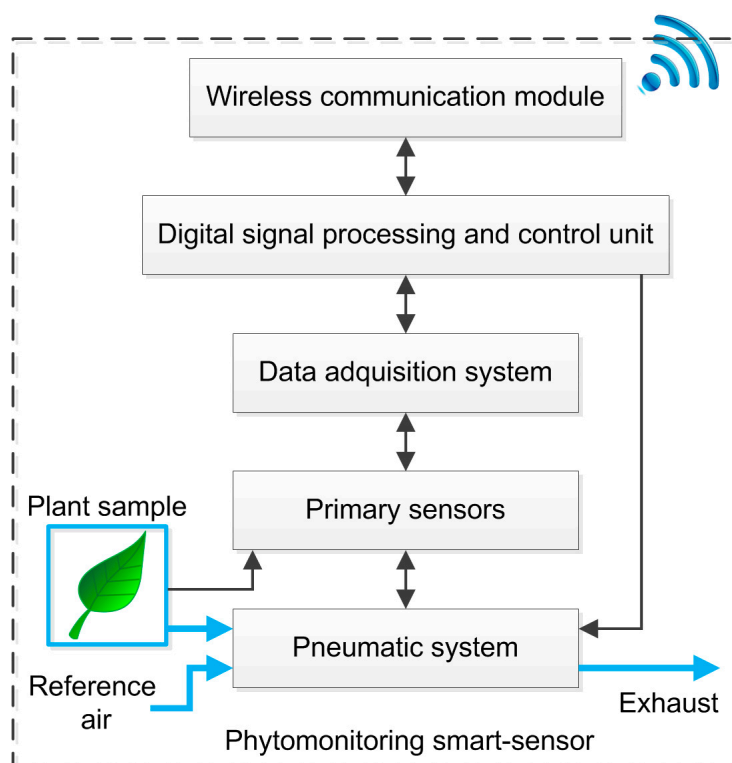
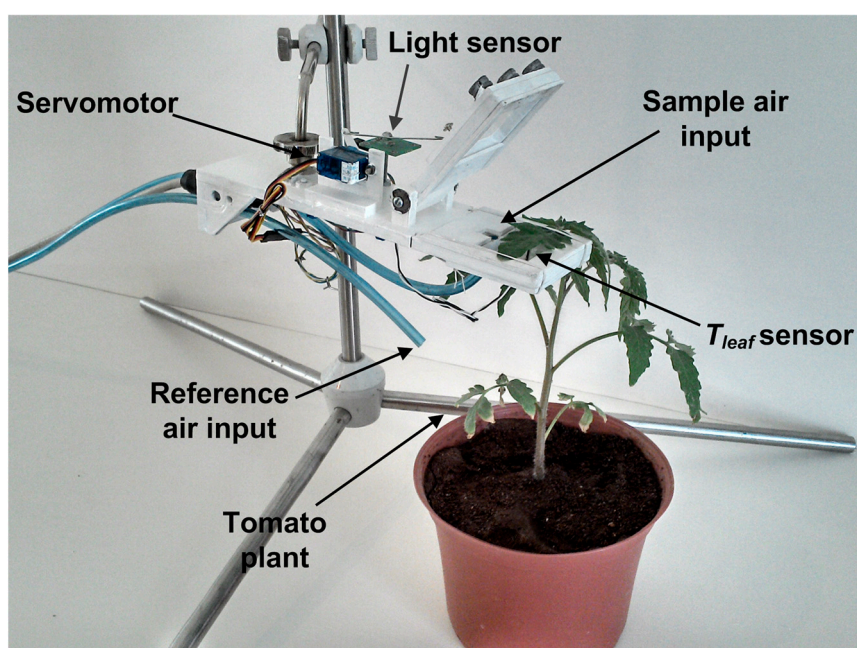


**Figure 2.** Leaf chamber and sensors arrangement.



The signals of all primary sensors are standardized to a 0 to 5 V output format by using OpAmp-based modules. Then, each sensor reading is entered into the Data Acquisition System (DAS) through an analog front end, 2nd order anti-alias low pass filter with a cut-off frequency of 20 Hz. A 12-bit Analog to Digital Converter Texas Instruments ADS7844 sampled the previously filtered sensor signals. The ADS7844 communicates via SPI with the third stage, the Digital Signal Processing and Control Unit (DSPCU) which is embedded in a low-cost EP2C35F672C6 FPGA that manages the ADS7844 at 200 kg samples per second (ksps), and also communicates via a 2-wire serial interface with the digital SHT75 sensor. This FPGA-processor is also responsible for controlling the mechanism used in the pneumatic line. The aforementioned tasks are performed simultaneously because of the parallel capabilities of the FPGA. Moreover, this unit performs data filtering operations in order to improve the quality of signals. Finally, the DSPCU estimates and transmits the physiological processes together with environmental readings to a coordinator device by using a wireless communication module.

### Digital Signal Processing Techniques

Because the experiment is performed in a noisy environment where the greenhouse microclimate presents sudden changes due to the influence of external weather, two stages of signal processing units are embedded inside the FPGA in order to reduce the amount of noise in primary sensors readings. As is illustrated in Figure 3, previously the estimation of plant processes, the signals  $X(k)$  from the primary sensors pass through a 1024th order average decimation filter, where a single average sample reduced in quantization and undesirable noise is obtained every second. Furthermore, the oversampled versions of sensor readings  $X_{os}(k)$  are introduced into the Kalman filters to obtain new filtered signals  $X_{ost}(k)$  [32].

As can be seen in Figure 3, once all the  $X_{ost}(k)$  are calculated, the plant physiological process estimator computes  $P_n$ ,  $E$ ,  $g_s$ ,  $VPD$ , and  $LATD$  from primary sensors readings. In addition, the proposed smart sensor provides a new version of the aforementioned process, in which spatial variations induced for the solar radiation can be reduced by using the simple index expressed in Equation (1). Herein,  $X_{norm}(k)$  represents the normalized version of the signals  $P_n$ ,  $E$ ,  $g_s$ ,  $VPD$  or  $LATD$ . Meanwhile  $Rad_{norm}(k)$  is the normalized version of radiation, but considers the maximum  $Rad$  value from all nodes. Finally,  $X_{rad\_index}(k)$  is the index that relates the physiological process to the radiation at the time when the sample was acquired:

$$X_{rad\_index}(k) = \frac{X_{norm}(k)}{Rad_{norm}(k)} \quad (1)$$

Moreover, the plant physiological estimator unit calculates the first derivative of  $P_n'$ ,  $E'$ ,  $g_s'$ ,  $VPD'$ , and  $LATD'$  in order to explore phenomena involved in the changes of physiological activity. This task is performed by using a discrete derivative as described in Equation (2), which can easily be implemented in the FPGA. Herein,  $X'(k)$  can represent any of the physiological processes previously estimated:

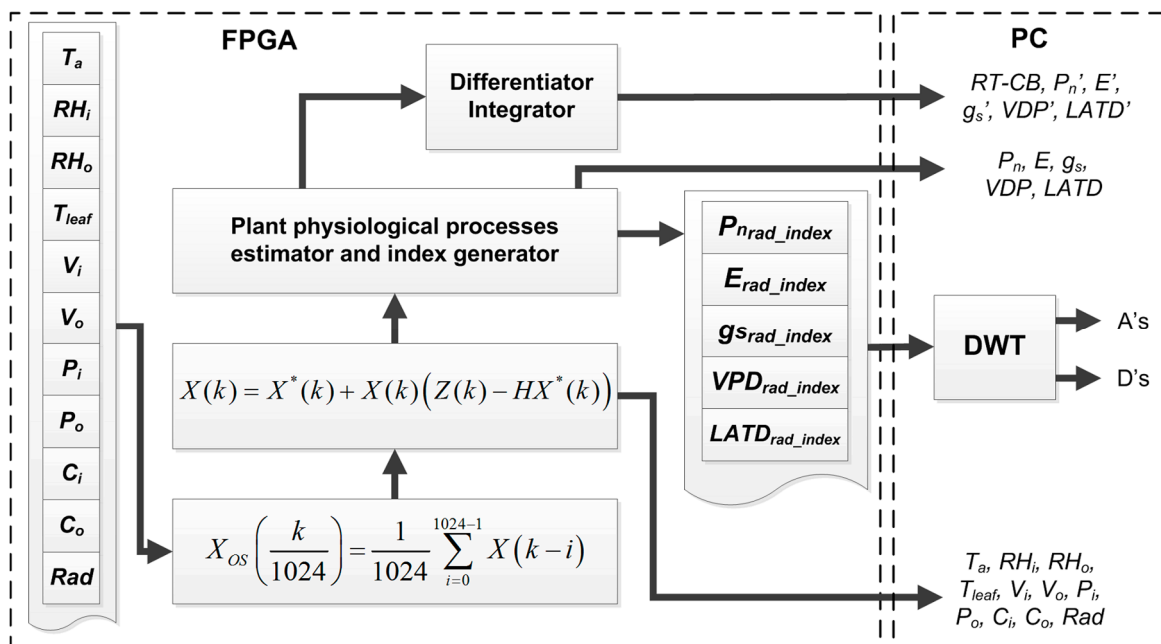
$$X'(k) = \frac{X(k) - X(k-1)}{T_s} \quad (2)$$

This unit also computes the Real Time-Carbon Balance (*RT-CB*), by integrating  $P_n$ , this index, as was previously reported in [22], describes the accumulation of carbon due to the photosynthesis activity. It is calculated by using Equation (3), which is the discrete time version of the integral:

$$RT - CB = T_s \sum_{k=0}^N P_n(k) \quad (3)$$

Furthermore, these signals are transmitted to a PC together with data from primary sensors to be stored and plotted. In addition, the PC performs a DWT to  $X_{rad\_index}(k)$  signals in order to explore the responses at different frequencies.

**Figure 3.** FPGA filtering stage and plant physiological estimator unit.



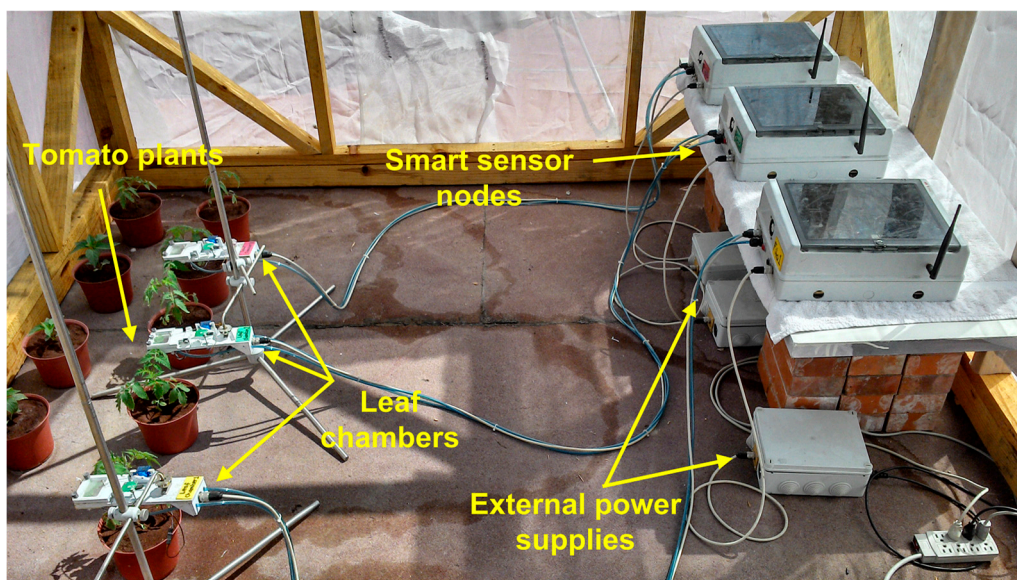
## 4. Experimentation and Results

### 4.1. Experimental Setup

The experiment illustrated in Figure 4 was conducted during 2013 in a research greenhouse located at an altitude of 54 m, in the Universidad Autonoma de Sinaloa, School of Biology, Culiacan Rosales, Sinaloa, Mexico (24°48'0"N, 107°23'0"W). The greenhouse was a single span arch type with 30 m<sup>2</sup> of ground, equipped with a commercial climate controller. The plants used for the experiment were single genotype tomatoes (*Solanum lycopersicum* L.) variety Raffaello; it is an indeterminate tomato appropriate for cultivation within greenhouse conditions and it is resistant to pests and diseases.

The variation factor in the experiment was the content of water in the soil at two levels: (a) The reference that represents plants irrigated at field capacity and (b) The drought treatment where the irrigation is recurrently suspended one day in order to reach water deficit in the soil. Three smart sensor nodes were used to measure the responses of plants to different irrigation levels. In addition, three tensiometers Irrometer model R were installed in the monitored plants in order to monitor the content of water in the soil. These sensors have a 0 to 100 kPa range with an accuracy rating of ±2%.

**Figure 4.** Experimental setup for smart sensors under real operating conditions.



#### 4.2. Sample Preparation

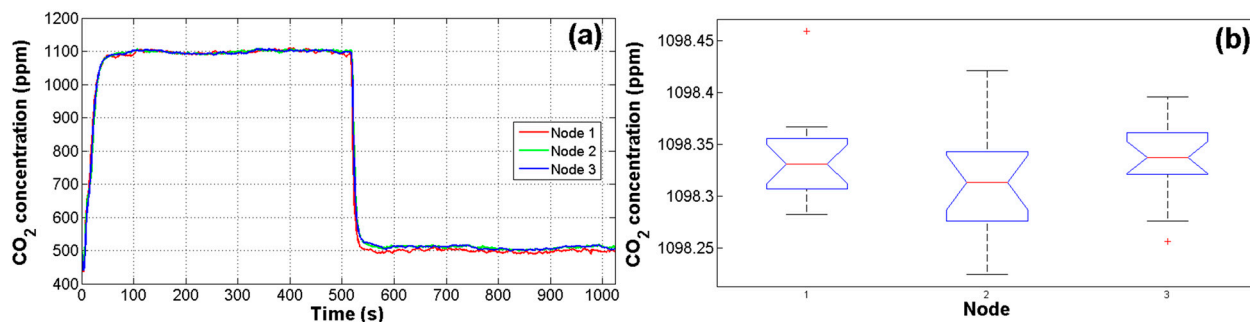
The tomato plants were germinated and transplanted into two liters containers where the plants were grown in greenhouse conditions until they were an appropriate size to attach the sample in the leaf chambers. The substrate used was a volcanic stone called tezontle, screened to homogenize the particles diameter and ensure same soil conditions (apparent density of  $605 \text{ kg}\cdot\text{m}^{-3}$ ). In order to avoid other variation factors, all the plants were irrigated with Steiner solution at a concentration according to the plant growth stage. Finally, in order to obtain reliable responses between different plants, it was necessary to standardize a method to select the leaves that would be monitored. The selected leaves were located at the same height, not to low leaves because it is reported that they are the first to lose the photosynthetic activity due to aging, and not the top leaves because they are the last to respond to drought [33].

#### 4.3. In-Situ Node Adjustment and Validation

Due to the high noise in  $\text{CO}_2$  signals and the fact that reliability of estimations depends on measurements of primary sensors, a test was performed in order to assess the responses of the IRGA  $\text{CO}_2$  sensors using an 1100 ppm  $\text{CO}_2$  reference. As can be seen in Figure 5a, the first 512 samples correspond to the  $\text{CO}_2$  reference and the next 512 samples correspond to the inside air of the closed greenhouse without plants. This test was performed for 16 cycles for the three nodes. Finally, with the average of cycles, an ANOVA was carried out to evaluate the response of nodes. The value of alpha  $\alpha$  for this and other tests in this work was set to 0.05 (95% of confidence). The resulting  $p$ -value of the analysis was 0.2205, which is higher than 0.05 that represents the upper boundary considered for statistical differences between treatments [34]. In this manner, the resulting  $p$ -value represents no significant difference between node readings. As it can be observed in Figure 5b there are only two outlier data points in node 1 and 3. The means in the analysis were 1098.4, 1098.3, and 1098.3 ppm with standard deviations of 4.49, 4.31, and 4.67 ppm respectively for nodes 1, 2, and 3.



**Figure 5.** Validation test of IRGA CO<sub>2</sub> sensors. (a) 1 cycle monitoring with an 1100 ppm CO<sub>2</sub> reference; (b) Analysis of variance boxplot results.



#### 4.4. Filtering Results

Figure 6 illustrates improvements over signal quality after the filtering stages. In the Figure 6a (CO<sub>2</sub> concentration) the amount of noise presented on the CO<sub>2</sub> signal can be easily appreciated. Consequently, the estimation of photosynthesis showed in Figure 6b is too noisy. Furthermore, it can be observed that filtering stages have improved the overall signal quality of CO<sub>2</sub> concentration at Figure 6c and net photosynthesis in Figure 6d.

**Figure 6.** Digital filtering results over photosynthesis estimation. (a) Non-filtered CO<sub>2</sub> signal; (b)  $P_n$  estimation based on raw signals; (c) filtered CO<sub>2</sub> signal; and (d)  $P_n$  estimation based on filtered signals.

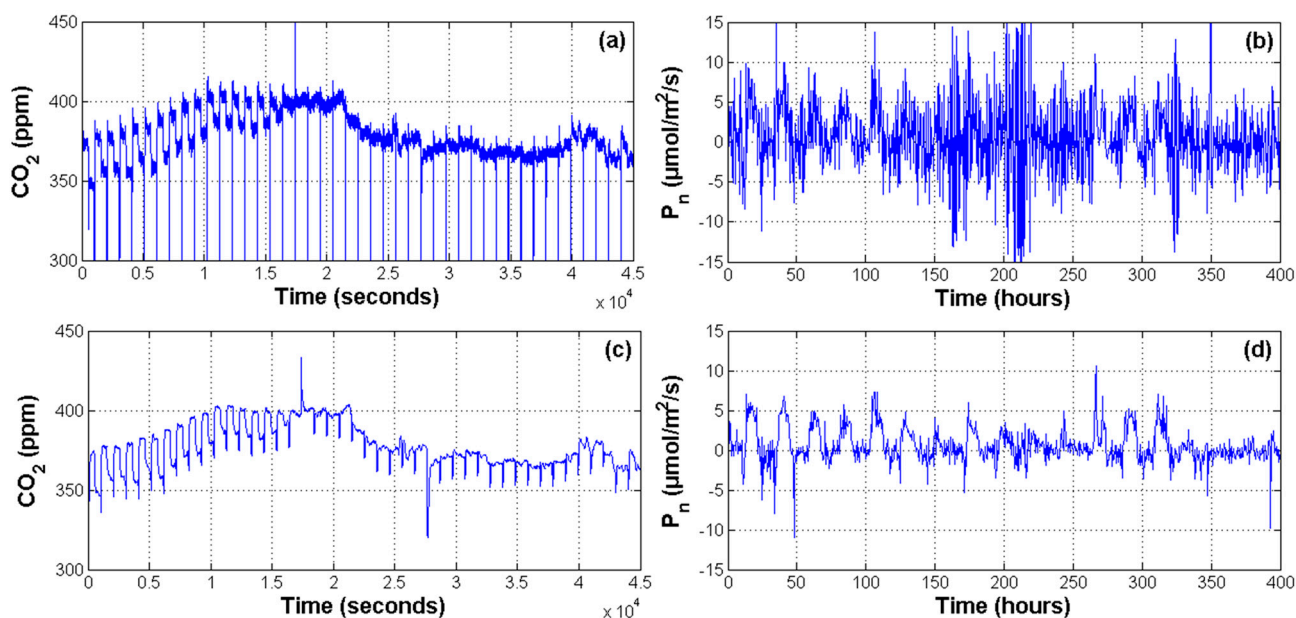


Figure 6 shows only the result of 1 node, but similar results were obtained for the other nodes of the network. In order to quantify how the filtered signals improved the estimation of physiological processes, a Pearson correlation between raw and filtered photosynthesis signals against radiation signal was conducted. Results presented in Table 2 suggest that the behavior of  $P_n$  when it was estimated with non-filtered signals do not correspond with the radiation pattern. In contrast, a better correlation between  $Rad$  and the  $P_n$  estimated with filtered signals was found. In Table 2,

photosynthesis with the subscript *osk* is the estimated one with filtered primary signals. The *R*-value shows the correlation weight while *p*-values below 0.05 confirm the existence of correlation between signals.

**Table 2.** Correlation analysis results for radiation against photosynthesis with and without filtering.

Variables	Photosynthesis–Radiation		Photosynthesis <sub>osk</sub> –Radiation	
	<i>R</i>	<i>p</i>	<i>R</i>	<i>p</i>
Node 1	0.0672	0.0515	0.5146	<0.0001
Node 2	0.2023	<0.0001	0.5307	<0.0001
Node 3	0.1027	0.0028	0.6557	<0.0001

#### 4.5. Environmental Signals

Because the experiment was carried out in a commercial greenhouse, spatial differences in the microclimate produced changes on physiological processes, even for plants undergoing the same water stress treatment. Then, it was necessary to monitor the microclimate related variables in order to understand these changes. Figure 7 illustrates the most important environmental variables monitored inside the greenhouse at three different locations. Figure 7a shows the readings for radiation during the entire experiment. This variable is noteworthy because it modifies the temperature (Figure 7b), *VPD* (Figure 7c) and *RH* (Figure 7d) of the air inside the greenhouse and therefore the transpiration rates of plants. Moreover, the photosynthesis is more sensitive to radiation than to any other factor.

**Figure 7.** WSN environmental readings inside the greenhouse at locations of Nodes 1, 2 and 3. (a) Solar radiation; (b) air temperature; (c) vapor pressure deficit; and (d) relative humidity.

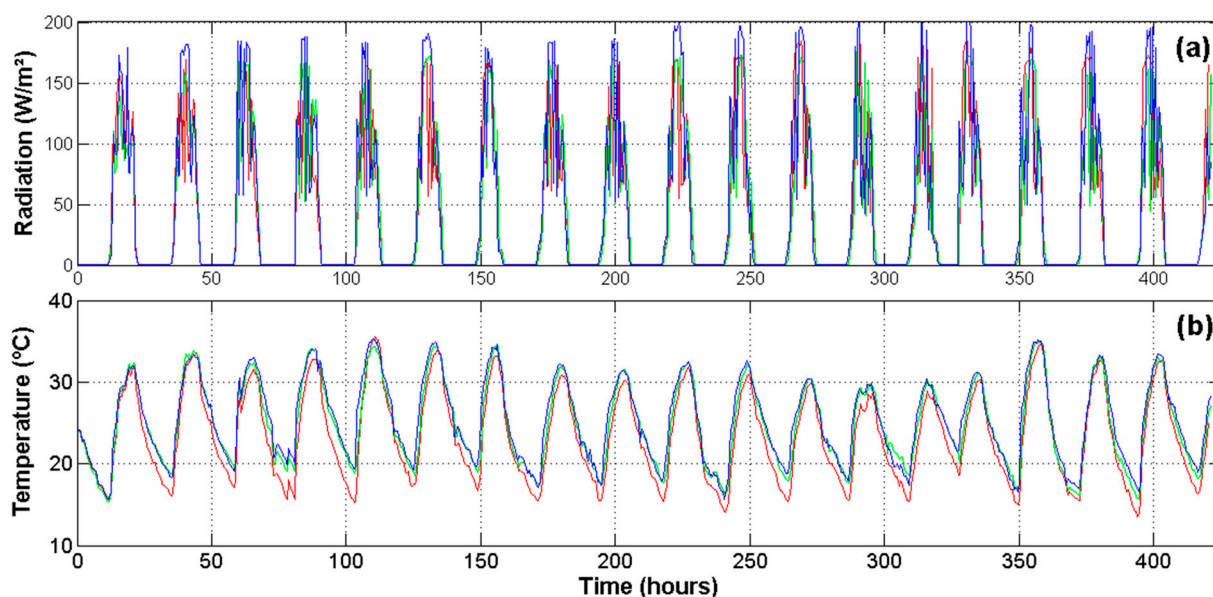
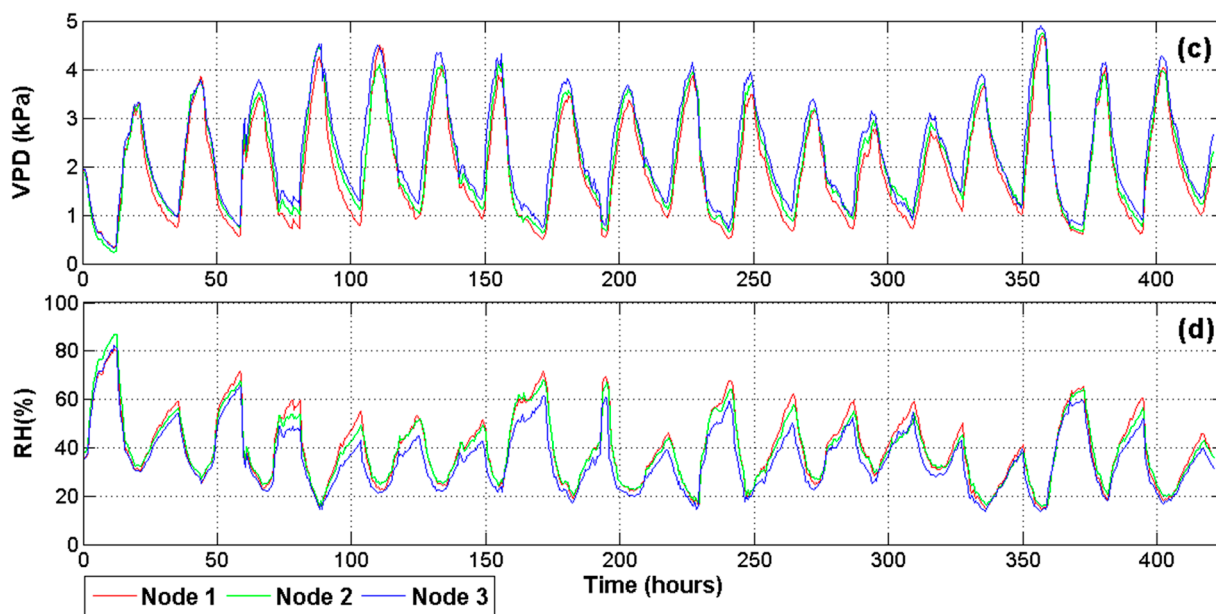
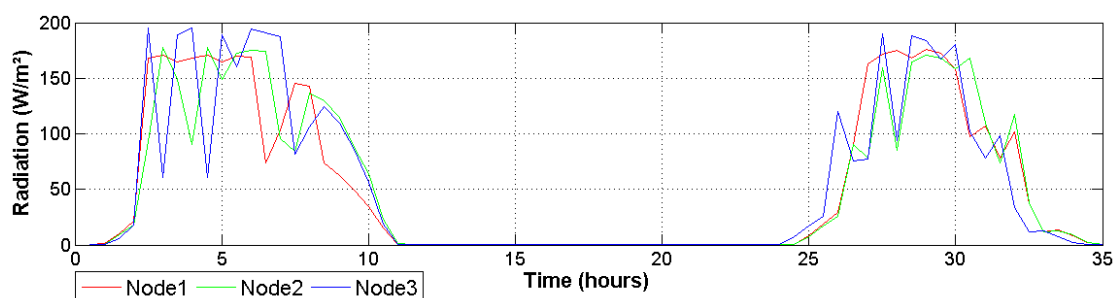


Figure 7. Cont.



Differences between node readings change throughout the day, but keep a relatively regular pattern in which node 3 registers a higher temperature and drier air conditions. As can be seen in Figure 8, this behavior is influenced by the total solar radiation received by this node. This figure illustrates how the greenhouse presents spatial variations provoked mainly by the structure geometry. This is important because it helps investigators to understand abrupt changes in transpiration and photosynthetic signals estimated by the system. Finally, it is important to note that received radiation was around  $175 \text{ W/m}^2$ , which is a suitable quantity to grow Raffaello variety of tomatoes [35].

Figure 8. Image zooms for two days of radiation.



#### 4.6. Physiological Signals

The methodology to induce drought stress was as follows: The first two days of monitoring were a stabilizing period in which plants were watered at field capacity (10 kPa); on day three, the irrigation was suspended so that two plants could reach 30–40 kPa soil drought conditions. Then, plants were rehydrated in order to avoid reaching permanent wilting point (PWP). After one rehydration day, the drought treatment began again. The experiment lasted 19 days. As is illustrated in Figure 9, red and green signals correspond to plants suffering from drought stress (SP1 and SP2 respectively). The reference plant (RP) that was continuously irrigated at 10 kPa is represented with the blue signal. The

light blue shadow indicates irrigation and light orange means water depletion. The brown arrows indicate irrigation interruption for the RP. After two days the irrigation was resumed, this is indicated by the blue arrows.

**Figure 9.** Physiological signals. (a) Photosynthesis; (b) transpiration; (c) stomatal conductance; and (d) leaf to air temperature difference.

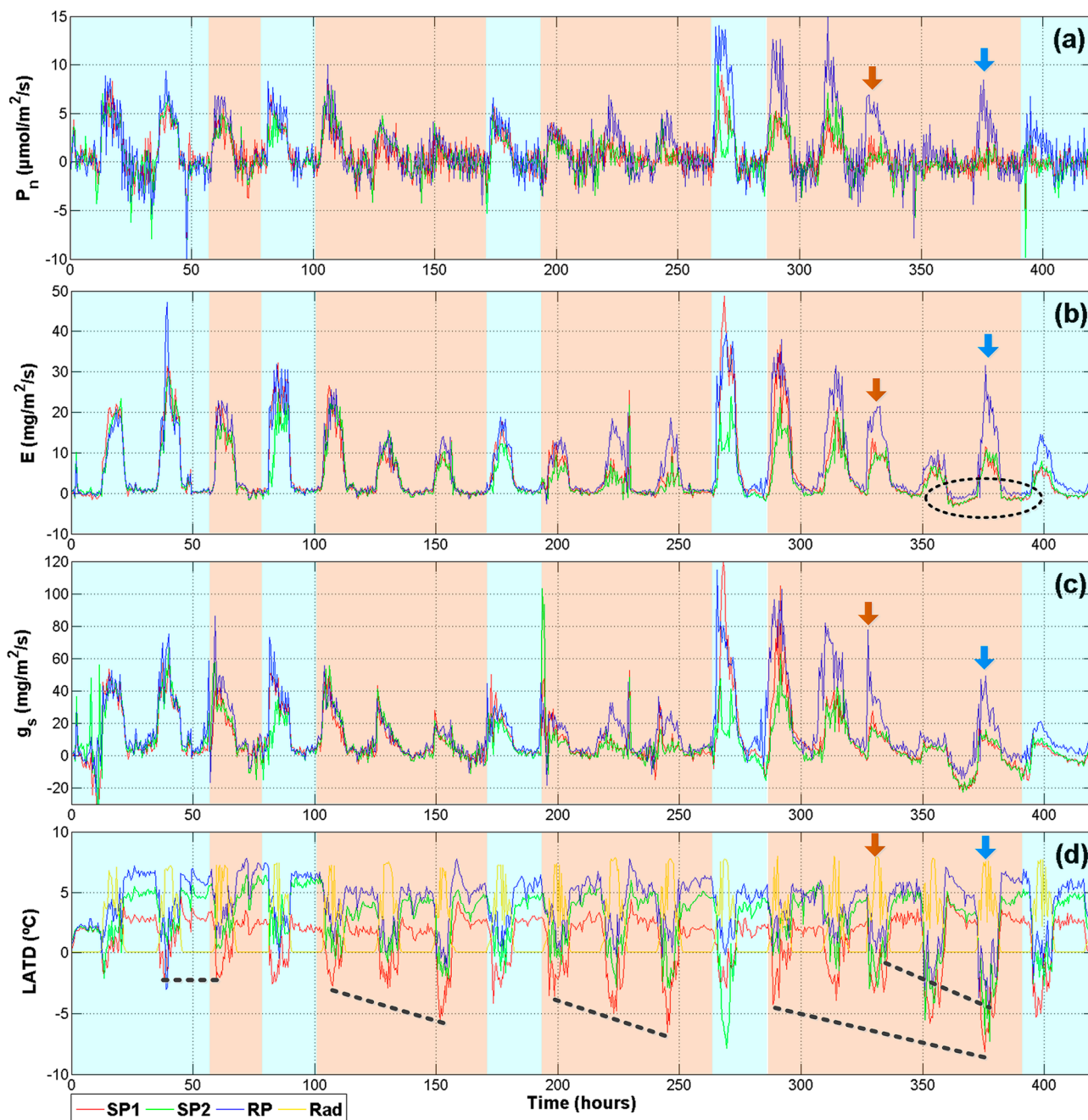


Figure 9 summarizes the physiological signals that provide more information related to plant status ( $P_n$ ,  $E$ ,  $g_s$ , and  $LATD$ ). As was expected, photosynthesis is not sensitive to early stages of drought. In Figure 9a, a difference between the RP and the treatments can be noticed only after three periods of stress near hour 225. Furthermore, after the fourth period of stress around hour 400, net photosynthetic activity for SP1 and SP2 was not recovered after being rehydrated. This behavior can be explained

because drought periods generate an accumulative oxidative stress in the leaves until damaging photosystem II in a permanent way by reactive oxygen species [2,36].

Transpiration results (Figure 9b) show an early response to treatments, especially in the second and third stages of stress. However, the most interesting behavior is at the end, enclosed by the dark ellipse, a low amplitude negative transpiration rate indicates that leaves are taking water vapor from the atmosphere instead of expelling it. This is a defense mechanism observed in plants under severe drought [37]. The stomatal conductance (Figure 9c) presents more marked differences as compared with  $P_n$ . Even in the first day of drought, SP1 and SP2 present a sudden drop in  $g_s$ . This is explained because the stomata closure and the decrease of  $g_s$  are the first defenses plants employ in order to reduce the amount of water loss through the stomata and it is related more to soil drought than leaf water status [2]. The higher decrease in the third stage of drought could be related to a decrease of  $g_m$  because the leaves are preparing for severe stress conditions.

The final graph (Figure 9d) illustrates the difference between air temperature and leaf temperature. Herein, a yellow line illustrates the day where the  $LADT$  must be zero or slightly positive. This is a normal behavior because in well-watered plants the  $T_{leaf}$  is cooler than  $T_a$ . However, if plants are under drought conditions, the  $T_{leaf}$  is higher than  $T_a$ . This tendency is clearly noticed in Figure 9d, where once the water depletion begins an increase in negative readings appears. This tendency is illustrated with the dashed black lines. Nevertheless, despite being under the same conditions, SP2 always presented a better tolerance to the stress than SP1. This can be noted because the red line presents more negative and sudden changes in  $LADT$ . On the other hand, the reference plant showed stable behavior with zero or positive values until the irrigation was suspended at hour 330. After this point, the drought was maintained for two days and a clear drop of blue line appears. After the rehydration day during hour 375, the  $LADT$  of RP slowly returns to zero and positive values.

Finally, it is important to mention that a significant reduction in height and the leaf areas of plants under drought was expressed. At the end of the experiment, plants under drought conditions maintained heights of approximately 80% of non-stressed plants.

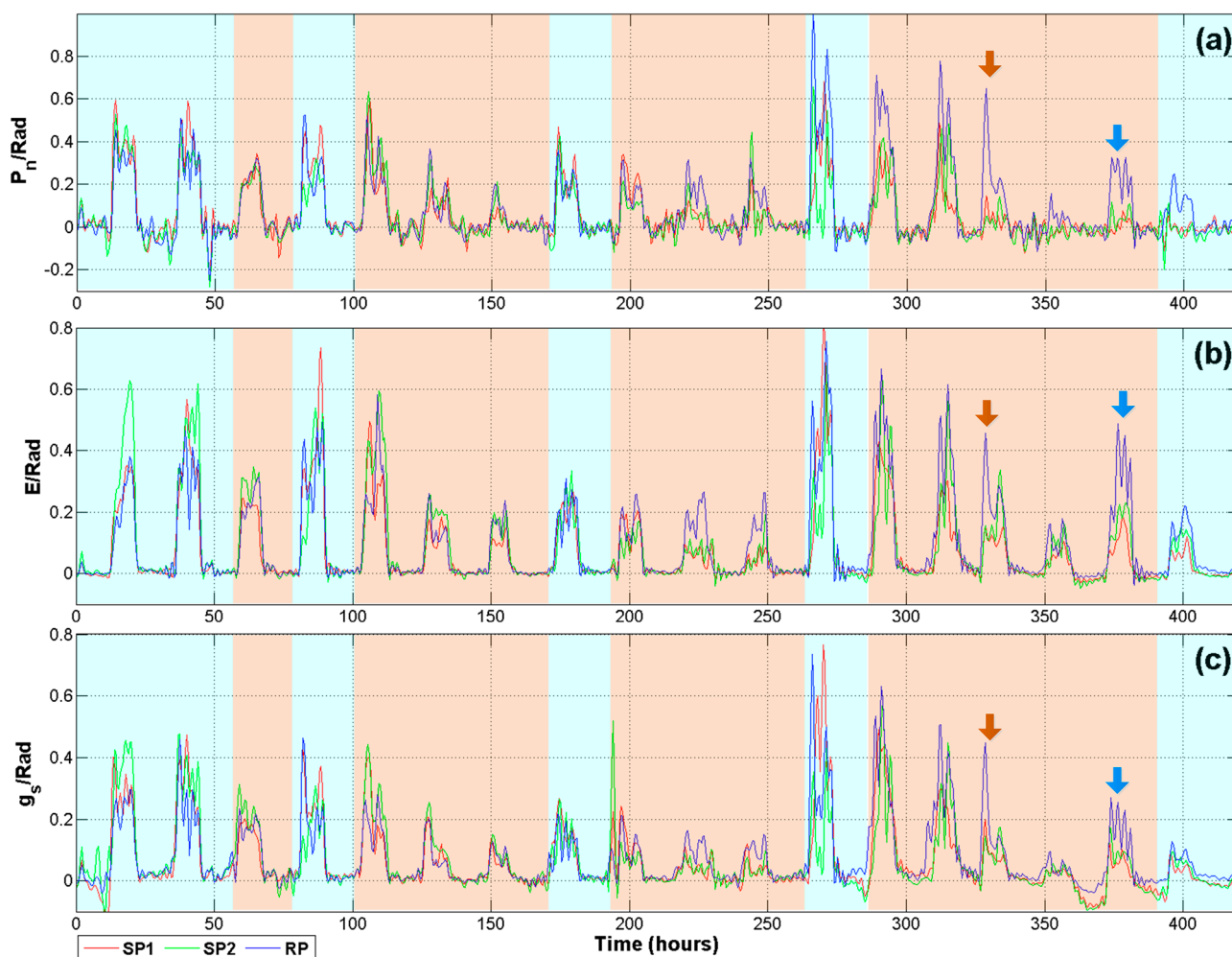
#### 4.7. Indexes and DWT Analysis

Despite the fact that Figure 9 provides important information about effects of drought on plants, the analysis requires data from at least two days in order to be able to notice a behavioral pattern. The problem with performing single day assessment is the amount of remnant noise, mainly for  $P_n$  and  $g_s$  signals. Another problem is the variation in growing conditions throughout the greenhouse, which may cause plants under the same treatment to respond quite differently. The variable that mainly affects the results is the solar radiation. This problem was addressed using the index previously described in Equation (1). Therefore, if plants under the same treatment receive different radiation levels, the difference in variable responds is mitigated permitting a better comparison. This methodology was useful for  $P_n$ ,  $E$ , and  $g_s$  signals which presented a higher component of noise as compared with  $VPD$  or  $LADT$ .

As it can be seen in Figure 3, after the normalization process, these signals were analyzed using the DWT. In a preliminary experiment, several configurations were performed in order to explore the best one to extract information from signals. Finally, the DWT applied to filter the signals illustrated in

Figure 10 uses a mother wavelet Daubechies db40 at a level A2 that rejects signals outside the range from 0 to 0.27 mHz bandwidth. This criterion was selected because lower mother wavelet levels discriminate important information related with abrupt changes due to radiation. Also, db40 mother wavelet required less computational resources compared with other wavelets such as Symmlets. The high frequency analysis of D levels is not reported because no clear patterns were found; this behavior could be a consequence of the system slow sampling frequency. The new version of  $P_n$  signals corresponding to Figure 10a presents a considerable reduction in the high frequency noise compared to Figure 9a, where after several stages of filtering, the  $P_n$  signal maintains a considerable amount of noise, this could be probably an aliasing of a frequency generated for the IRGA Sensor itself. However, after the use of DWT analysis such as an extra filtering stage, this component of noise was reduced allowing a comparison along one single day.

**Figure 10.** Wavelet of processes/Radiation indexes. (a) Photosynthesis; (b) transpiration; and (c) stomatal conductance.



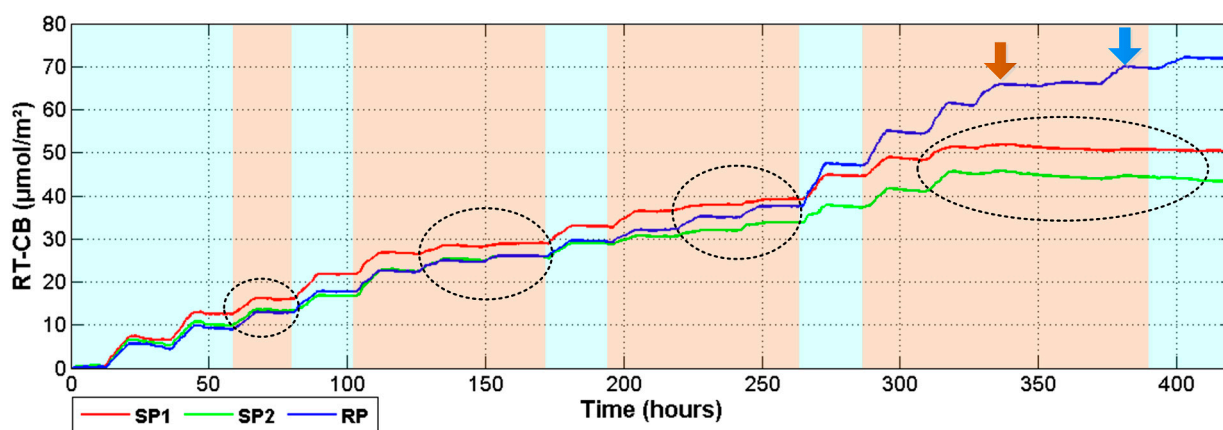
Furthermore, in order to avoid the removal of information related with the plant response and considering that  $P_n$  is highly related with  $Rad$ , a Pearson correlation was conducted to compare  $Rad$  with  $P_n$  before the DWT processing. The correlation results are presented in Table 3 to support the idea that DWT rejects the noise on photosynthesis signal but it keeps the information related with

photosynthesis itself. As it can be appreciated, the correlation between  $P_n$  and  $Rad$  slightly increases when  $P_n$  is filtered with the DWT. Only node 3 did not repeat this trend. However, the decrease in the correlation is not too high. Table 3 presents the results of the hypothesis test of no correlation. The  $p$ -values suggest that null hypothesis is rejected.

**Table 3.** Photosynthesis–radiation correlation results with and without DWT filtering.

Variables	Photosynthesis <sub>Sosk</sub> –Radiation		Photosynthesis <sub>DWT</sub> –Radiation	
	<i>R</i>	<i>p</i>	<i>R</i>	<i>p</i>
Node 1	0.5146	<0.0001	0.5600	<0.0001
Node 2	0.5307	<0.0001	0.5574	<0.0001
Node 3	0.6557	<0.0001	0.6308	<0.0001

**Figure 11.** Real Time-Carbon Balance (*RT-CB*).



Finally, in order to understand the impact of drought for long-term development and health of the plants, the analysis of  $P_n$  integral calculation which is named as Real Time-Carbon Balance index was proposed to explore the response of plants under drought conditions. As it can be seen in Figure 11, during the day *RT-CB* increases but stops or slightly decreases during the nights. This behavior is a result of the photosynthetic and respiration activity; but, as it is indicated with dark ellipses, when the plants were subjected to drought, the *RT-CB* signals remained constant until the rehydration day. Here it is important to state that the first day of drought did not significantly affected plant response and changes appeared until day two. During the rehydration days corresponding to hours 75, 175, and 275; the plants were recovered and photosynthetic activity was normalized. Nevertheless, SP1 and SP2 did not recover after the fourth period of drought, even when plants were watered at approximately hour 380. Here, the *RT-CB* index maintains the negative tendency which means that the photosynthetic activity stops, and the net respiration increases causing a loss of dry matter. Figure 11 also shows the exponential behavior of the photosynthesis activity as the plant grows, because around hour 275 of experimentation, the *RT-CB* registered an important increase for the reference plant. However, this tendency changed when the irrigation was suspended. The first day of scarcity, as indicated with the brown arrow did not change the plant response. However, the next day a fall in the Carbon assimilation was reported. This tendency continues until normal irrigation was re-established in the day marked with the blue arrow.

## 5. Conclusions

In this investigation, a smart sensor system was developed to monitor primary variables in plants. Then, this information was then used to estimate physiological processes such as photosynthesis, transpiration, and stomatal conductance. The proposed experiment demonstrates the capabilities of the system to detect stress in plants submitted to soil drought conditions. It also reveals that even under real operation conditions (greenhouse applications) the system properly estimates the aforementioned physiological processes. However, important considerations must be taken into account if the system pretends to be operated outside due to sunlight and rain conditions. But it is important to state that this is a prototype that can be improved in a future. Another central consideration relies on the leaf chamber design and stress conditions that are produced on isolated leaves. During the experiment, it was necessary to periodically changed between leaves. However, during periods of three days not important damage over the samples was appreciated. This may be due to the Nylamid-acrylic materials utilized in the leaf chamber design, which do not overheat under sunlight such as aluminum based chambers that are used in commercial devices.

In addition, the DWT was used to process the signal combined with an index that adjusts the estimation according to the plants surrounding environment. It resulted useful in order to perform a day by day comparison for drought detection, which is important because conventional analysis requires long time to detect drought conditions. Moreover, the *RT-CB* index provides an alternative method for monitoring plant growth without using destructive laboratory analysis. Therefore, *RT-CB* provides information about irregular growing circumstances such as drought. Finally, the proposed digital signal processing methodology implemented in the gas exchange system represents an alternative that can be used to detect and monitor drought under real growth conditions. Also, this methodology can be utilized for filtering purposes in precision agriculture applications where the signal-to-noise ratio is high (like chlorophyll fluorescence or impedance sensor applications). Furthermore, it can be utilized to explore time-frequency properties of different kinds of signals.

## Acknowledgments

This project was partially supported by CONACYT scholarship 231946, PROINNOVA-20501059, and by PROFAPI 2012-111 and PROFAPI 2013-116. The authors wish to thank Ismael Urrutia for his support and advice related with the biological part of this investigation. Also thanks to M.C. Gilberto Marquez Salazar for providing the greenhouse where the experiments were conducted and Texas Instruments for providing device samples tested in this project. Finally, the authors wish to thank Silvia C. Stroet for her support by doing the English language edition.

## Author Contributions

Guevara-Gonzalez and Carrillo-Serrano designed the study. The experiments and the signal processing and analysis were performed by Duarte-Galvan, Millan-Almaraz, and Romero-Troncoso. All authors discussed the results and implication and everyone provided helpful feedback and commented on the manuscript at all stages.



## Conflicts of Interest

The authors declare no conflict of interest.

## References

1. Taiz, L.; Zeiger, E. *Plants Physiology*; Sinauer Associates, Incorporated: Sunderland, MA, USA, 2010.
2. Aroca, R. *Plant Responses to Drought Stress: From Morphological to Molecular Features*; Springer: Berlin/Heidelberg, Germany, 2012.
3. García-Mier, L.; Guevara-González, R.G.; Mondragón-Olguín, V.M.; del Rocío Verduzco-Cuellar, B.; Torres-Pacheco, I. Agriculture and bioactives: Achieving both crop yield and phytochemicals. *Int. J. Mol. Sci.* **2013**, *14*, 4203–4222.
4. Fernandez-Jaramillo, A.A.; Duarte-Galvan, C.; Contreras-Medina, L.M.; Torres-Pacheco, I.; Romero-Troncoso, R.D.J.; Guevara-Gonzalez, R.G.; Millan-Almaraz, J.R. Instrumentation in developing chlorophyll fluorescence biosensing: A review. *Sensors* **2012**, *12*, 11853–11869.
5. Agam, N.; Cohen, Y.; Berni, J.A.J.; Alchanatis, V.; Kool, D.; Dag, A.; Yermiyahu, U.; Ben-Gal, A. An insight to the performance of crop water stress index for olive trees. *Agric. Water Manag.* **2013**, *118*, 79–86.
6. Udompetaikul, V.; Upadhyaya, S.K.; Slaughter, D.; Lampinen, B.; Shackel, K.; House, G. Plant Water Stress Detection Using Leaf Temperature and Microclimatic Information. In Proceedings of 2011 ASABE Annual International Meeting Sponsored by ASABE Galt House, Louisville, KY, USA, 7–10 August 2011.
7. Jiménez-Bello, M.A.; Ballester, C.; Castel, J.R.; Intrigliolo, D.S. Development and validation of an automatic thermal imaging process for assessing plant water status. *Agric. Water Manag.* **2011**, *98*, 1497–1504.
8. Abboud, T.; Bamsey, M.; Paul, A.-L.; Graham, T.; Braham, S.; Noumeir, R.; Berinstain, A.; Ferl, R. Deployment of a fully-automated green fluorescent protein imaging system in a high arctic autonomous greenhouse. *Sensors* **2013**, *13*, 3530–3548.
9. Millan-Almaraz, J.R.; Guevara-Gonzalez, R.G.; Romero-Troncoso, R.; Osornio-Rios, R.A.; Torres-Pacheco, I. Advantages and disadvantages on photosynthesis measurement techniques: A review. *Afr. J. Biotechnol.* **2009**, *8*, 7340–7349.
10. Hsiao, S.-C.; Chen, S.; Yang, I.C.; Chen, C.-T.; Tsai, C.-Y.; Chuang, Y.-K.; Wang, F.-J.; Chen, Y.-L.; Lin, T.-S.; Lo, Y.M. Evaluation of plant seedling water stress using dynamic fluorescence index with blue led-based fluorescence imaging. *Comput. Electron. Agric.* **2010**, *72*, 127–133.
11. Kim, Y.; Glenn, D.M.; Park, J.; Ngugi, H.K.; Lehman, B.L. Hyperspectral image analysis for water stress detection of apple trees. *Comput. Electron. Agric.* **2011**, *77*, 155–160.
12. Mirzaie, M.; Darvishzadeh, R.; Shakiba, A.; Matkan, A.A.; Atzberger, C.; Skidmore, A. Comparative analysis of different uni- and multi-variate methods for estimation of vegetation water content using hyper-spectral measurements. *Int. J. Appl. Earth Obs. Geoinf.* **2014**, *26*, 1–11.

13. Senay, G.; Budde, M.; Verdin, J.; Melesse, A. A coupled remote sensing and simplified surface energy balance approach to estimate actual evapotranspiration from irrigated fields. *Sensors* **2007**, *7*, 979–1000.
14. Ghulam, A.; Li, Z.-L.; Qin, Q.; Yimit, H.; Wang, J. Estimating crop water stress with ETM + NIR and SWIR data. *Agric. Forest Meteorol.* **2008**, *148*, 1679–1695.
15. Barbagallo, S.; Consoli, S.; Russo, A. A one-layer satellite surface energy balance for estimating evapotranspiration rates and crop water stress indexes. *Sensors* **2009**, *9*, 1–21.
16. Suárez, L.; Zarco-Tejada, P.J.; González-Dugo, V.; Berni, J.A.J.; Sagardoy, R.; Morales, F.; Fereres, E. Detecting water stress effects on fruit quality in orchards with time-series PRI airborne imagery. *Remote Sens. Environ.* **2010**, *114*, 286–298.
17. Atherton, J.J.; Rosamond, M.C.; Zeze, D.A. A leaf-mounted thermal sensor for the measurement of water content. *Sens. Actuators A Phys.* **2012**, *187*, 67–72.
18. Wang, Z.-Y.; Leng, Q.; Huang, L.; Zhao, L.-L.; Xu, Z.-L.; Hou, R.-F.; Wang, C. Monitoring system for electrical signals in plants in the greenhouse and its applications. *Biosyst. Eng.* **2009**, *103*, 1–11.
19. Tomkiewicz, D.; Piskier, T. A plant based sensing method for nutrition stress monitoring. *Precis. Agric.* **2012**, *13*, 370–383.
20. Passaro, V.; De Leonardis, F. Investigation of SOI raman lasers for mid-infrared gas sensing. *Sensors* **2009**, *9*, 7814–7836.
21. Escalona, J.M.; Fuentes, S.; Tomás, M.; Martorell, S.; Flexas, J.; Medrano, H. Responses of leaf night transpiration to drought stress in *Vitis vinifera* L. *Agric. Water Manag.* **2013**, *118*, 50–58.
22. Millan-Almaraz, J.R.; Torres-Pacheco, I.; Duarte-Galvan, C.; Guevara-Gonzalez, R.G.; Contreras-Medina, L.M.; Romero-Troncoso, R.d.J.; Rivera-Guillen, J.R. FPGA-based wireless smart sensor for real-time photosynthesis monitoring. *Comput. Electron. Agric.* **2013**, *95*, 58–69.
23. Schmidt, U. Low-cost system for on-line measurement of plant transpiration and photosynthesis in greenhouse production. *Acta Hort.* **1998**, *421*, 249–258.
24. Sánchez, J.A.; Rodríguez, F.; Guzmán, J.L.; Arahál, M.R. Virtual sensors for designing irrigation controllers in greenhouses. *Sensors* **2012**, *12*, 15244–15266.
25. Millan-Almaraz, J.R.; Romero-Troncoso, R.D.J.; Guevara-Gonzalez, R.G.; Contreras-Medina, L.M.; Carrillo-Serrano, R.V.; Osornio-Rios, R.A.; Duarte-Galvan, C.; Rios-Alcaraz, M.A.; Torres-Pacheco, I. FPGA-based fused smart sensor for real-time plant-transpiration dynamic estimation. *Sensors* **2010**, *10*, 8316–8331.
26. Centritto, M.; Brilli, F.; Fodale, R.; Loreto, F. Different sensitivity of isoprene emission, respiration and photosynthesis to high growth temperature coupled with drought stress in black poplar (*populus nigra*) saplings. *Tree Physiol.* **2011**, *31*, 275–286.
27. Flexas, J.; Ribas-Carbó, M.; Hanson, D.T.; Bota, J.; Otto, B.; Cifre, J.; McDowell, N.; Medrano, H.; Kaldenhoff, R. Tobacco aquaporin NtAQP1 is involved in mesophyll conductance to CO<sub>2</sub> *in vivo*. *Plant J.* **2006**, *48*, 427–439.
28. Munné-Bosch, S.; Mueller, M.; Schwarz, K.; Alegre, L. Diterpenes and antioxidative protection in drought-stressed *Salvia officinalis* plants. *J. Plant Physiol.* **2001**, *158*, 1431–1437.
29. Munné-Bosch, S.; Alegre, L. Plant aging increases oxidative stress in chloroplasts. *Planta* **2002**, *214*, 608–615.

30. Hubbard, R.; Ryan, M.; Stiller, V.; Sperry, J. Stomatal conductance and photosynthesis vary linearly with plant hydraulic conductance in ponderosa pine. *Plant Cell Environ.* **2001**, *24*, 113–121.
31. CI-340. *Hand-Held Photosynthesis System Instruction Manual*; CID Inc.: Camas, WA, USA, 2008.
32. Rodriguez-Donate, C.; Osornio-Rios, R.A.; Rivera-Guillen, J.R.; Romero-Troncoso, R.D.J. Fused smart sensor network for multi-axis forward kinematics estimation in industrial robots. *Sensors* **2011**, *11*, 4335–4357.
33. Ton, Y.; Kopyt, M. Phytomonitoring information and decision-support system for crop growing. In Proceedings of the 2nd IS on Intelligent Information Technology in Agriculture, Beijing, China, October 2003.
34. Goodman, S.N. Toward evidence-based medical statistics. 1: The p value fallacy. *Ann. Intern. Med.* **1999**, *130*, 995–1004.
35. Vazquez-Cruz, M.A.; Luna-Rubio, R.; Contreras-Medina, L.M.; Torres-Pacheco, I.; Guevara-Gonzalez, R.G. Estimating the response of tomato (*solanum lycopersicum*) leaf area to changes in climate and salicylic acid applications by means of artificial neural networks. *Biosyst. Eng.* **2012**, *112*, 319–327.
36. Sharma, P.; Jha, A.B.; Dubey, R.S.; Pessarakli, M. Reactive oxygen species, oxidative damage, and antioxidative defense mechanism in plants under stressful conditions. *J. Bot.* **2012**, *2012*, doi:10.1155/2012/217037.
37. Beebe, S.E.; Rao, I.M.; Blair, M.W.; Acosta-Gallegos, J.A. Phenotyping common beans for adaptation to drought. *Front. Physiol.* **2013**, *4*, doi:10.3389/fphys.2013.00035.

© 2014 by the authors; licensee MDPI, Basel, Switzerland. This article is an open access article distributed under the terms and conditions of the Creative Commons Attribution license (<http://creativecommons.org/licenses/by/4.0/>).



## FPGA-based wireless smart sensor for real-time photosynthesis monitoring



Jesus Roberto Millan-Almaraz<sup>a,\*</sup>, Irineo Torres-Pacheco<sup>b</sup>, Carlos Duarte-Galvan<sup>b</sup>,  
Ramon Gerardo Guevara-Gonzalez<sup>b</sup>, Luis Miguel Contreras-Medina<sup>b</sup>, Rene de Jesus Romero-Troncoso<sup>c</sup>,  
Jesus Rooney Rivera-Guillen<sup>d</sup>

<sup>a</sup> Facultad de Ciencias Físico-Matemáticas, Universidad Autónoma de Sinaloa, Av. de las Américas y Blvd. Universitarios, Cd. Universitaria, 80000 Culiacan, Sinaloa, Mexico

<sup>b</sup> CA Ingeniería de Biosistemas, División de Investigación y Posgrado, Facultad de Ingeniería, Universidad Autónoma de Queretaro, Cerro de las Campanas s/n, 76010 Queretaro, Qro., Mexico

<sup>c</sup> HSPdigital – CA Telemática, DICIS, Universidad de Guanajuato, Carr. Salamanca-Valle km 3.5+1.8, Palo Blanco, 36885 Salamanca, Gto., Mexico

<sup>d</sup> Department of Aerospace Engineering, Ryerson University, 350 Victoria Street, Toronto, Ontario, Canada M5B 2K3

### ARTICLE INFO

#### Article history:

Received 24 November 2011

Received in revised form 7 February 2013

Accepted 5 April 2013

#### Keywords:

Smart sensor  
Photosynthesis  
Precision agriculture  
Phytomonitoring  
FPGA  
Wireless monitoring

### ABSTRACT

Photosynthesis is considered the most important physiological function because it constitutes the main biomass entrance for the planet and consequently it permits the continuance of life on earth. Therefore, accurate photosynthesis measurement methods are required to understand many photosynthesis-related phenomena and to characterize new plant varieties. This project has been carried out to cover those necessities by developing a novel FPGA-based photosynthesis smart sensor. The smart sensor is capable of acquiring and fusing the primary sensor signals to measure temperature, relative humidity, solar radiation, CO<sub>2</sub>, air pressure and air flow. The measurements are used to calculate net photosynthesis in real time and transmit the data via wireless communication to a sink node. Also it is capable of estimating other response variables such as: carbon content, accumulated photosynthesis and photosynthesis first derivative. This permits the estimation of carbon balance and integrative and derivative variables from net photosynthesis in real time due to the FPGA processing capabilities. In addition, the proposed smart sensor is capable of performing signal processing, such as average decimation and Kalman filters, to the primary sensor readings so as to decrease the amount of noise, especially in the CO<sub>2</sub> sensor while improving its accuracy. In order to prove the effectiveness of the proposed system, an experiment was carried out to monitor the photosynthetic response of chili pepper (*Capsicum annum* L.) as case of study in which photosynthetic activity can successfully be observed during the excitation light periods. Results revealed useful information which can be utilized as new tool for precision agriculture by estimating the aforementioned variables and also the derivative and integrative new indexes. These indexes can be utilized to estimate carbon accumulation over the crop cycle and fast derivative photosynthesis changes in relation to the net photosynthesis measurement which can be utilized to detect different stress conditions in the crops, permitting growers to apply a correction strategy with opportunity.

© 2013 Elsevier B.V. All rights reserved.

### 1. Introduction

The photosynthesis process is the biochemical reaction in which plants transform sunlight energy into chemical energy. In this process, plants fix carbon dioxide (CO<sub>2</sub>) and release oxygen (O<sub>2</sub>). This process is considered the most important biochemical reaction in the world because it produces 90% of the planet biomass (Taiz and Zeiger, 2002). On the other hand, photoinhibition is a term utilized to describe all the environmental conditions that can negatively affect the photosynthetic activity. The most common stress

factor is light. Consequently, accurate photosynthesis measurements are necessary to establish comparisons and understand plant productivity or biomass accumulation at the leaf, plant, canopy, or community levels as well as their interaction and response to environmental (Bakker et al., 2001), chemical (Marschner, 1995), or biological (Stout et al., 1999) factors that generate stress conditions.

Due to the great importance of photosynthesis, accurate measurement methods are required to gather more information about this process. These methods are commonly classified as destructive and non-destructive. Destructive methods are those that cause partial or total destruction of the plant, leaf or tissue during the measurement process. These methods include techniques like dry matter accumulation that consists of drying the plant sample in

\* Corresponding author. Tel.: +52 6677161154x117.

E-mail address: [jrmillan@uas.edu.mx](mailto:jrmillan@uas.edu.mx) (J.R. Millan-Almaraz).

an oven and measuring dry weight to determine accumulated photosynthesis (Hodson et al., 2005), and the isotope method based on the use of carbon isotopes like  $^{11}\text{C}$ ,  $^{12}\text{C}$  and  $^{14}\text{C}$  to obtain marked  $\text{CO}_2$  that is traceable through the plant body, but contaminates the analyzed plant with radioactive  $\text{CO}_2$  as was mentioned by Kawachi et al. (2006) and Millan-Almaraz et al. (2009). Non-destructive photosynthesis measurement methods in contrast, are those that seek to avoid plant damage. These methods include electrochemical methods that consist of red-ox reaction based sensors used to measure oxygen liberation in aqueous algae solutions (Hunt, 2003). Acoustic methods are based on an uncommon technique that measure sea photosynthesis by a quantification of the under-sea sound interruption occurring as a result of the liberation of small  $\text{O}_2$  bubbles through algae photosynthesis (Hermand, 2004). Chlorophyll fluorescence is one of the most utilized photosynthesis measurement techniques. It consists of determining the amount of chlorophyll present in the analyzed sample; this is performed by enclosing the plant sample in a dark chamber, applying light excitation and quantifying the red fluorescence emitted by the plant after the excitation light interruption as was reported by Fedack et al. (2005) and Sayed (2003). This method presents the advantage of being less sensitive to environment factors compared with the  $\text{CO}_2$  exchange method which is the most widely utilized for photosynthesis measurement (Wang et al., 2004).

Gas exchange ( $\text{CO}_2$  and  $\text{H}_2\text{O}$ ) within leaves constitutes the basis of most photosynthesis measurement methods. Since  $\text{CO}_2$  intake and  $\text{H}_2\text{O}$  release share the same biochemical pathway, photosynthesis measurements commonly include the estimation of photosynthesis itself also known as the assimilation or  $\text{CO}_2$  uptake or the stomatal conductance and transpiration (Field et al., 1991). It consists of partially isolating the plant sample in a transparent chamber, using Infrared Gas Analyzer (IRGA)  $\text{CO}_2$  sensors to measure the difference between intake ambient  $\text{CO}_2$  concentration and the final concentration after a period of time to permit plant photosynthesis inside the leaf chamber as reported by Takahashi et al. (2001) and Millan-Almaraz et al. (2009).

Consequently, it can be inferred that the  $\text{CO}_2$  exchange method is more sensitive to environmental factors than chlorophyll-fluorescence based techniques. However,  $\text{CO}_2$  exchange has several advantages over other methods. First, a higher amount of information regarding variables as product of the photosynthesis measurement process can be gathered. These include net photosynthesis itself, carbon content, transpiration, stomatal conductance, dew point, to name but a few. Another advantage is to be less prone to errors due to spatial heterogeneity of stomatal conductance and photosynthetic capacity given by the variability across leaf surfaces. Further, this method permits investigators to determine the exact leaf-area of measurement in the majority of cases, with the exception of small or narrow leaves which do not fill the small chambers (Long and Bernachi, 2003). Due to these aforementioned advantages, the  $\text{CO}_2$  exchange method has been chosen in this investigation.

In previous investigations, the  $\text{CO}_2$  exchange method has been used to measure net photosynthesis ( $P_n$ ) in many photosynthesis measurement systems (Phytech Inc., 2005; CID Inc., 2008). Net photosynthesis is an indirect indicator of the plant's whole biomass production and consequently can be used to estimate crop yield. In biotechnology research,  $P_n$  can be used to characterize the photosynthetic response of new genetically-improved plant varieties. Due to the demands to constantly develop new plant varieties, it is very important to maintain pest and disease resistances in a changing world in which pathogens are continuously mutating to counteract natural and artificially induced plant resistance mechanisms (Torres-Pacheco et al., 2007). Consequently, it is necessary to perform genetic, biochemical and physiological characterizations in order to better understand information regarding

the variety being developed to determine if it is affordable to be utilized for agricultural processes or not. Moreover, it is necessary to characterize the behavior of improved plants in order to add this information in patent documents. In biology research  $P_n$  is studied to understand many processes in wild plants. Forestry and ecological research has also used photosynthesis monitoring as an ecological indicator of pollution as well as to investigate certain properties of trees (Schulze, 1972).

Due to the increasing demand for food, extra efforts and special techniques to increase the food production and information technology is now heavily relied upon in agriculture. Because of the advancements of technologies and reduced size of sensors, the use of sensors and wireless technology are supporting agricultural practices very positively. According to Aqeel-ur-Rehman et al. (in press), the agricultural domain possesses various requirements, some of them requires the collection of weather, crop and soil information. In order to accomplish this, it is necessary to employ parallel and distributed applications. Consequently, these technological advances permit to collect important information and to react to different situations. The commercial equipment used for photosynthesis monitoring in the aforementioned applications perform offline measurements, yet lack the capability of multipoint instrumentation systems for measurement of large crop extensions where using wired communication is expensive and impractical. Consequently, any abnormal or stress conditions cannot be detected *in situ* with opportunity; therefore, it is necessary to have a technician to take the measurements manually in the field or greenhouse. The data collected then has to be manually downloaded to be analyzed offline and make decisions regarding proactive measures with at least a 1 day delay (Ton et al., 2004). In precision agriculture, a 1 day delay can easily represent the loss of the total crop (Millan-Almaraz et al., 2010). Due to the aforementioned shortfalls of multipoint monitoring of photosynthesis response to characterize and monitor diverse physiological responses on plants of commercial interest, a new multipoint monitoring system with wireless communication capabilities to monitor photosynthesis response in a real time way is proposed herein.

A smart sensor is defined as a sensor that provides functions beyond those necessary for generating a correct interpretation of a sensed or controlled quantity (Frank, 2000), based on this; smart sensors must incorporate processing, communication and integration (Rivera et al., 2008). In this investigation the use of oversampling and Kalman filters in order to decrease the amount of noise received in the data collected is proposed, with special emphasis on data that is coming from the  $\text{CO}_2$  sensor. Further, the capability of fusing the information of nodes inside of the sensor network must be taken into consideration. To accomplish this, high performance computational capabilities are required. These days, Field Programmable Gate Arrays (FPGAs) are devices that are being employed in applications where high demand computational resources are necessary (Contreras-Medina et al., 2012). Consequently, these devices have been gaining popularity primarily because of their parallelism, high-speed processing and high reconfigurability (Contreras-Medina et al., 2010). Due to the demands for high computation required in this research the use of FPGA-based smart sensor with capabilities of acquiring the primary sensor readings, memory management, signal processing, photosynthesis calculation, wireless communication management and *in situ* real time photosynthesis signal visualization in a color LCD screen is proposed.

The contribution of this research project is to develop a novel photosynthesis smart sensor capable of acquiring and fusing the primary sensor signals to measure temperature, relative humidity, solar radiation,  $\text{CO}_2$ , air pressure and air flow in order to calculate in real time net photosynthesis and transmit this data via wireless communication to a data server. The wireless communication is

based on Zigbee technology which is preferred over other technologies, such as: Bluetooth, Wibree, and WiFi, mainly because of its long range, low power consumption, and cost (Aqeel-ur-Rehman et al., in press). The photosynthesis calculation is carried out in a specific processing unit embedded in a FPGA. In addition, it is capable of estimating other response variables such as: carbon content, accumulated photosynthesis and transpiration related information as was previously proposed (Millan-Almaraz et al., 2010). It is designed using a combination of several hardware architectures and techniques in order to function in real time. The communication of the proposed smart sensor is composed of a data server for storage and control purposes and a single photosynthesis monitoring smart sensor end point, but it can be upgraded in a future to many end points within the neighborhood of the system.

In order to prove the effectiveness of the proposed smart sensor, an experimental setup was carried out to monitor the photosynthetic response of chili pepper (*Capsicum annuum*) as a case of study.

This paper is organized into four sections: the first presents an introduction to this project; the second presents the materials and methods section to describe devices, methods and all the elements which were utilized in this research for the experiment; the third section illustrates an analysis of the obtained results with a respective discussion; and finally, the fourth section presents conclusions.

## 2. Materials and methods

### 2.1. Photosynthesis measurement

CO<sub>2</sub> gas exchange is the most widely utilized method used for photosynthesis measurement. It is often used to build commercial and experimental photosynthesis monitoring systems by equipment manufacturers. In the technique described herein, closed systems are used with IRGA CO<sub>2</sub> sensors to measure the initial concentration in an isolation chamber where the sample is tested to measure the final concentration after a period of time to permit the photosynthesis of the plant (Phytech Inc., 2005). Open-flow systems have great advantages in comparison to closed systems because photosynthesis occurring delay is not required to record the final concentration of CO<sub>2</sub>. Instead, photosynthesis sampling at higher frequencies than closed systems is permitted. Therefore, it becomes more useful for fast monitoring of photosynthetic phenomena. This also enables the chamber to be interchanged with other chambers possessing differing leaf sizes or shapes, depending on the specie of plant that needs to be monitored.

In order to calculate the net photosynthesis in an open flow system, it is necessary to convert the volumetric air flow into a mass flow by calculating the  $W$  factor by using Eq. (1) as was previously reported by (Millan-Almaraz et al., 2010), in which  $V$  corresponds to the volumetric air flow in the pneumatic line expressed in liters per minute (lpm),  $P$  corresponds to pressure in Bar,  $T_a K$  to air temperature in Kelvin,  $A$  is the leaf chamber area in cm<sup>2</sup>, and the 2005.39 is a constant factor to convert minutes to seconds and centimeters to meters.

$$W = 2005.39 \times \left( \frac{V \times P}{T_a K \times A} \right) \quad (1)$$

Once the  $W$  factor has been calculated,  $P_n$  calculation can be performed using Eq. (2) in which  $C_i$  corresponds to the leaf chamber intake CO<sub>2</sub> concentration in ppm and  $C_o$  is the exhaust CO<sub>2</sub> concentration also in ppm to express net photosynthesis in μmol/m<sup>2</sup>/s.

$$P_n = W \times (C_i - C_o) \quad (2)$$

### 2.2. Smart sensor methodology

The design and development of a photosynthesis smart sensor network requires integrating many subsystems. It involves a data acquisition unit (DAS), a whole pneumatic gas exchange system, a signal processing unit and a wireless communication subsystem. The combination of different primary sensors permits integration of many measurement points. The FPGA-based photosynthesis processor is described in the following subsections.

#### 2.2.1. Pneumatic process

The procedure for photosynthesis measurement is illustrated in Fig. 1. Here, the primary sensors are orange and the two pneumatic lines shown as black arrows can be seen. In the upper part of the figure, there is a reference air channel, which is analyzed to determine the environment properties of the plant neighborhood air such as: air temperature ( $T_a$ ), input relative humidity ( $RH_i$ ), reference air flow ( $V_i$ ), reference pressure ( $P_i$ ) and input CO<sub>2</sub> ( $C_i$ ). The lower pneumatic line corresponds to the air channel that is connected to the leaf gas exchange chamber called a sample air channel. Therefore, it is necessary to analyze the same environmental variables such as the reference channel to establish a comparison between these properties because this is the basis of the gas exchange method. Here, the measured variables are: leaf temperature ( $T_{leaf}$ ), output relative humidity ( $RH_o$ ), reference air flow ( $V_o$ ), sample pressure ( $P_o$ ) and output CO<sub>2</sub> ( $C_o$ ). Furthermore, the data acquisition system can be observed in the middle of Fig. 1 in which all the primary sensors from both reference and sample air channels are connected plus an additional solar radiation sensor to have reference of the start and end of day information which is much related to the photosynthetic activity. Both pneumatic lines were monitored as was aforementioned in order to determine the specific properties of both air channels and later in order to be able to establish a difference between both.

#### 2.2.2. Wireless communication subsystem

The development of the wireless communication subsystem, involves the evaluation of different communication technologies. As an example of this, there are factors such as: bandwidth, transmission rate, total range, scalability and power consumption that need to be taken into consideration. As was previously established by Moreno-Tapia et al. (2010), the IEEE 802.15.4 ZigBee standard which has a theoretical transmission rate of 250 kbps and a maximum range of 1000 m which results in this being the most suitable for this application. This standard works in three different frequency bands and could theoretically contain up to 65,536 nodes managed by a single coordinator on a network and has low energy consumption (IEEE, 2006). Due to these aforementioned benefits, the ZigBee standard is considered as the optimum for this application.

The end point is the smart sensor node equipped with the necessary instrumentation systems to calculate net photosynthesis from the measurement of certain primary sensors. The coordinator node is implemented on a similar platform as the rest of the nodes, but it is responsible for the management of the starting measurement commands up to the smart sensor and to gather its respective photosynthesis results in its personal area network (PAN). The proposed wireless system is capable of communicating directly to a PC through a USB interface in the coordinator device to enable mass storage and better display purposes.

The wireless subsystem is constituted by a star topology network architecture in which a single coordinator node is deployed to manage the smart sensor node which is dedicated to perform photosynthesis analysis. For this application, only one smart sensor is connected for the experiment tests, but additional smart sensor devices can be added in future upgrades.

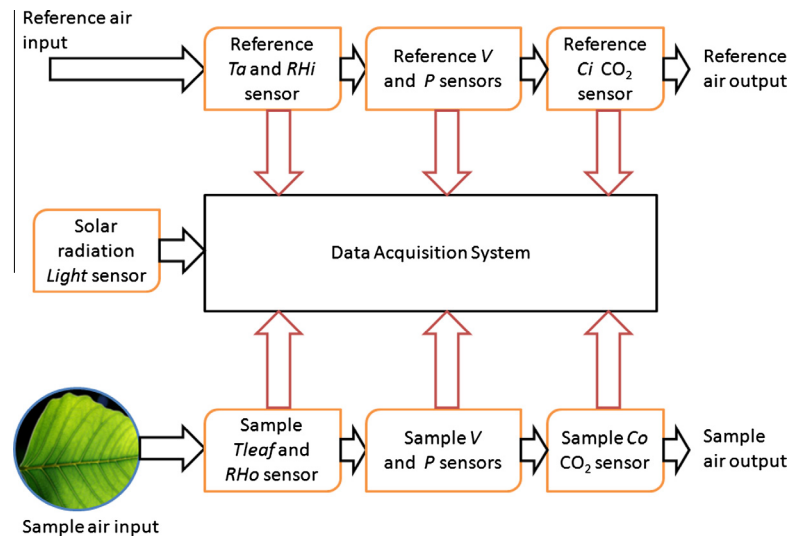


Fig. 1. CO<sub>2</sub> exchange based pneumatic system design.

The smart sensors are composed of three stages: data acquisition card, FPGA unit and a commercial transceiver based on XBEE-Pro transceivers with physical layer, media access control (MAC) and antenna integrated inside the module (Digi International, 2008). Furthermore, the coordinator node consists of the same FPGA module, but with its corresponding coordinator firmware connected to the same Zigbee transceiver and a by USB connection to the PC. The hardware processing unit utilizes low cost FPGA devices to control both smart sensor node and coordinator, but with photosynthesis smart sensor and coordinator firmware respectively.

In order to understand the operation protocol of this system, it is necessary to understand some specifications about the measurement process. Once a measurement command is received by the smart sensor node, it is necessary to acquire the measurements of eleven primary sensors which are  $T_a$ ,  $T_{leaf}$ ,  $RH_i$ ,  $RH_o$ ,  $C_i$ ,  $C_o$ ,  $V_i$ ,  $V_o$ ,  $P_i$ ,  $P_o$  and ambient light (*Light*) at the data acquisition stage. Each of those sensors consists of a two byte format, so 22 bytes are required to start each photosynthesis calculation process. Furthermore,  $P_n$  among others are calculated inside the smart sensor node FPGA-based processing unit. As a result, a row of eleven primary sensor variables plus three response variables are given by each smart sensor; therefore, fourteen variables of two bytes each are used. Consequently, each photosynthesis measurement consists of a 28-byte data frame for each measurement request.

The communication protocol utilizes a star topology network limited to point-to-point for this application to establish the link between coordinator and smart sensor. Each node has a specific 16-bit PAN address, device ID and advanced encryption standard (AES) 128-bit security key configured and stored in the flash memory of the XBee-based transceivers. The coordinator is responsible for associating or disassociating the smart sensor as required by the user as well as sending data request commands to measure, or gather smart sensor status. On the other hand, the smart sensor node has the specific tasks of the photosynthesis measurement process, having association only with the coordinator and being responsible for sending data by request to the coordinator as a reduced functionality device (RFD).

Therefore, the wireless operation consists of sending a measurement command from the coordinator to the smart sensor. Once the command is recognized as start process, the measurement round is initiated and synchronized in time. The whole photosynthesis measurement process takes approximately 7.5 min due to the

complex gas analysis process. Furthermore, the smart sensor sends an “end of process” command to advise to the coordinator that the measurement process is completed. Once the result data is ready, the coordinator starts gathering the results from the smart sensor byte by byte. Finally, the data round is sent to the PC via USB interface for mass storage and display purposes.

A special note regarding the wireless performance of the proposed system. It is necessary to start from the specifications of the utilized transceivers model Xbee-PRO from Digi International (Digi International, 2008), which claim to have an effective communication range of 1.6 km without obstacles, a maximum speed of 250 kbps and a power consumption of approximately 250 mA. Due to the specific environment conditions in this case study, the effective communication range was approximately 500 m, the power consumption was the same as the manufacturer specs and the transmission speed was set to a secure 9600 bps in order to avoid package loss which experimented with transmission speeds of more than 115,200 bps.

### 2.2.3. Wireless coordinator device

The coordinator architecture is controlled by a FPGA device unit which utilizes a Terasic DE0-Nano development board which is based on an Altera EP4CE22F17C6N Cyclone IV device with 22,000 LE, low power consumption and 32 MB of external SDRAM. It embeds many subsystems in order to manage the wireless communication by itself, saving data and graphically demonstrating the smart sensor measurements as can be seen in Fig. 2. The first step has an IEEE 802.15.4 ZigBee transceiver model XBee-PRO (Digi International, 2008) which is connected to a communications management unit which is embedded in the FPGA. This unit is the responsible for the remote administration and data gathering from the smart sensor node. The coordinator block RAM is the storage part of the system in which all the information gathered is concentrated and packaged in order to be sent to a data server through the embedded USB 2.0 interface. The graphics engine is a unit which permits reading of the data which is stored in the block RAM in order to plot in real time the multiple monitored variables in a TFT LCD color display model (Terasic Corporation, 2008). Furthermore, the master control unit performs the process synchronization to manage all of the aforementioned processes which are carried out inside of the coordinator module. The FPGA resource utilization is around 2% of the logic elements (LEs) and 76% of the RAM bits as can be seen in Table 1.

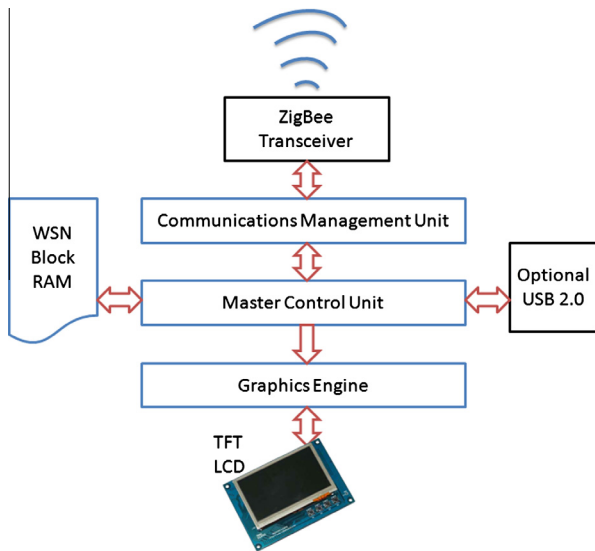


Fig. 2. Coordinator architecture.

As was aforementioned, the coordinator is the responsible for managing the smart sensor node for photosynthesis measurement. Consequently, each measurement which is carried out in the smart sensor node consists of a 28-byte data burst which requires 224-bit from the 608,256-bit available in the internal block RAM of the selected FPGA device. Furthermore, in order to determine the theoretical capability for managing smart sensor nodes by the proposed coordinator it is necessary to divide the maximum RAM availability of 608,256-bit by 224 for each node measurement memory requirement obtaining a theoretical maximum of 2715 nodes that can be managed by a single coordinator device. For this case study, the communication is restricted to only one smart sensor and the coordinator as was aforementioned. The measurement cycle starts when the coordinator sends a measurement command to the smart sensor node to start the gas exchange analysis. Seven minutes later the data is ready and the coordinator starts to gather the results and stores these in its RAM block. Once the data round is completed, the results are sent to a PC through a USB connection to backup measurements in a database.

#### 2.2.4. Smart sensor node

The proposed methodology and its corresponding architecture for the photosynthesis smart sensor are illustrated in Fig. 3. It describes the architecture in the smart sensor in which data acquisition; signal processing and communication capabilities are embedded.

The data acquisition stage includes seven analog primary sensors with corresponding signal conditioning units standardized at a 0–5 V format to measure  $V_i$ ,  $P_i$ ,  $C_i$ ,  $V_o$ ,  $P_o$ ,  $C_o$ , and Light. Air flow for  $V_i$  and  $V_o$  is measured using an Omron D6F Micro Electro Mechanical System (MEMS) based sensors with an accuracy of

$\pm 3\%$  of its measured value and a measurement range of 0–5 lpm (Omron Electronic Components LLC, 2008).  $P_i$  and  $P_o$  are measured using Honeywell Trustability SSC sensors (Honeywell Sensing and Control, 2010). Sensing  $\text{CO}_2$  is the most important part for photosynthesis measurement; consequently, it has been carried out using Edinburgh Instruments Gascheck 2 IRGA based  $\text{CO}_2$  sensors with a measurement range of 0–3000 ppm and an accuracy of  $\pm 30$  ppm (Edinburgh Instruments, 2010). The ambient light sensor is OSRAM SFH5711 with a measurement range of 0–100,000 lux and an accuracy of  $\pm 0.4\%$  of its measured value (Osram Opto-semiconductors Inc., 2007). Each of the previous sensors is sampled via an ADS7844 analog to digital converter which has eight channels, 12-bit resolution, 200 kilo samples per second (ksps) as a maximum sampling frequency ( $f_s$ ) and a serial peripheral interface (SPI) (Burr Brown Corp., 2003). In addition, there are two digital temperature/relative humidity sensors model Sensirion SHT75, which are responsible for measuring  $T_a$ ,  $RH_i$ ,  $T_{leaf}$  and  $RH_o$  with a resolution of 12-bits for RH and 14-bits for temperature and an accuracy of  $\pm 0.4^\circ\text{C}$  of its measured value for temperature and  $\pm 1.8\%$  for RH (Sensirion Co. Ltd., 2009).

The blue modules are embedded inside a FPGA device, model Altera Cyclone IV EP4CE22F17C6N, similar to the one utilized in the coordinator device. It includes all the digital systems (Altera Corp., 2010). The data acquisition control unit is embedded inside the low cost EP4CE22F17C6N FPGA device and is responsible for reading both SHT75 sensors managed in parallel by two embedded controllers for its specific I<sup>2</sup>C modified interface at the same time in which the ADS7844 converter is operated via SPI interface. It is achieved as a result of the FPGA parallel computation capabilities. Moreover, this module controls the RAM access to store the acquired sensors data and to guarantee data access to the next signal processing stage. The signal processing unit is used to perform the primary sensors data filtering operations in order to improve the signal quality and reduce the amount of noise as was previously utilized for robotics vibration monitoring (Rodriguez-Donate et al., 2010) and plant transpiration dynamics real time calculation (Millan-Almaraz et al., 2010). Furthermore, the photosynthesis processor is the real time calculation module utilized to obtain the  $P_n$  value from the primary sensor readings. The communications management unit is the stage which controls the wireless communication between the smart sensor and its coordinator node. It involves recognition of the start measurement command which is sent by the coordinator to begin each measurement cycle and the data sending command to begin the result transmission to the coordinator at the end of the measurement process. Finally, the leaf chamber opening mechanism and vacuum pump is controlled by the FPGA hardware signal processing (HSP) unit. All the aforementioned modules which are embedded inside the FPGA device consume approximately 4% of logic elements, 26% of the total pins, less than 1% RAM bits and 8% of the available  $9 \times 9$ -bit multiplier blocks as can be seen in Table 2.

#### 2.2.5. FPGA-based signal processing unit

The signal processing unit is a stage of the embedded processor included as part of the firmware of each end-point FPGA device which is graphically illustrated in Fig. 4. Here two signal processing stages and response variables calculation processors can be seen. Substantial noise is present in photosynthesis measurements when it is based on the  $\text{CO}_2$  exchange. This is present in the  $\text{CO}_2$  measurements because of the direct dependent relation with the gas law, in which pressure, temperature and volume are involved. Consequently, average decimation filters of 128th order are proposed as a first step to decrease the amount of  $\text{CO}_2$  signal noise. These decimation filters are embedded inside of the FPGA-based signal processing stage of the proposed smart sensor system. Furthermore, each of the primary sensor readings from the ADS7844 such

Table 1  
FPGA resource utilization for the coordinator.

Logic element	Used	Available	Percentage (%)
Total logic elements	430	22,320	2
Total combinational functions	375	22,320	2
Dedicated logic registers	316	22,320	1
Total pins	30	154	19
Total memory bits	458,752	608,256	76
Embedded multiplier 9-bit elements	0	132	0
Total PLLs	0	4	0



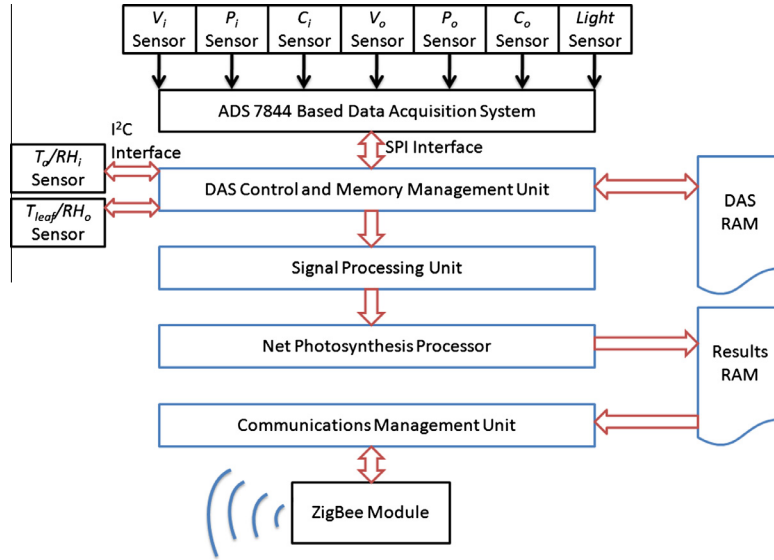


Fig. 3. Photosynthesis smart sensor architecture.

**Table 2**  
FPGA resource utilization for the smart sensor node.

Logic element	Used	Available	Percentage (%)
Total logic elements	920	22,320	4
Total combinational functions	846	22,320	4
Dedicated logic registers	462	22,320	2
Total pins	40	154	26
Total memory bits	224	608,256	<1
Embedded multiplier 9-bit elements	10	132	8
Total PLLs	0	4	0

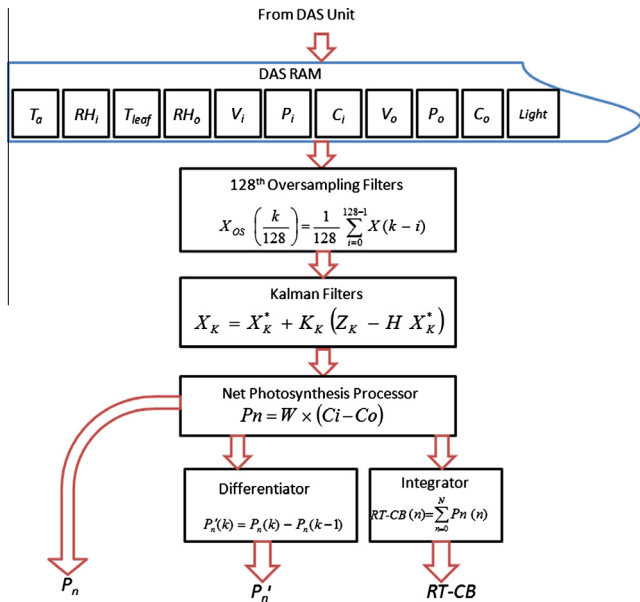


Fig. 4. FPGA signal processing and smart processor unit.

as:  $V_i$ ,  $P_i$ ,  $C_i$ ,  $V_o$ ,  $P_o$ ,  $C_o$ , and Light are introduced to the parallel decimation filters, oversampled and averaged 128 times in order to reduce the quantization and undesired noise based on Eq. (3). Using this method, new signal versions of the primary sensor reading are obtained and distinguished from previous versions by utilizing the

suffix  $os$ , as occurs in (3) where  $X(k)$  can be any primary sensor reading introduced to the decimation filters and  $X_{os}(k)$  is the average decimation filtered version of  $X(k)$ .

$$X_{os}\left(\frac{k}{128}\right) = \frac{1}{128} \sum_{i=0}^{128-1} X(k-i) \quad (3)$$

The Kalman filters are also embedded in the FPGA unit and its algorithm is based on Rodriguez-Donate et al. (2011) description which is based on previously described equations (Marsland, 2009). The Kalman filter is based on statistical processing in which the filter obtains the next state of the signal called prediction and calculates the feedback that is used to apply the correction to the predicted state which is presented in Eqs. (4) and (5).  $S$  is the matrix that relates the previous state and the estimated actual state,  $Q$  is the covariance of the interest signal and  $P^*(k)$  is the a priori estimated error covariance.

$$X^*(k) = S X(k-1) + B u(k-1) \quad (4)$$

$$P^*(k) = S P(k-1) S^T + Q \quad (5)$$

The correction stage is based on Eqs. (6)–(8) where  $R$  is the noise covariance when the interest phenomenon is in steady state,  $H$  relates the sensor measurements ( $Z(k)$ ) with the current state  $X(k)$ ,  $K(k)$ , is the Kalman gain factor which is utilized to minimize the a posteriori error covariance ( $P(k)$ ).

$$K(k) = P^*(k) H^T (H P^*(k) H^T + R)^{-1} \quad (6)$$

$$X(k) = X^*(k) + K(k) (Z(k) - H X^*(k)) \quad (7)$$

$$P(k) = (I - K(k) H) P^*(k) \quad (8)$$

Furthermore,  $X_{os}(k)$  oversampled signals are introduced in the Kalman filters stage to obtain new filtered signals  $X_{osk}(k)$ . To accomplish this,  $S$  is considered to be an identity matrix, previous values  $X = [V_{iosk}^*, P_{iosk}^*, C_{iosk}^*, V_{oosk}^*, P_{oosk}^*, C_{oosk}^*, \text{and } \text{Light}_{osk}^*]^T$  and sensor measurement values  $Z = [V_{iosk}, P_{iosk}, C_{iosk}, V_{oosk}, P_{oosk}, C_{oosk}, \text{and } \text{Light}_{osk}]^T$  where  $Q$  is a diagonal matrix which contains the covariance of each  $X_{os}(k)$  signal. Therefore,  $R$  is also a diagonal matrix that includes the noise covariance of each variable. Finally,  $H$  is an identity matrix.

Once  $X_{osk}(k)$  signals are calculated, the net photosynthesis processor performs the  $P_n$  computation based on the primary sensor readings. To accomplish this,  $W$  is calculated as a first step to convert from volumetric gas flow into mass gas flow. Consequently,  $W$  is multiplied by the difference between carbon intake and carbon out in order to obtain  $P_n$  according to Eq. (2) as written above.

**2.2.5.1. Net photosynthesis integration.** It is frequently important to obtain quantitative assessment of plant growth, primary productivity and the impact of climate change on vegetation. One way to achieve this is by having knowledge of the crop carbon balance which is based in part on photosynthesis measurements (Albrizio and Steduto, 2003) based on responses of  $CO_2$  gains. Sakai et al. (2000) calculated carbon daily gain and carbon total gain during an experiment by integrating the net photosynthesis and gross photosynthesis measurements to study the impact of different levels of  $CO_2$  in rice. Choudhury, 2000 obtained gross photosynthesis by integrating instantaneous measurements to study the impact of biophysical parameters related to radiation use efficiency of wheat during its vegetative period; similarly, Albrizio and Steduto (2003) correlated the generated biomass with cumulative photosynthesis measurements to study carbon use and growth efficiency; consequently, in several studies it is important to associate the crop yield with the photosynthetic activity or obtain gross photosynthesis measurements by integrating instantaneous measurements in order to have an indicator of the quantity of the production based on the photosynthesis data or evaluate the impact of different treatments or management practices. Consequently, the real time-carbon balance (rtcb) is a novel term that is proposed in this research project as a new index which was obtained experimentally and can serve to indicate the accumulation of carbon due to the photosynthetic activity. It can be calculated by obtaining the integral of  $p_n$  function as can be described in Eq. (9), where rtcb is the continuous time version. It can be utilized in future applications to estimate, in real time, carbon fixing via accumulated photosynthetic activity and carbon losses due to night respiration. It permits investigators to determine the carbohydrate accumulation in a way that can be utilized to determine the crop yield early; therefore, constituting a new tool for precision agriculture. In order to have a digitally implementable equation of (9), it can be translated to its discrete time version of real time carbon balance (RTCB) to obtain Eq. (10), where the integral is changed into an accumulated addition and obtaining the discrete time versions of the variables such as: RTCB and  $P_n$

$$rtcb(t) = \int_a^b p_n(t) dt \quad (9)$$

$$RTCB(k) = \sum_{k=0}^N P_n(k) \quad (10)$$

**2.2.5.2. Net photosynthesis first derivative.** The study of growth efficiency of the plants and the impact of different treatments in biomass production results are of great importance in agricultural investigations (Sakai et al., 2000; Albrizio and Steduto, 2003). Albrizio and Steduto (2003) obtained the slope of regressions between photosynthesis and respiration measurements to evaluate the carbon use and growth efficiency of certain  $C_3$  and  $C_4$  plants. Consequently, the first derivative factor of net photosynthesis in continuous time ( $p'_n$ ) and its discrete time version ( $P'_n$ ) as another novel indicator obtained through experimentation to analyze diverse phenomena involved in the changes of photosynthetic activity such as the carbon use and growth efficiency is proposed herein. This index can also be used in future investigations to analyze and quantify the effect of different treatments and

management practices on the rate of photosynthetic activity in plants.  $p'_n$  is calculated by performing the first derivative of  $p_n$  as is established in Eq. (11). As occurred with RTCB, in order to be able to implement  $p'_n$  in a digital system it is necessary to obtain its discrete time version  $P'_n$  which result from Eq. (12).

$$p'_n = \frac{p_n}{dt} \quad (11)$$

$$P'_n(k) = P_n(k) - P_n(k-1) \quad (12)$$

### 2.3. Photosynthesis smart sensor and commercial equipment

Once the proposed photosynthesis smart sensor was explained in the previous sections, it is necessary to clarify the advantages and disadvantages of the proposed project in comparison with commercial equipment alternatives. In Table 3, it can be observed a detailed comparison of the main characteristics between commercial photosynthesis monitoring systems and the proposed smart sensor. Here can be observed a similar tendency in the commercial equipment by having only one leaf chamber, microprocessor based system and non-automated leaf chamber mechanism in the Li-6400XT (LI-COR Inc., 2010), CIRAS-2 (PP Systems, 2012), CI-340 (CID Inc., 2008) and GFS-3000 (Heinz Walz GmbH, 2012). Also, they have similar communication interfaces such as RS232, RS485 and USB connection and lack of wireless capability. The PTM-48M is a little bit different by having four leaf chamber which are automated by a pneumatic mechanism but have less memory capacity to store data and delivers less response variables (Phytech Inc., 2005). In contrast, the proposed wireless smart sensor for photosynthesis monitoring have wireless capability to communicate between the data storage computer and the smart sensor, allowing to be deployed in the field as a stand-alone device due to its automated leaf chamber mechanism which is based in a miniature servomotor. Another significant advantage of the proposed system is the use on a FPGA device as digital controller which allows performing digital signal processing *in situ* to add complex digital filtering stages such as 128 order oversampling and Kalman filters to improve signal quality which is difficult to be implemented in a microprocessor based system. Furthermore, two novel indexes can be calculated by the proposed system which are RTCB and  $P'_n$  to describe additional photosynthesis related information.

### 2.4. Experiment setup

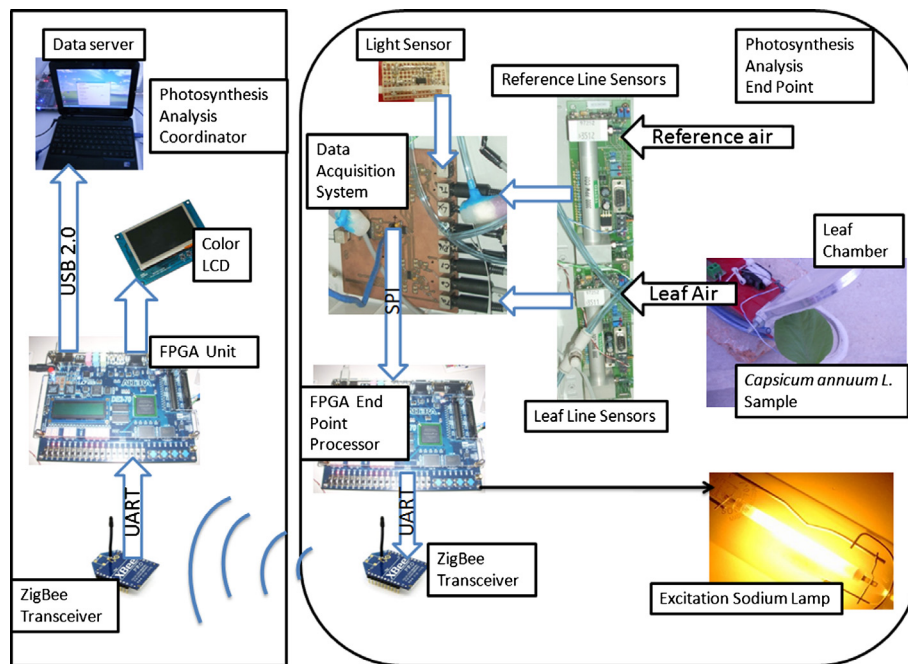
In this section, the experiment setup which is utilized to test the proposed photosynthesis smart sensor is presented. This includes the primary sensor reading results and its corresponding signal processing treatments to improve these signals plus a graphic comparison in the primary sensor signals  $X(k)$ ,  $X_{os}(k)$  and  $X_{osk}(k)$ . Further, a subsection to include the photosynthesis real time analysis and its results is also presented. Finally, the last subsection presents results to detect on line and in real time photosynthesis stress conditions which can hinder achieving a good  $P_n$  rate.

The experiment setup can be seen in Fig. 5 and it is based on coordinator linked to smart sensor architecture. The smart sensor device was based on the aforementioned DAS where both reference and leaf sample air was analyzed by the temperature, RH, pressure, flow and  $CO_2$  sensors. The DAS is controlled via SPI in the FPGA unit. As biological material, a *C. annum* L. plant is utilized as case study. In order to induce photosynthesis related activity on the plant sample, a high pressure sodium lamp (HPSL) capable of supplying a 10,000 lux artificial light source is utilized to excite the plant sample. The lamp was controlled by the FPGA,

**Table 3**

Comparison of commercial photosynthesis measurement systems with the proposed smart sensor.

	PTM-48M	Li-6400XT	CIRAS-2	CI-340	GFS-3000	Proposed smart sensor
Manufacturer	Phytech Inc.	Li-cor Biosciences	PP Systems	CID Inc.	Heinz Walz GmbH	Authors
Clamp isolation mechanism	Pneumatic	Manual	Manual	Manual	Manual	Servomotor
ADC resolution	12-bit	Not specified	Not specified	Not specified	Not specified	12-bit
Number of leaf chambers	4	1	1	1	1	1 per node
Communication interface	RS232	RS232, Ethernet	RS232, USB	RS232, USB	RS485, USB	RS232, USB and ZigBee
Storage capacity	256 samples	Compact Flash	RAM	4 MB RAM	7.4 GB Compact flash	32 MB Onboard SDRAM/Server HDD
CPU type	Microprocessor	Microprocessor	Microprocessor	Microprocessor	Microprocessor	FPGA
Real time photosynthesis processing	No	Yes	Yes	No	Yes	Yes
Sensor measured variables	$T_a$ , $RH$ , $CO_2$ , $V$ , $P$	$T_a$ , $RH$ , $CO_2$ , $V$ , $P$ , $Light$	$T_a$ , $RH$ , $CO_2$ , $V$ , $P$ , $Light$	$T_a$ , $RH$ , $CO_2$ , $V$ , $P$ , $Light$	$T_a$ , $RH$ , $CO_2$ , $V$ , $P$ , $Light$	$T_a$ , $RH$ , $CO_2$ , $V$ , $P$ , $Light$
Response calculated variables	$E$ , $P_n$ , $VPD$	$E$ , $g_s$ , $P_n$ , Dew point	$E$ , $g_s$ , $P_n$ , Dew point	$E$ , $g_s$ , $P_n$ , Dew point	$E$ , $g_s$ , $P_n$ , Dew point, $VPD$	$E$ , $g_s$ , $P_n$ , Dew point, $VPD$ , $P_n'$ , $RTCB$
In situ graphic capabilities	No	Yes, B&W LCD	Yes, Color LCD	Yes, B&W LCD	Yes, Color LCD	Yes, Color LCD
Automatic mechanism capabilities	Yes	No	No	No	No	Yes
Wireless capability	No	No	No	No	No	Yes
Digital signal processing capabilities (Oversampling and Kalman filters)	No	No	No	No	No	Yes
Multi node measurement capabilities	No	No	No	No	No	Yes

**Fig. 5.** Experiment setup for the proposed smart sensor.

which turned it on at 9 AM and off at 9 PM. The light sensor permits observation of the exact moment when the lamp is activated and deactivated. All the information gathered is processed by the FPGA smart sensor unit and sent to the coordinator system via ZigBee RF communication when it is required. The coordinator unit gathers the primary sensor readings and photosynthesis response variables from the ZigBee network to be sent to a data server via USB interface for data backup purpose and plotted in parallel in a 4.5 in. TFT color LCD to visualize the acquired data. The data sampling was configured to acquire one photosynthesis measurement every 30 min in order to permit the pneumatic line transient filling when the system is started and avoid excessive plant damage when the servomotor based mechanism performs the isolating process.

### 3. Results and discussion

#### 3.1. Primary sensor results

The signal processing unit, which is embedded inside of the FPGA device, is responsible for carrying out all the necessary signal treatment algorithms in order to reduce the noise in the primary sensor readings. The general procedure consists of acquiring any primary sensor signals as  $X(k)$ , then applying a 128th oversampling filter to reduce the noise as a first improvement in obtaining the oversampled version of the signal as  $X_{os}(k)$  and finally passing it through a Kalman filter to obtain the most noise filtered version  $X_{osk}(k)$ . This procedure is applied to any primary sensor signal.

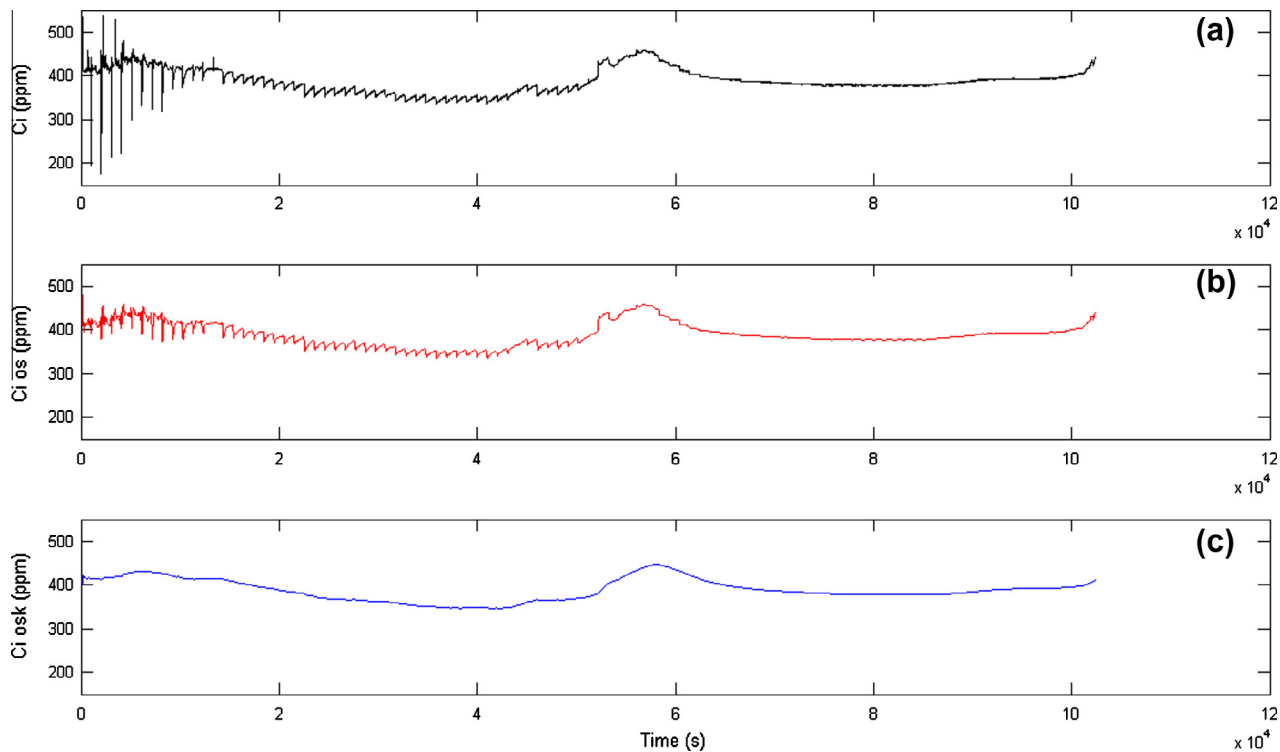


Fig. 6. Difference between CO<sub>2</sub> signals. (a) CO<sub>2</sub> signal acquired directly from the CO<sub>2</sub> gas analyzer. (b) Intermediate CO<sub>2</sub> signal obtained by filtering previous signal through the oversampling filter. (c) Final CO<sub>2</sub> signal obtained by filtering the previous CO<sub>2</sub> oversampled signal through Kalman filter.

In photosynthesis measurement, it is very difficult to obtain a good  $P_n$  estimation results due to the CO<sub>2</sub> sensors low stability. An example of this is the fact that, commercial CO<sub>2</sub> sensors have accuracies of  $\pm 100$  ppm to as low as  $\pm 20$  ppm with a pricing increase when the accuracy is better. The main problem is that photosynthesis is a phenomenon in which the carbon fixing rates are approximately less than 1–50 ppm with typical fixing of 5 ppm. Consequently, it can be inferred that it is impossible to measure results of a phenomenon in which the interest measurement is a difference of 5 ppm using a sensor with  $\pm 100$  ppm of noise. Consequently, advanced signal processing techniques are applied to the CO<sub>2</sub> readings as example of the rest of the primary sensors because this sensor is the noisiest. In Fig. 6, three signals can be seen. The black one represents the original CO<sub>2</sub> sampling signal sampled at 1 sample per second (SPS). Here, a large amount of glitches at the star of the measurements can be noticed due to the CO<sub>2</sub> sensor accuracy, gas law noise which can be derived from pressure, flow, and temperature. It is noteworthy that moisture interferes with the IRGA sensor infrared absorption principle because hetero-atomic molecules such as CO<sub>2</sub> or also H<sub>2</sub>O can absorb the infrared radiation. All of this results in a very noisy black signal which must be digitally filtered. As a result, the aforementioned 128th average decimation filter is applied to the black signal and the red signal is obtained as a first stage filtered signal where the initial glitches are reduced as a consequence of the oversampling process in which 128 samples were taken averaged and finally only one result is delivered at its output. Furthermore, the red signal is introduced to a Kalman filter stage which is fine tuned to track and filter the CO<sub>2</sub> signal resulting in a very clear CO<sub>2</sub> measurement in which the accuracy noise and other perturbations are eliminated. This result in a new blue signal that has the necessary stability to be used for photosynthesis measurement purposes in which 5 ppm differences between  $C_i$  and  $C_o$  are common differences and noisy sensors are not suitable to measure this.

### 3.2. Acquisition of primary sensor signals

As a result of the requirement to have a new smart sensor that fuses many primary sensor signals, a novel photosynthesis smart sensor is proposed in order to be able to measure photosynthesis in real time that possesses graphic visualization, instant value measurement and longtime data logging capabilities in a multi-point instrumentation scheme. The results of the acquired signals at the output of the Kalman filters can be seen in Fig. 7. These signals from the primary sensors of temperature, moisture to name but a few which are required to calculate the photosynthesis related variables such as  $P_n$ ,  $RTCB$  and  $P'_n$ . This acquisition process was carried out in a 1 week monitoring cycle to be able to demonstrate day and night changes in the data. It includes air and leaf temperature measurement, moisture, air flow, carbon dioxide and ambient light. Furthermore, these signals are introduced to the processing unit in the FPGAs of the smart sensor unit to continue with the processing stage to calculate the photosynthesis related information.

### 3.3. Fused real time photosynthesis analysis

Due to the parallel and reconfigurable capabilities of the FPGA based smart sensor, a new methodology for real time photosynthesis analysis which involves many factors such as  $P_n$ ,  $RTCB$  and  $P'_n$  to better explain all the photosynthesis related phenomena that occurs in plants is proposed. A light measurement is included in this fused analysis to track the photosynthesis process and its excitation light source activity. In Fig. 8 a graphical description of the fused photosynthesis analysis is presented.

#### 3.3.1. Photosynthesis results

First, the light primary reading can be seen in order to track the excitation light source. It is noteworthy that this process was

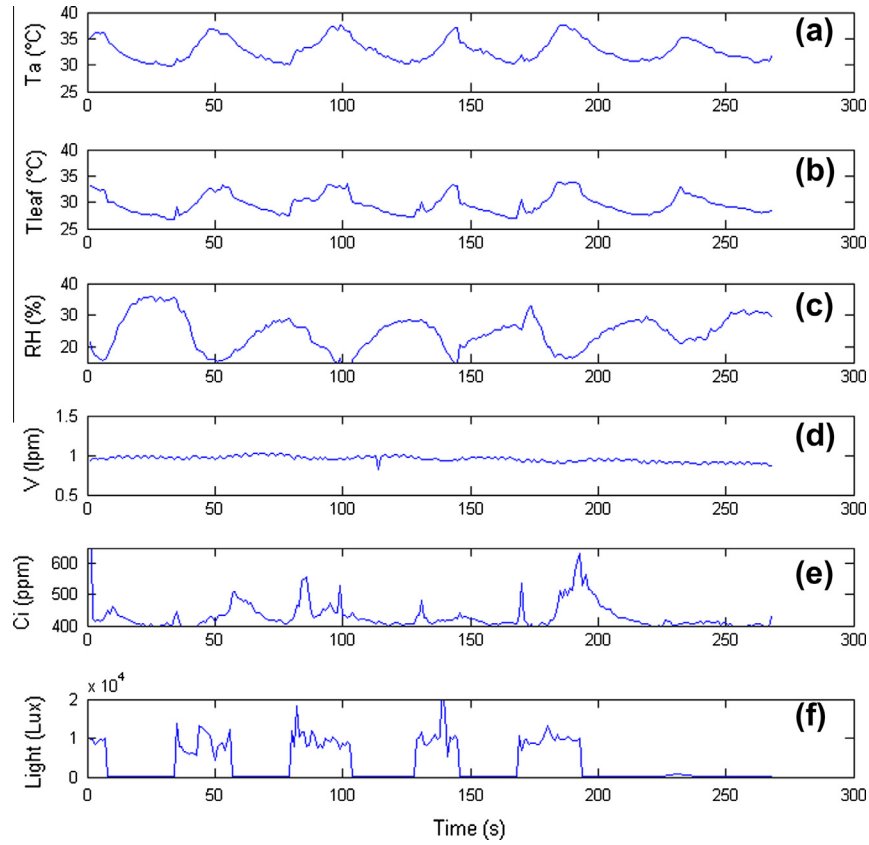


Fig. 7. Signals acquired by the primary sensors. (a) Air temperature. (b) Leaf temperature. (c) Air relative humidity. (d) Volumetric air flow. (e) Input carbon dioxide. (f) Light.

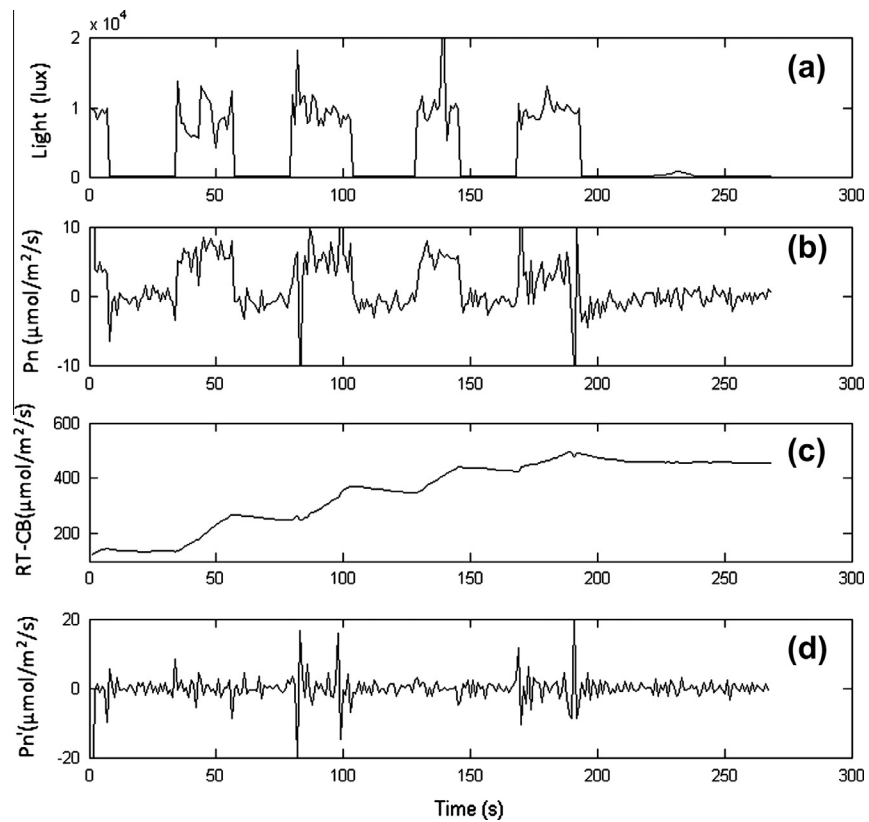


Fig. 8. Real time photosynthesis analysis for *Capsicum annum L.* (a) Ambient light signal, (b) Net photosynthesis measurement signal, (c) Real time carbon balance and (d) First derivative of net photosynthesis.

running for 6 days with a photosynthesis sampling frequency of 1 sample each 30 min. In the second signal which corresponds to  $P_n$ , as seen in Fig. 8, there is a direct relationship between light and  $P_n$  because  $P_n$  is activated only in the periods when the sodium lamp is activated. This is only from 9 AM to 9 PM and there are respiration periods during the nights where a negative photosynthesis is measured as a consequence of  $\text{CO}_2$  release activity where dry matter is lost.

### 3.3.2. Real time-carbon balance RTCB results

As was aforementioned, RTCB is a novel index that results from the  $P_n$  integral calculation and it is proposed as a tool for photosynthesis analysis. As can be seen in Fig. 8 the RTCB takes an increasingly line like behavior when the plant sample has a good photosynthetic activity with a decreasing tendency during the nights when the sodium lamp is disconnected. Furthermore, it can be noted that this behavior continues until the night of the 200th sample. After this point in time the sodium lamp was not turned on the following day, to induce photo-inhibition conditions. In such a situation the RTCB behavior stops its increasing behavior because the low photosynthetic activity turns to respiration and loses dry matter. This novel index can be utilized in future research to measure the global carbon assimilation without the need for destructive methods to dehydrate plant samples. Also it can be utilized for many applications such as estimating the crop yield based on real time RTCB measurements.

### 3.3.3. Net photosynthesis first derivative factor results

This is another novel index being proposed in this article for real time photosynthesis analysis that as was previously established. It results from the  $P_n$  differentiation. In Fig. 8, the last signal in which the high frequency components of  $P_n$  are extracted through the first derivative can be seen. This permits one to observe the changing factor of  $P_n$  where a high frequency activity increase can be seen before the photosynthesis process starts. It can be checked by comparing the changes in photosynthesis related activity in  $P_n$ , RTCB and  $P'_n$ . This index can be used to detect external perturbations in precision agriculture applications, for example, to study phenomena with fast photosynthesis changes that may be observed in  $P'_n$ .

## 4. Conclusions

A novel photosynthesis analyzer based on smart sensor architecture is proposed in order to establish a new real time analysis methodology that includes wireless capabilities. Each smart sensing node includes many fused primary sensor readings that can be useful to determine environmental conditions that can harm and affect the plant global photosynthetic activity that will be reflected in the final crop yield. This sensor network permits detection of photosynthesis inhibition conditions in real time by relating the primary sensor readings with the response variables such as net photosynthesis that have been widely studied for many years already. Further, novel variables such as RTCB and  $P'_n$  can be used in future research primarily as quantitative indicators of plant growth, carbon use and growth efficiency and principally to evaluate different treatments or management practices that can negatively affect the plant biomass production. All of the aforementioned variables can be utilized together to analyze in an on-line method different crops as a result of wireless capabilities. The proposed wireless monitoring system constitutes a new tool that can be used in future research in precision agriculture and biotechnology seed improvement to characterize photosynthesis related phenomena.

## Acknowledgements

This project was partially supported by CONACYT Ph. D. scholarship 207684 and post-doctoral scholarship 161832. Also thanks to Altera Corp. for the donation of an Altera DE2-70 3 in 1 FPGA development kit used in this project and Texas Instruments for providing device samples tested in this project. Finally, the authors wish to thank Silvia C. Stroet for her support by doing the English language edition.

## References

- Albrizio, R., Steduto, P., 2003. Photosynthesis, respiration and conservative carbon use efficiency of four field grown crops. *Agricultural and Forest Meteorology* 116 (1–2), 19–36.
- Altera Corp., 2010. Cyclone II Hand Book Volume 1. Altera Corp., San Jose, CA, USA.
- Aqeel-ur-Rehman, Abbasi, A.Z., Islam, N., Shaikh, Z.A., in press. A review of wireless sensors networks applications in agriculture. *Computer Standards and Interfaces*.
- Bakker, J.C., Bot, G.P.A., Challa, H., Braak, N.J., 2001. *Greenhouse Climate Control: An Integrated Approach*. Wageningen Academic Publishers.
- Burr Brown Corp., 2003. ADS7844 Data Sheet. Burr Brown Corp., Dallas, TX, USA.
- Choudhury, B.J., 2000. A sensitivity analysis of the radiation use efficiency for gross photosynthesis and net carbon accumulation by wheat. *Agricultural and Forest Meteorology* 101 (2–3), 217–234.
- CID Inc., 2008. CI-340 Hand-held Photosynthesis System Instruction Manual. CID Inc., Camas, WA, USA.
- Contreras-Medina, L.M., Osornio-Rios, R.A., Torres-Pacheco, I., Romero-Troncoso, R.J., Guevara-Gonzalez, R.G., Millan-Almaraz, J.R., 2012. Smart sensor for real-time quantification of common symptoms present in unhealthy plants. *Sensors* 12 (1), 784–805.
- Contreras-Medina, L.M., Romero-Troncoso, R.J., Cabal-Yepez, E., Rangel-Magdaleno, J.J., Millan-Almaraz, J.R., 2010. FPGA based multiple-channel vibration analyzer for industrial application in induction motor failure detection. *IEEE Transactions on Instrumentation and Measurement* 59 (1), 63–72.
- Digi International, 2008. XBEE Multipoint RF Modules Product Datasheet, Digi International, Minnetonka, MN, USA.
- Edinburgh Instruments, 2010. Gascheck 2 User manual. Edinburgh Instruments, Livingston, UK.
- Fedack, V., Kytav, O., Klochan, P., Romanov, V., Voytovych, I., 2005. Portable chlorofluorometer for express-diagnostics of photosynthesis. *IEEE Workshop on Intelligent Data Acquisition and Advanced Computing Systems: Technology and Applications*, Sofia, Bulgaria, September 2005, pp. 287–288.
- Field, C.B., Ball, J.T., Berry, J.A., 1991. *Photosynthesis: Principles and Field Technique. Field Methods and Instrumentation: Plant Physiological Ecology*. Chapman and Hall, pp. 209–253.
- Frank, R., 2000. *Understanding Smart Sensors*, second ed. Artech House, Norwood, MA, USA, pp. 1–15.
- Heinz Walz GmbH, 2012. GFS-3000 Portable Gas Exchange Fluorescence System Brochure. Heinz Walz GmbH, Effeltrich, Germany.
- Hermand, J.P., 2004. Photosynthesis of seagrasses observed In Situ from acoustic measurements. *OCEANS '04. Mts./IEEE Technol. Ocean.*, pp. 433–437, IEEE.
- Hodson, M.J., White, P.J., Mead, A., Broadley, M.R., 2005. Phylogenetic variation in the silicon composition of plants. *Annals of Botany* 96, 1027.
- Honeywell Sensing and Control, 2010. Trustability Silicon Pressure Sensors: SSC Series-Standard Accuracy Datasheet. Honeywell Sensing and Control, Golden Valley, MN, USA.
- Hunt, S., 2003. Measurements of photosynthesis and respiration in plants. *Physiologia Plantarum* 117, 314–325.
- IEEE, 2006. IEEE 802.15.4 Standard. Part 15.4: Wireless Medium Access Control (MAC) and Physical Layer (PHY) Specifications for Low-Rate Wireless Personal Area Networks (LR-WPANs). IEEE, Piscataway, NJ, USA.
- Kawachi, N., Sakamoto, K., Ishii, S., Fujimaki, S., Suzui, N., Ishioka, N.S., Matsushashi, S., 2006. Kinetic analysis of carbon-11-labeled carbon dioxide for studying photosynthesis in a leaf using positron emitting tracer imaging system. *IEEE Transactions on Nuclear Science* 53 (5), 2991–2997.
- LI-COR Inc., 2010. LI-6400XT User Manual. LI-COR Inc., Lincoln, NE, USA.
- Long, S.P., Bernachi, C.J., 2003. Gas exchange measurements, what can they tell us about the underlying limitations to photosynthesis? Procedures and sources of error. *Journal of Experimental Botany* 54 (392), 2393–2401.
- Marschner, H., 1995. *Mineral Nutrition of Higher Plants*. Academic Press, San Diego, CA, USA.
- Marsland, S., 2009. *Machine Learning: An Algorithmic Perspective*, first ed. Chapman and Hall/CRC, Boca Raton, FL, USA, pp. 356–359.
- Millan-Almaraz, J.R., Guevara-Gonzalez, R.G., Romero-Troncoso, R.J., Osornio-Rios, R.A., Torres-Pacheco, I., 2009. Advantages and disadvantages on photosynthesis measurement techniques: a review. *African Journal of Biotechnology* 8 (25), 7340–7349.
- Millan-Almaraz, J.R., Romero-Troncoso, R.J., Guevara-Gonzalez, R.G., Contreras-Medina, L.M., Carrillo-Serrano, R.V., Osornio-Rios, R.A., Duarte-Galvan, C., Rios-Alcaraz, M.A., Torres-Pacheco, I., 2010. FPGA-based fused smart sensor for real-time plant-transpiration dynamic estimation. *Sensors* 10 (9), 8316–8331.

- Moreno-Tapia, S.V., Vera-Salas, L.A., Osornio-Rios, R.A., Dominguez-Gonzalez, A., Stiharu, I., Romero-Troncoso, R.J., 2010. A field programmable gate array-based reconfigurable smart-sensor network for wireless monitoring of new generation computer numerically controlled machines. *Sensors* 10 (8), 7263–7286.
- Omron Electronic Components LLC, 2008. MEMS Flow Sensor D6F-01/02/05 Datasheet. OMRON Electronic Components LLC, Schaumburg, IL, USA.
- Osram Opto Semiconductors Inc., 2007. SFH-5711 Data sheet. OSRAM Opto Semiconductors Inc., Munich, Germany.
- Phytech Inc, 2005. PTM-48M User Manual. Phytech Inc., Yad Mordechai, Israel.
- Systems, P.P., 2012. CIRAS-2 User Manual. PP Systems, Amesbury, MA, USA.
- Rivera, J., Herrera, G., Chacon, M., Acosta, P., Carillo, M., 2008. Improved progressive polynomial algorithm for self-adjustment and optimal response in intelligent sensors. *Sensors* 8 (11), 7410–7427.
- Rodriguez-Donate, C., Morales-Velazquez, L., Osornio-Rios, R.A., Herrera-Ruiz, G., Romero-Troncoso, R.J., 2010. FPGA-based fused smart sensor for dynamic and vibration parameter extraction in industrial robot links. *Sensors* 10 (4), 4114–4129.
- Rodriguez-Donate, C., Osornio-Rios, R.A., Rivera-Guillen, J.R., Romero-Troncoso, R.J., 2011. Fused smart sensor network for multi-axis forward kinematics estimation in industrial robots. *Sensors* 11 (4), 4335–4357.
- Sakai, H., Yagi, K., Kobayashi, K., Kawashima, S., 2000. Rice carbon balance under elevated CO<sub>2</sub>. *New Phytologist* 150 (2), 241–249.
- Sayed, O.H., 2003. Chlorophyll fluorescence as a tool in cereal crop research. *Photosynthetica* 41 (3), 321–330.
- Schulze, E.D., 1972. A new type of climatized gas exchange chamber for net photosynthesis and transpiration measurements in the field. *Oecologia* 10, 243–251.
- Sensirion Co. Ltd., 2009. Datasheet SHT7x (SHT71, SHT75) Humidity and Temperature Sensor. Sensirion Co. Ltd., Staefa, ZH, Switzerland.
- Stout, M.J., Fidantsef, A.L., Duffey, S.S., Bostock, R.M., 1999. Signal interactions in pathogen and insect attack: systemic plant-mediated interactions between pathogens and herbivores of the tomato, *Lycopersicon esculentum*. *Physiological and Molecular Plant Pathology* 54 (3–4), 115–130.
- Taiz, L., Zeiger, E., 2002. *Plant Physiology*, fifth ed. Sinauer Associates, Sunderland Mass, pp. 111–192.
- Takahashi, M., Ishiji, T., Kawashima, N., 2001. Handmade oxygen and carbon dioxide sensors for monitoring the photosynthesis process as instruction material for science education. *Sensors Actuators B* 77, 237–243.
- Corporation, Terasic., 2008. LTM User Manual. Terasic Corporation, Hsinchu, TW.
- Ton, Y., Kopyt, M., Nilov, N., 2004. Phytomonitoring technique for tuning irrigation of vineyards. *Acta Horticulturae* 646, 133–139.
- Torres-Pacheco, I., Gonzalez-Chavira, M.M., Villaseñor-Mir, H.E., Huerta-Espino, J., Villordo-Pineda, E., Espitia-Rangel, E., Guevara-Gonzalez, R., 2007. Genetic markers of resistance to rust stem (*Puccinia graminis* Persoon f. sp. *avenae*) in oat (*Avena sativa* L.). *Agricultura Técnica en México* 33 (3), 221–230.
- Wang, C., Xing, D., Chen, Q., 2004. A novel method for measuring photosynthesis using delayed fluorescence of chloroplast. *Biosensors and Bioelectronics* 20 (3), pp. 454–259.

Review

## Instrumentation in Developing Chlorophyll Fluorescence Biosensing: A Review

Arturo A. Fernandez-Jaramillo <sup>1</sup>, Carlos Duarte-Galvan <sup>1</sup>, Luis M. Contreras-Medina <sup>1,2</sup>, Irineo Torres-Pacheco <sup>1</sup>, Rene de J. Romero-Troncoso <sup>2</sup>, Ramon G. Guevara-Gonzalez <sup>1</sup> and Jesus R. Millan-Almaraz <sup>3,\*</sup>

<sup>1</sup> Biosystems Engineering CA, Postgraduate Study Division, Engineering Faculty, Autonomous University of Queretaro, Cerro de las Campanas St., Querétaro, 76010, Qro., Mexico; E-Mails: aafernandez@hspdigital.org (A.A.F.-J.); cduarte20@alumnos.uaq.mx (C.D.-G.); mcontreras@hspdigital.org (L.M.C.-M.); irineo.torres@uaq.mx (I.T.-P.); ramon.guevara@uaq.mx (R.G.G.-G.)

<sup>2</sup> HSPdigital-CA Mecatronics, Engineering Faculty, Autonomous University of Queretaro, Campus San Juan del Rio, 249 Rio Moctezuma St., San Juan del Rio, 76807, Qro., Mexico; E-Mail: troncoso@hspdigital.org

<sup>3</sup> Faculty of Physics and Mathematics, Autonomous University of Sinaloa, Universitarios Blvd., De las Americas Ave., Cd. Universitaria, Culiacan, 80000, Sinaloa, Mexico

\* Author to whom correspondence should be addressed; E-Mail: jrmillan@uas.edu.mx; Tel.: +52-667-716-1154 (ext. 117).

Received: 25 June 2012; in revised form: 9 August 2012 / Accepted: 13 August 2012 /

Published: 29 August 2012

---

**Abstract:** Chlorophyll fluorescence can be defined as the red and far-red light emitted by photosynthetic tissue when it is excited by a light source. This is an important phenomenon which permits investigators to obtain important information about the state of health of a photosynthetic sample. This article reviews the current state of the art knowledge regarding the design of new chlorophyll fluorescence sensing systems, providing appropriate information about processes, instrumentation and electronic devices. These types of systems and applications can be created to determine both comfort conditions and current problems within a given subject. The procedure to measure chlorophyll fluorescence is commonly split into two main parts; the first involves chlorophyll excitation, for which there are passive or active methods. The second part of the procedure is to closely measure the chlorophyll fluorescence response with specialized instrumentation systems. Such systems utilize several methods, each with different characteristics regarding to cost,



resolution, ease of processing or portability. These methods for the most part include cameras, photodiodes and satellite images.

**Keywords:** fluorescence; chlorophyll; photosynthesis; instrumentation; LED; laser; Kautsky

---

## 1. Introduction

Plants are among the most evolved beings on the planet; for example, unlike humans they are capable of producing their own nourishment through the process of photosynthesis. During this process sunlight energy is stored, and subsequently, in conjunction with water and carbon dioxide, forms carbohydrates and expels oxygen into the atmosphere [1]. However, plants cannot assimilate all the stored energy and approximately 5–10% of the total absorbed energy is accumulated as dry matter [2]. Consequently, plants are considered to be low-efficiency organisms. The excess energy is absorbed by the leaves must be dissipated through different paths involving thermal dissipative process, fluorescence emissions and photochemistry [3]. These losses can be utilized to research certain physiological behaviors in plants, such as photochemical and non-photochemical quenching.

Chlorophyll fluorescence is the red and far-red light emitted by photosynthetic tissue when it is excited by a light source [4]. Chlorophyll measurement is a non-invasive method for imaging photosynthetic fluxes because fluorescence depends directly on photosynthetic activity and it can be inferred through this [5–7].

This article reviews many applications in the measurement of fluorescence, most notably the detection of plant stress factors, with the objective of improving comfort conditions for the plant and providing higher production rates [8–11]. There are many factors that can produce plant diseases like stress caused by the environmental factors, among others [12]; however, these are not the only applications. Recently there has been climate impact research utilizing chlorophyll fluorescence analysis, along with satellite images [13] and manual measurement systems [14].

In order to develop instrumentation systems for measuring chlorophyll fluorescence, it is necessary to merge electrical engineering and plant biology. In this review, one vertex between the respective fields of electrical engineering and plant biosystems, is examined, especially the instrumentation when applied to the measurement of chlorophyll fluorescence. This phenomenon is common in some algae, bacteria and especially plants.

There are even some applications of chlorophyll fluorescence that focus on the quality, chemistry or physical characteristics of fruits; for instance, there are destructive methods which are commonly used in the process of detecting anthocyanin or flavonoids in specific fruits [1]. With chlorophyll fluorescence methods, this can be avoided. Regarding quality, there is research focused on plant nutrition characteristics to determine the types of elements that are beneficial for the plant and in what amounts [15,16]. Another important physical characteristic is the measurement of biomass, because it can be reflected directly in agricultural production [16], even in climate research through this characteristic [13].

None of the aforementioned techniques can be carried out without the appropriate instrumentation or equipment. The procedure proposed is made up of two main parts: the first being the chlorophyll

excitation, for which there are active and passive methods. The active methods use lamps [17–19], LEDs [6,9,20–25], or lasers [16,26,27] to excite the chlorophyll before beginning the measurements. The passive methods takes advantage of solar radiation to achieve the same goal [28,29]. The second part of the procedure is the measurement of the chlorophyll fluorescence. This can include several methods, each with different characteristics such as cost, resolution, ease of processing or portability. These characteristics primarily take into account the cameras [19,30], photodiodes [6,21], optical fiber [31] and satellite images [13] used during the process.

This article is both an update and overarching review regarding the instrumentation and sensing methods for measuring chlorophyll fluorescence; the objective is to provide a panoramic view of this field of research to aid in future developments and research projects. The long term objective of this review is to provide useful information and key data: primarily, the wavelength, intensity, and operating conditions that a given source of active or passive chlorophyll excitation requires. Next, the proper handling of the sample for correct measurement is reviewed. After that, the connections, methods, and electronic devices to maximize fluorescence response acquisition are described. Finally, data processing of the fluorescence response which includes filters, algorithms and equations, is examined.

## 2. Evolving Knowledge of Chlorophyll Fluorescence

Hans W. Kautsky and his collaborator, A. Hirsh, discovered a time dependent fluorescence when they observed an increase in fluorescence intensity when dark-adapted photosynthetically active samples were illuminated [32]. This phenomenon is also known as fluorescence transient, OJIP curve, fluorescence induction, fluorescence decay or the Kautsky effect.

All plants, from higher specimens to unicellular green algae, possess a chloroplast with thylakoid membranes containing photosystems I (PSI) and II (PSII), which are connected to each other by the cytochrome  $b_6/f$  complex. PSI is capable of producing fluorescence, but in very small quantities which are negligible. PSII is the only viable contributor to variable fluorescence [20,33].

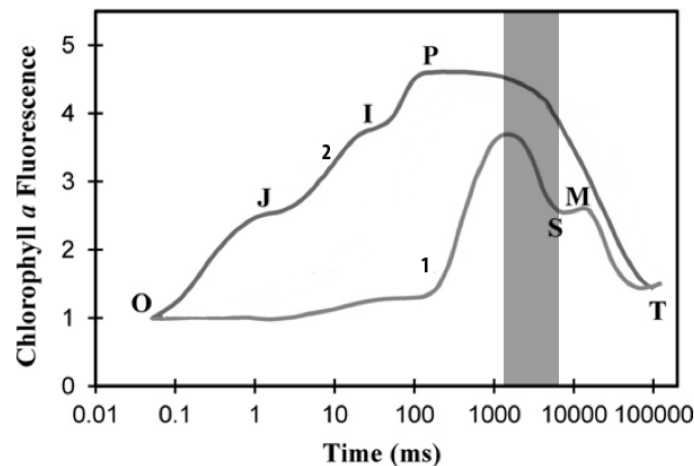
PSII consists of pigments and proteins in the thylakoid membrane of chloroplasts, which is the major target of many environmental stresses [34]. Based on this, chlorophyll fluorescence is widely used to determine the quality of growth conditions particularly in precision agriculture, where the parameters can be manipulated to improve the comfort conditions of plants.

Recent research suggests that the methods to dissipate excessive sunlight energy can be considered as a slowly reversible, protective mechanism, because inactive PSII complexes can act as protective shields [35]. Therefore, these mechanisms decrease the photochemical efficiency of PSII by interrupting the equilibrium between the radical pair and excitons in the light-harvesting antenna [36]. Consequently, photosynthetic energy harvesting is reduced and photon re-emitting by fluorescence is increased. Based in these facts, many techniques have been developed in the measurement of fluorescence for the improvement of comfort conditions in the plant and have increased production rates through the early detection of stress conditions [8–11].

In order to make accurate measurements of chlorophyll fluorescence, it is necessary to obtain the chlorophyll a fluorescence induction transient. This process is divided into two parts: the fast phase, which occurs within a second is labeled OJIP as shown in Figure 1, where O is the origin, P is the peak, and the two intermediate states are J-I [33]. This phase can be divided into two sub-phases;

(1) the photochemical phase that consists of O-J, and is directly dependant on the intensity of the excitation light; and (2) the nonphotochemical phase that consists of the J-I-P transient and is dominated by mechanisms for the excitation-dependent thermal dissipation of energy from PSII [37,38].

**Figure 1.** Chlorophyll *a* fluorescence induction transient, wavelength of excitation 650 nm and (1) 32 and (2) 3,200  $\mu\text{mol photons m}^{-2} \text{s}^{-1}$  at the leaf surface respectively (modified from [33]).



In this part, the main characteristics of the OJIP curve are described. Due to the fact that  $F_O$  and  $F_M$  are the most common parameters, these can be translated to O and P, respectively. In normal non-stressed plant leaves, the ratio of  $F_M/F_O$  is a constant high value [39]. There is another parameter called the variable fluorescence,  $F_V$ , which is the difference between  $F_M$  and  $F_O$  as shown in Equation (1). The ratio shown in Equation (2) is related to the maximum quantum yields of primary PSII photochemistry [37,40,41]. The relative variable fluorescence,  $V(t)$  at time  $t$  is a parameter frequently used in graphical representations of fluorescence inductions data, as stated in Equation (3). This is a double normalization of the fluorescence induction curve that permits a comparison of fluorescence transient measured under different conditions and/or within different samples:

$$F_V = F_M - F_O \quad (1)$$

$$\phi_{Po} = \frac{F_V}{F_M} = 1 - \frac{F_O}{F_M} \quad (2)$$

$$V(t) = \frac{(F(t) - F_O)}{(F_M - F_O)} \quad (3)$$

The above processes are applied to photosynthetic samples that have been kept in darkness, but, for samples that are kept in light, there are variants of this analysis. These measurements are commonly made during the decrease stage of fluorescence induction, utilizing a pulse of intense light between P and S time intervals as is highlighted in Figure 1. This leads to a transient increase of the fluorescence to a maximum value that, for the samples kept in light, this is called  $F'_M$ . This is usually lower than the  $F_M$  measured in dark-adapted samples. This decrease of maximum fluorescence during the slow phase of fluorescence induction is attributed to the non-photochemical process [42]. Similarly, the  $F_O$  value

of the sample kept in light is labeled as  $F'_O$ , being slightly different [43]. Nevertheless, the change is small enough to be negligible and it can be assumed that  $F_O = F'_O$ .

To calculate the non-photochemical quenching of samples kept in light, the expression in Equation (4), is used [44]. As has been observed, it is not necessary to differentiate the  $F_O$  and  $F'_O$  values. However, it is noted that  $F'_M$  is affected by photochemical quenching too. There are definitive results with samples that had been kept in darkness, and these can serve as reference for the normalization of data obtained from samples that have been kept in light. In such cases the formula for non-photochemical quenching is Equation (5). Taking into consideration that  $F'_O = F_O$ , the non-photochemical quenching formula for light-kept samples becomes Equation (6), whereas the photochemical quenching formula for light-kept samples is expressed as Equation (7). It must be taken into account that  $q_N$  and  $q_P$  are not two complementary terms, meaning that  $q_N$  and  $q_P$  are not equal to one [33]:

$$\frac{(F_M - F'_M)}{F'_M} \quad (4)$$

$$q_N = 1 - \frac{(F'_M - F'_O)}{(F_M - F_O)} \quad (5)$$

$$q_N = \frac{(F_M - F'_M)}{(F_M - F_O)} \quad (6)$$

$$q_P = 1 - \frac{(F'_M - F(t))}{(F'_M - F'_O)} \quad (7)$$

To begin with, the first instrumentation systems for chlorophyll fluorescence measurement evolved slowly. This happened because there was not much variety in the electronic devices available to develop these instruments, limiting possible research projects for lack of suitable technology. For example, in earlier tests, quartz fluorescence tubes with lens, prisms and photoelectric cells had to be used to acquire the fluorescence response. Today, far more advanced instrumentation and new technologies are available in order to provide a light source for this procedure.

### 3. Instrumentation in Chlorophyll Fluorescence

Most applications of chlorophyll fluorescence are focused on herbaceous plants, as these represent the main part of agricultural production. There are many kinds of measurements for monitoring plant variables, but these methods always attempt to be less invasive; that is, to make the measurements without causing damage and with a minimum amount of stress to the plant. This is why the chlorophyll fluorescence method is so successful. The instrumentation methods used to carry this out are thought to be the least invasive possible, even when the measurements are made in the laboratory.

The complete methodology to measure chlorophyll fluorescence is shown in Figure 2. First, it is necessary to prepare the sample to be measured. For example, if the measurement is carried out in dark-adapted conditions, the sample must be put inside a light isolation chamber to avoid ambient light interference. Sometimes, microorganisms need pre-treatments to improve the measurement and avoid stress conditions. The next step is the development of system instrumentation, using lamps, LEDs,

lasers, among others as excitation light source on active methods. However, there are passive methods which utilize only sunlight. This can be an advantage when the designer wants to save on light source devices, but it commonly requires more processing capabilities. The next stage consists of designing and selecting the proper optical detection devices, to obtain the fluorescence response from the previously excited sample for subsequent data storage and analysis. Later, it is necessary to process the response by applying signal processing techniques and displaying data in order to analyze the conditions of the sample.

**Figure 2.** Stages of chlorophyll fluorescence measurement process.

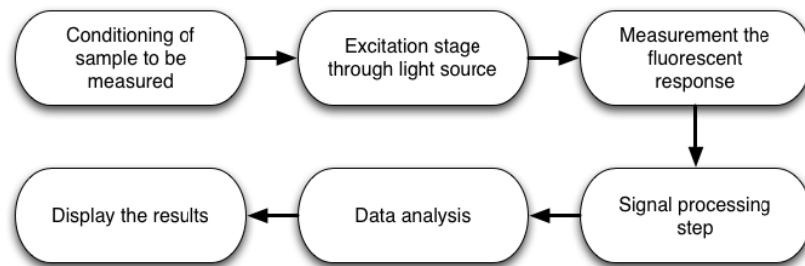
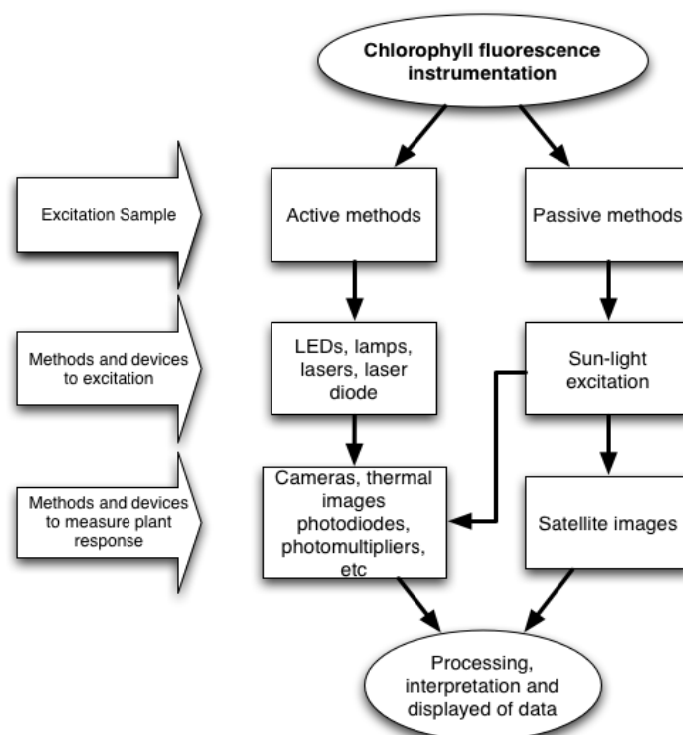


Figure 3 shows two possible ways to perform the measurement process. Active methods are those in which excitation light is provided by electronic devices such as LEDs, lamps, lasers, laser diodes, *etc.* On the other hand, passive methods, utilize only the sunlight energy as an excitation source. Furthermore, there are different ways to obtain the fluorescence response, depending on the excitation method and sample conditions. This can be achieved by using photodetector devices such as, cameras, photodiodes, photomultipliers, among others. It is necessary to process the collected data in order to obtain the chlorophyll fluorescence response to perform a proper interpretation and display results.

**Figure 3.** Chlorophyll fluorescence measurement routes by excitation source.



### 3.1. Light Sources for Excitation of Chlorophyll

As mentioned before, chloroplasts are very sensitive to stress. Consequently, the instrumentation applied to the plant for chlorophyll excitation should affect as little of the plant as possible. The first objective of study is the excitation light source. Correct selection is critical. First, taking into consideration the stress it is inflicting on the study subject, and second, the kinds of energy being emitted by the light source. It is well known that light sources are not very efficient devices, and often waste too much energy on others types of radiations, such as heat. The chlorophyll needs high light intensity to be activated and submit a response, and herein lays the problem. If the light source is intense, this could cause a harmful increase in temperature, especially when the subject is isolated via a dark chamber [6,18,22].

An appropriate light source must be selected. The first consideration for any light source is a lamp; yet, common lamps emit light primarily through filaments, which are low-efficiency devices due to the wasted energy in the form of heat and infrared emissions. Nevertheless, some kinds of lamps are widely used for plant growth. For example, high-pressure sodium lamps likes GroLux [17] do not use filament, but instead function through the excitation of the gas inside them. However, this type of lamp, like the filament lamp, emits heat that can cause stress to the plant; consequently, causing a disruption in the sample measurement.

New and more efficient alternatives for lighting are constantly being generated; one of the most current is the *Light Emitter Diode* (LED). The LED commonly takes up less space, generates less heat, and has a higher efficiency. This technology is being used regularly as a chlorophyll fluorescence source [6,9,20–25].

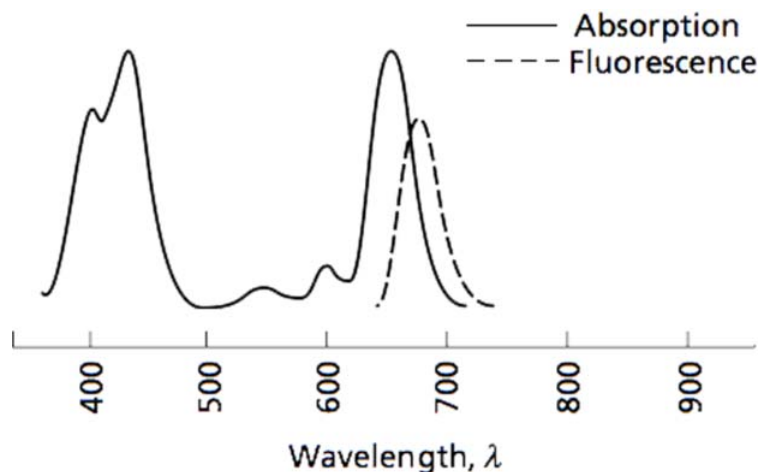
Some applications do not need to excite the entire subject, only a small part of it. In these cases lasers or laser diodes are an excellent choice, taking advantage of their special characteristic of emitting coherent light. This means that all of the electromagnetic waves emitted by the laser are pointed in a single direction. In contrast to what occurs with a common lamp where the emissions are dispatched in all directions, also referred to as omnidirectional. The coherent light emitted by these devices is quite a handy feature because a considerable amount of energy can be directed to a small area. This can cut down on the amount of necessary devices, and in some cases even lower costs. Also, these are a good choice for implementing portable chlorophyll fluorescence sensing systems. Such positive attributes are what makes the laser a frequently used device in these applications [16].

Another important factor to consider for the application of chlorophyll excitation is the wavelength. It is critical to choose the correct excitation wavelength to get the expected response. It is common knowledge that chlorophyll absorbs blue and red wavelengths, but reflects green, which is why the human eyes perceive plants in this hue [1]. The chlorophyll absorption zone on the electromagnetic spectrum and its fluorescence wavelength response are shown in Figure 4. Despite this standard, each chlorophyll excitation application uses a specific wavelength. This is because depending on what intensity or spectrum is the excitation source, the subject will have a different response.

Regarding the correct choice of wavelength, different selections are considered depending on the applications or electronic devices that were used in carrying out the experiment. This is based on the fact that the fluorescence of the plant is a re-emitting process of the absorbed photons with increased wavelength [1]. For example, for a plant that absorbs light in the blue (440 nm) and red (660 nm)

wavelengths the chlorophyll fluorescence will manifest as a red and infrared wavelength approximately 700 nm. This happens because energy is lost through heat, as seen in Figure 4.

**Figure 4.** Light absorption and emission by chlorophyll (modified from [1]).



Depending on the target applications, researchers select different wavelengths for excitation, as well as the appropriate light source, to carry out the fluorescence measurement. Table 1, shows a revision of the wavelengths utilized to excite samples, via various chlorophyll fluorescence sensing systems. Most are in the range from the ultra-violet to infrared.

**Table 1.** Wavelength use rate in chlorophyll sample excitation.

Wavelength (nm)	365	375	400	450	460	470	477	520	528	454	580	600	628	630	640	650	655	660	665	700	740
Use rate	1	1	1	1	1	1	1	1	1	1	1	1	1	1	1	3	1	2	1	1	1

### 3.2. Detection Devices for Chlorophyll Fluorescence

After the proper selection of chlorophyll excitation light-emitting devices and wavelengths, the second step is to have a way of identifying the response of the excited plant. This is achieved through different methods or sensing devices, depending on the system's design. For example, sometimes when an isolation chamber is used, optical fibers may be needed to convey the plant response to be processed outside of the chamber [14,22,24]. Photodiodes are widely used in these applications, often because they have both a good response time and are low-cost optical sensing devices along with other options for detecting the fluorescence (e.g., photomultipliers, thermal cameras, interferometry, *etc.*). As was aforementioned, photomultipliers are also used [45,46]. These are optical detectors like photodiodes, but with a base of vacuum tubes, and are particularly sensitive to low radiation.

However, the fluorescent response is not always acquired and processed as a one-dimensional signal. On many occasions image processing is also applied, and this is where the use of cameras comes in [19,26]. Generally, researchers tend to be more familiar with cameras as the sensing devices, because it is easy to understand how cameras can capture the response of the excited plant, not only on the visible spectrum but also through thermal imaging. It is possible that the use of thermal imaging is not taking fluorescence into account, only the temperature of the plant. But one must remember that

visible light makes up just a small part of the electromagnetic spectrum, and that thermal emissions are located just below the visible, in the infrared spectrum. Taking this into account, thermal cameras are just as common and necessary as those that process visible light, the only difference being that they exhibit greater sensitivity to longer wavelengths.

The application of cameras in this field sometimes has different objectives than those of two-dimensional imaging. For instance, there are camera-based applications that can be used in the quality-control area, such as the research carried out by Lefcourt *et al.* in 2005 [30]. In this study, special filters and edge detections were found to be able to detect when a fruit, in this case a red-delicious apple, was contaminated by fecal waste. In other cases, camera application can be used to detect pathogens even when there are no symptoms visible to the human eye.

Image processing for chlorophyll fluorescence is not only used for small-subject analysis; it is also widely applied for large-scale analysis, as in cases where it is necessary to analyze the fluorescence of high plants, or even large sets of plants, via satellite imaging.

#### 4. Measurement Methods for High Plants

It tends to be more difficult to make measurements for high plants, or in other words trees, because they are less manageable than herbaceous plants for either laboratory or field measurements. Therefore, it is sometimes impossible to use the aforementioned techniques for this type of procedure.

This section of the review will focus on the techniques that differ from those used for herbaceous plants. However, it is important to note that some of the chlorophyll fluorescence sensing systems are used in a similar fashion, especially with commercial products such as PEA Hansatech Instruments Ltd., which is used in applications with high as well as herbaceous plants [10].

Some of the methods used in chlorophyll excitation are called passive since they do not use an excitation device, the only excitation source employed being natural sunlight. This can lead to problems, since most of the active measurements are performed under controlled conditions; for example, the sample isolation chamber used in many laboratory measurements. However, when using the sun as a source of chlorophyll excitation the main problem lies in the photon emission response from the plant. This is below that which is emitted by the sun, less 1% [28].

To perform these types of measurements with environmental noise present, different methods have been developed to combat solar interference and obtain an accurate response from the plant. One way to solve this problem is through Fraunhofer lines. This technique is based on the capacity of gases in the atmosphere to absorb certain wavelengths. This means that band-reject filters can be used in such a manner that when determined by the incursion of gas, they can suppress an absorbed wavelength [13,28,47].

This technique can exploit oxygen capability by suppressing the 688 nm and 760 nm wavelengths, which is the bandwidth where chlorophyll fluorescence occurs [11]. Through the suppression of these wavelengths the fluorescence emitted by the plant can be viewed in order to make measurements.

Another way to make measurements on high plants is through the use of satellite [48] or airborne images [49], sometimes even both [50]. In contrast to ground applications, the estimation of chlorophyll fluorescence from air or space-borne sensors complicates the results. Consequently, the chlorophyll fluorescence, which is emitted by plants, needs to be separated from the reflected light by the sample



and the atmosphere path radiance conditions, which creates accuracy problems on the sensor [29]. These techniques, due to their nature, are applied to large numbers of subjects at the same time, even on a global level. Because a single subject emitting chlorophyll fluorescence is negligible using this method, such techniques can be used for large-scale environmental and ecological analysis. They can also be used for the analysis of photosynthesis in primary sector production, because it is well known that these variables are highly related. The methods of chlorophyll excitation for these applications are always passive, due to the nature of their collective analysis.

## 5. Measurement Methods for Micro Organisms

There are other applications of this process contrasting greatly with the mega-analysis methods covered in the previous section; these processes focus on analyzing microorganisms such as phytoplankton, algae, and bacteria. Method-wise, however, these procedures are not significantly different since photosynthetic reactions occur at a cellular level. Some of the commercial tools used to make the fluorescence measurements are actually used in both whole plants and unicellular organisms [50–53].

Despite the similarities in the chlorophyll excitation process and fluorescence response acquisition in both single cells and whole plants, a serious factor to consider is that the manipulation of samples changes noted for microorganisms, as compared to leaf-level measurements. Single-cell samples need special consideration and complex treatment. For example, there is a custom spectrometer modified to carry out measurement of the delayed fluorescence spectra of *Chlorella vulgaris* [52]. In conjunction with the commercial PAM-2000, it is possible to measure the efficiency of photochemical energy conversion in PSII reaction centers in microorganism samples [43].

Another sample type with similar features is algae. One specific case, in an experiment carried out by Drinovec in 2011 [54], the delayed fluorescence excitation spectra were measured with a custom-built delayed fluorescence spectrometer. The excitation was performed by halogen lamp and linear filter, while light was detected with a Perkin Elmer C1393 channel photomultiplier in photon-counting mode, assisted by two electromagnetic shutters used to protect the photomultiplier from the excitation light. This is because, as was aforementioned, the photomultiplier is a highly sensitive device and is subsequently used in lower light conditions.

Cyanobacteria are another type of microorganism capable of being analyzed via these methods. Cyanobacteria are thought, evolutionarily speaking, to be among the oldest organisms; they can perform oxygenic photosynthesis and respiration simultaneously, and many species are able to fix nitrogen. Within cyanobacteria similar conditions can be found and reactions such as those found in plants; for example, stress caused by heavy metal effects. These kinds of stress conditions can be detected by the previously detailed commercial methods, but these need to have been previously modified for this application. The container, especially, is different in this context. A cuvette equipped with sensors, such as piezoelectric transducers attached to its wall, usually serves as a detection system [53].

Wavelengths for chlorophyll excitation and subsequent fluorescence responses are not much different in analysis, between plants and microorganisms. However, it is necessary to perform tests to determine the most appropriate wavelength to use with any appliance, because the fluorescence excitation spectrum of fluorescence depends on the various cell pigments [52]. It is even possible to

take advantage of this situation, since samples in different taxonomic groups can be discriminated using delayed fluorescence spectroscopy by applying a sweep of wavelength, for example in a range between 400 nm and 700 nm [53].

## 6. Chlorophyll Fluorescence Signal Processing and Drivers

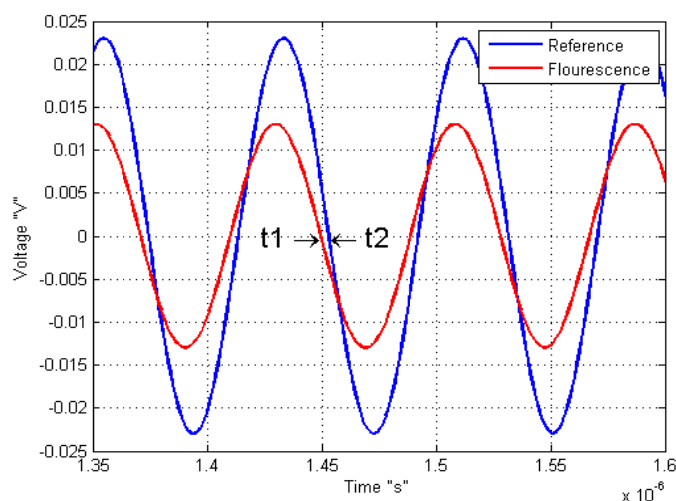
In this review the methods and electronic devices to elicit the chlorophyll fluorescence as well as the measurement of the response have been analyzed. Nevertheless, none of these are functional without data or signal processing, with the overall goal of estimating the condition or characteristics of the sample being measured.

Some equipment just displays the fluorescence behavior graphs and the operator is responsible for interpreting those graphs. Yet, other equipment is able to process information to show clear results such as photochemical and non-photochemical quenching. Depending on the pretreatment of the sample, the formula is selected like light-adapted or dark-adapted quenching [33].

Commercial equipment, generally known as PAM, functions with a Pulse Amplitude Modulated and operates without isolation chambers, which means that it is susceptible to environmental noise. In these cases, it is necessary to separate the fluorescent plant response in sunlight from fluorescence caused by chlorophyll excitation device. This is achieved by the pulse modulation of light source device, which induces a pulsed chlorophyll fluorescence signal form, the sample within conditions where ambient light is excluded with the assistance of optical filters permitting only three types of light signals: ambient light, non-pulsed fluorescence signal induced by the ambient light, and pulsed fluorescence signal induced by the modulation light source. It is noteworthy that this process is an active method, because the source light is different from the sun.

Another example of modified light source is used by Kissinger and Wilson on 2011, where they connected an oscillator to vary the LED source, with the objective to know the response of the sample by a sine-modulated excitation. This means that the phase difference between the reference or signal excitation and the output signal of the sample response indicates the fluorescence lifetime response as shown on Figure 5.

**Figure 5.** Sine waveform of light source chlorophyll excitation with a fluorescent response (Modified of [21]).



There are a variety of commercial or custom instruments to measure fluorescence, all of these aim to be less expensive and more accurate than other complex and inefficient methods. The fluorescence measurement has many advantages compared with other photosynthesis measurement methods. Chlorophyll fluorescence has the advantages of low energy consumption, fast measurement process, portability, lower cost, to name but a few when it is compared with carbon dioxide exchange method.

## 7. Main Applications of Chlorophyll Fluorescence

Chlorophyll fluorescence is a defense mechanism or excess energy dissipation performed by the subject [33] that is highly linked to the photosynthetic process. Consequently, it is one of the main applications used to estimate the photosynthesis level. Considering photosynthesis maintains autotrophic life, it is imperative to seek new alternatives for its measurement estimations. Chlorophyll fluorescence is one of them.

The main reason behind of these chlorophyll fluorescence sensing systems is to determine the comfort status of the plant, which gives one an idea of how productive the plant will become. However, these comfort conditions are not only reflected in the photosynthesis estimate, but also in the measurement of chlorophyll fluorescence. This means that it is not necessary to perform photosynthesis estimation procedures, because stress can also be detected through the sole use of chlorophyll fluorescence measurement. The quenching curves alone reflect several types of stress, including hydric or drought [55,56], frost damage [57], ozone [8], nutritional (such as boron) [15] and nitrogen [16,27,47].

There are other interesting features that can be detected by fluorescence as well; one being the amount of anthocyanins and flavonoids present in a subject. These can be detected by the surface skin fluorescence, as has been done with grapes [58]. Such uses are not as common as stress detection but are a good alternative to avoid destructive methods in these types of processes.

A method of identifying traces of feces in food was previously discussed. This takes advantage of the bacteria or plant remains found in feces, which are made to fluoresce. Through filters and image processing, the contaminating material can be detected. This can be applied to evaluate fruit washing methods, and therefore result in cleaner food without risk of disease [30]. As can readily be seen, the chlorophyll fluorescence method is a heavily exploited and is a useful tool in the areas of industry, agriculture, food, and research, including the area of global climate change.

## 8. Conclusions

The main advantage of chlorophyll fluorescence measurement is that it has the possibility of being a non-invasive technique. This differs from other stress-detection methods in which the measurement itself causes undue stress to the plant, which in turn can alter the resulting measurements. Based on these facts, many techniques for chlorophyll fluorescence measurement have been developed with the aim of improving comfort conditions for the plant and of obtaining increased production rates. However, these are not the only applications, because significant research on climate and environmental impact can also be carried out via chlorophyll fluorescence, which can be measured with the use of satellite images or manual methods. Due to various ecological problems, this is now more important than ever before.

Taking into account that electronic devices are constantly evolving and becoming more efficient, equipment to measure chlorophyll fluorescence will constantly improve; therefore, making smaller, more precise and more accurate measurements possible. However, there are many pathways to create new biosensors research. Therefore, this article review should be helpful in achieving a wide overview of state of the art investigations. For example, new methods and waveforms in the excitation light source could be utilized with the goal of finding new expressions in chlorophyll fluorescence response, and enhancing the methods of detecting bad conditions or problems in samples.

In modern fluorescence biosensing systems, it is necessary to perform the measurement in real time, with an optimal resolution and with portable biosensing systems. Furthermore, the aim is to improve the detection of stress conditions on plants of interest, as well as creating automated and easier measurement methods, in order to perform a large number of measurements at the same time without requiring highly qualified personnel. To carry out real-time measurement, it is necessary to design embedded sensor systems and reduce dependency on stationary and manual laboratory equipment.

However, none of these applications can be carried out without the appropriate instrumentation or equipment. As such, this review has been written with the goal of both widening general knowledge of these kinds of applications, and of providing the necessary information to develop novel and custom biosensors for chlorophyll fluorescence measurement.

## Acknowledgement

This project was partially supported by the CONACYT scholarship 226888 and the “Programa de Desarrollo e Innovación en Tecnologías Precursoras (PROINNOVA)”, by the program 20501059. The authors wish to thank Rebecca Baker and Silvia C. Stroet for English language editing. And finally, we wish to thank Universidad Autónoma de Querétaro (UAQ) for the academic support for this Ph. D. research.

## References

1. Taiz, L.; Zeiger, E. *Plant Physiology*, 5th ed.; Sinauer Associates: Sunderland, MA, USA, 2002; pp. 111–192.
2. Long, S.P.; Humphries, S.; Falkowski, P.G. Photoinhibition of photosynthesis in nature. *Annu. Rev. Plant. Mol. Biol.* **1994**, *45*, 633–662.
3. Losciale, P.; Hendrickson, L.; Grappadelli, L.C.; Chow, W.S. Quenching partitioning through light-modulated chlorophyll fluorescence: A quantitative analysis to assess the fate of the absorbed light in the field. *Environ. Exp. Bot.* **2011**, *73*, 73–79.
4. Zarco-Tejada, P.J.; Miller, J.R.; Mohammed, G.H.; Noland, T.L.; Sampson, P.H. Vegetation stress detection through chlorophyll a + b estimation and fluorescence effects on hyperspectral imagery. *J. Environ. Qual.* **2002**, *31*, 1433–1441.
5. Genty, B.; Briantais, J.M.; Baker, N.R. The relationship between the quantum yield of photosynthetic electron transport and quenching of chlorophyll fluorescence. *Biochim. Biophys. Acta* **1989**, *990*, 87–92.

6. Fedack, V.; Kytaev, O.; Klochan, P.; Romanov, V.; Voytovych, I. Portable Chronofluorometer for Express-Diagnostics of Photosynthesis. In *Proceedings of Intelligent Data Acquisition and Advanced Computing Systems: Technology and Applications*, Sofia, Bulgaria, 5–7 September 2005.
7. Espinosa-Calderon, A.; Torres-Pacheco, I.; Padilla-Medina, J.A.; Osornio-Rios, R.A.; Romero-Troncoso, R.J.; Villaseñor-Mora, V.; Rico-Garcia, E.; Guevara-Gonzalez, R.G. Description of photosynthesis measurement methods in green plants involving optical techniques, advantages and limitations. *Afr. J. Agric. Res.* **2011**, *12*, 2638–2647.
8. Bussotti, F.; Desotgiu, R.; Cascio, C.; Pollastrini, M.; Gravano, E.; Gerosa, G.; Marzuoli, R.; Nali, C.; Lorenzini, G.; Salvatori, E.; *et al.* Ozone stress in woody plants assessed with chlorophyll a fluorescence. A critical reassessment of existing data. *Environ. Exp. Bot.* **2011**, *73*, 19–30.
9. Faraloni, C.; Cutino, I.; Petruccelli, R.; Leva, A.R.; Lazzeri, S.; Torzillo, G. Chlorophyll fluorescence technique as a rapid tool for *in vitro* screening of olive cultivars (*Olea europaea* L.) tolerant to drought stress. *Environ. Exp. Bot.* **2011**, *73*, 49–56.
10. Mereu, S.; Gerosa, G.; Marzuoli, R.; Fusaro, L.; Salvatori, E.; Finco, A.; Spano, D.; Manes, F. Gas exchange and JIP-test parameters of two Mediterranean maquis species are affected by sea spray and ozone interaction. *Environ. Exp. Bot.* **2011**, *73*, 80–88.
11. Colls, J.J.; Hall, D.P. Application of a chlorophyll fluorescence sensor to detect chelate-induced metal stress in *Zea mays*. *Photosynthetica* **2004**, *42*, 139–145.
12. Contreras-Medina, L.M.; Torres-Pacheco, I.; Guevara-González, R.G.; Romero-Troncoso, R.J.; Terol-Villalobos, I.R.; Osornio-Rios, R.A. Mathematical modeling tendencies in plant pathology. *Afr. J. Agric. Res.* **2009**, *25*, 7399–7408.
13. Frankenberg, C.; Fisher, J.B.; Worden, J.; Badgley, G.; Saatchi, S.S.; Lee, J.E.; Toon, J.C.; Butz, A.; Jung, M.; Kuze, A.; *et al.* New global observations of the terrestrial carbon cycle from GOSAT: Patterns of plant fluorescence with gross primary productivity. *Geophys. Res. Lett.* **2011**, *38*, 1–6.
14. Piccotto, M.; Bidussi, M.; Tretiach, M. Effects of the urban environmental conditions on the chlorophyll a fluorescence emission in transplants of three ecologically distinct lichens. *Environ. Exp. Bot.* **2011**, *73*, 102–107.
15. Guidi, L.; Degl’Innocenti, E.; Carmassi, G.; Massa, D.; Pardossi, A. Effects of boron on leaf chlorophyll fluorescence of greenhouse tomato grown with saline water. *Environ. Exp. Bot.* **2011**, *73*, 57–63.
16. Thoren, D.; Schmidhalter, U. Nitrogen status and biomass determination of oilseed rape by laser-induced chlorophyll fluorescence. *Eur. J. Agron.* **2009**, *30*, 238–242.
17. Van Gaalen, K.E.; Flanagan, L.B.; Peddle, D.R. Photosynthesis, chlorophyll fluorescence and spectral reflectance in Sphagnum moss at varying water contents. *Oecologia* **2007**, *153*, 19–28.
18. Hideg, E.; Schreiber, U. Parallel assessment of ROS formation and photosynthesis in leaves by fluorescence imaging. *Photosynth. Res.* **2007**, *92*, 103–108.
19. Lichtenthaler, H.K.; Langsdorf, G.; Lenk, S.; Buschmann, S. Chlorophyll fluorescence imaging of photosynthetic activity with the flash-lamp fluorescence imaging system. *Photosynthetica* **2005**, *43*, 355–369.

20. Johnson, X.; Vandystadt, G.; Bujaldon, S.; Wollman, F.A.; Dubois, R.; Roussel, P.; Alric, J.; Béal, D. A new setup for *in vivo* fluorescence imaging of photosynthetic activity. *Photosynth. Res.* **2009**, *102*, 85–93.
21. Kissinger, J.; Wilson, D. Portable fluorescence lifetime detection for chlorophyll analysis in marine environments. *IEEE Sens. J.* **2011**, *11*, 288–295.
22. Wang, J.; Xing, D.; Zhang, L.; Jia, L. A new principle photosynthesis capacity biosensor based on quantitative measurement of delayed fluorescence *in vivo*. *Biosens. Bioelectron.* **2007**, *22*, 2861–2868.
23. Avercheva, O.V.; Berkovich, Y.A.; Erokhin, A.N.; Zhigalova, T.V.; Pogosyan, S.I.; Smolyanina, S.O. Growth and photosynthesis of chinese cabbage plants grown under light-emitting diode-based light source. *Russ. J. Plant. Phys.* **2009**, *56*, 14–21.
24. Bulgarea, G.; Boukadoum, M. A high-performance instrumentation system to measure the fluorescence kinetics of plants for *in vivo* photosynthesis research. *IEEE. T. Instrum. Meas.* **2001**, *50*, 679–689.
25. Ji, J.W.; Xu, M.H.; Li, Z.M. Research and application on chlorophyll fluorescence on-line monitoring technology. *Adv. Mat. Res.* **2010**, *139–141*, 2550–2555.
26. Kolber, Z.; Klimov, D.; Ananyev, G.; Rascher, U.; Berry, J.; Osmond, B. Measuring photosynthetic parameters at a distance: Laser induced fluorescence transient (LIFT) method for remote measurements of photosynthesis in terrestrial vegetation. *Photosynth. Res.* **2005**, *84*, 121–129.
27. Schächtl, J.; Huber, G.; Maidl, F.X.; Stickse, E. Schulz, J.; Haschberger, P. Laser-induced chlorophyll fluorescence measurements for detecting the nitrogen status of wheat (*Triticum aestivum* L.) canopies. *Prescis. Agric.* **2005**, *6*, 143–156.
28. Liu, L.; Zhang, Y.; Wang, J.; Zhao, C. Detecting solar-induced chlorophyll fluorescence from field radiance spectra based on the fraunhofer line principle. *IEEE Trans. Geosci. Remote* **2005**, *43*, 827–832.
29. Meroni, M.; Rossini, M.; Guanter, L.; Alonso, L.; Rascher, U.; Colombo, R.; Moreno, J. Remote sensing of solar-induced chlorophyll fluorescence: Review of methods and applications. *Remote. Sens. Environ.* **2009**, *113*, 2037–2051.
30. Lefcourt, A.M.; Kim, M.S.; Chen, Y. A transportable fluorescence imaging system for detecting fecal contaminants. *Comput. Electron. Agric.* **2005**, *48*, 63–74.
31. Agati, G.; Cerovic, Z.G.; Pinelli, P.; Tattini, M. Light-induced accumulation of ortho-dihydroxylated flavonoids as non-destructively monitored by chlorophyll fluorescence excitation techniques. *Environ. Exp. Bot.* **2011**, *73*, 3–9.
32. Kautsky, H.; Hirsch, A. Neue versuche zur kohlen säureassimilation. *Naturwissenschaften* **1931**, *19*, 964–964.
33. Stirbet, A.; Govindjee. On the relation between the Kautsky effect (chlorophyll a fluorescence induction) and photosystem II: Basics and applications of the OJIP fluorescence transient. *J. Photochem. Photobiol. B* **2011**, *104*, 236–257.
34. Lin, Z.; Liu, N.; Lin, G.; Pan, X.; Peng, C. Stress-induced alteration of chlorophyll fluorescence polarization and spectrum in leaves of *Alocasia macrorrhiza* L. Schott. *J. Fluoresc.* **2007**, *17*, 663–669.

35. Sun, Z.; Lee, H.; Matsubara, S.; Hope, A.B.; Pogson, B.J.; Hong, Y.; Chow, W.S. Photoprotection of residual functional photosystem II units that survive illumination in the absence of repair, and their critical role in subsequent recovery. *Physiol. Plant* **2006**, *128*, 415–424.
36. Hendrickson, L.; Förster, B.; Pogson, B.J.; Chow, W.S. A simple chlorophyll fluorescence parameter that correlates with the rate coefficient of photoinactivation of photosystem II. *Photosynth. Res.* **2005**, *84*, 43–49.
37. Campbell, D.; Hurry, V.; Clarke, A.K.; Gustafsson, P.; Öquist, G. Chlorophyll fluorescence analysis of cyanobacterial photosynthesis and acclimation. *Microbiol. Mol. Biol. Rev.* **1998**, *68*, 667–683.
38. Buonasera, K.; Lambreva, M.; Rea, G.; Touloupakis, E.; Giardi, M.T. Technological applications of chlorophyll a fluorescence for the assessment of environmental pollutants. *Anal. Bioanal. Chem.* **2011**, *40*, 1139–1151.
39. Björkman, O.; Demmig, B. Photon yield of O<sub>2</sub> evolution and chlorophyll fluorescence characteristics at 77 K among vascular plants of diverse origins. *Planta* **1987**, *170*, 489–504.
40. Govindjee. Sixty-three years since Kautsky: Chlorophyll a fluorescence. *Aust. J. Plant Physiol.* **1995**, *22*, 131–160.
41. Govindjee. Chlorophyll A Fluorescence: A Bit of Basics and History. In *Chlorophyll a Fluorescence A Signature of Photosynthesis*; Springer: Berlin, Germany, 2004; Volume 19, pp. 1–42.
42. Krause, G.H.; Jahns, P. Non-Photochemical Energy Dissipation Determined by Chlorophyll Fluorescence Quenching: Characterization and Function. In *Chlorophyll a Fluorescence: A Signature of Photosynthesis (Advances in Photosynthesis and Respiration)*; Papageorgiou, G.C., Govindjee, Eds.; Springer: Berlin, Germany, 2004; pp. 463–495.
43. Bilger, W.; Schreiber, U. Energy-dependent quenching of dark level chlorophyll fluorescence in intact leaves. *Photosynth. Res.* **1986**, *10*, 303–308.
44. Bilger, W.; Björkman, O. Role of the xanthophyll cycle in photoprotection elucidated by measurements of light-induced absorbance changes, fluorescence and photosynthesis in leaves of *Hedera canariensis*. *Photosynth. Res.* **1990**, *25*, 173–185.
45. Bürling, K.; Hunsche, M.; Noga, G. Use of blue-green and chlorophyll fluorescence measurements for differentiation between nitrogen deficiency and pathogen infection in winter wheat. *J. Plant Physiol.* **2011**, *168*, 1641–1648.
46. Hunsche, M.; Bürling, K.; Noga, G. Spectral and time-resolved fluorescence signature of four weed species as affected by selected herbicides. *Pestic. Biochem. Phys.* **2011**, *101*, 39–47.
47. Zhang, Y.; Liu, L.; Hou, M.; Liu, L.; Li, C. Progress in remote sensing of vegetation chlorophyll fluorescence. *J. Remote Sens.* **2009**, *13*, 971–978.
48. Xing, X.; Zhao, D.; Liu, Y.; Yang, J.; Xiu, P.; Wang, L. An overview of remote sensing of chlorophyll fluorescence. *Ocean Sci. J.* **2007**, *42*, 49–59.
49. Zarco-Tejada, P.J.; González-Dugo, V.; Berni, J.A.J. Fluorescence, temperature and narrow-band indices acquired from a UAV platform for water stress detection using a micro-hyperspectral imager and a thermal camera. *Remote Sens. Environ.* **2012**, *117*, 322–337.

50. Koponen, S.; Attila, J.; Pulliainen, J.; Kalliob, K.; Pyhälähtib, T.; Lindfors, A.; Rasmus, K.; Hallikainen, M. A case study of airborne and satellite remote sensing of a spring bloom event in the Gulf of Finland. *Cont. Shelf Res.* **2007**, *27*, 228–244.
51. Kurzbaum, E.; Eckert, W.; Yacobi, Y.Z. Delayed fluorescence as a direct indicator of diurnal variation in quantum and radiant energy utilization efficiencies of phytoplankton. *Photosynthetica* **2007**, *45*, 562–567.
52. Kurzbaum, E.; Beer, S.; Eckert, W. Alterations in delayed and direct phytoplankton fluorescence in response to the diurnal light cycle. *Hydrobiologia* **2010**, *639*, 197–203.
53. Dudkowiak, A.; Olejarz, B.; Łukasiewicz, J.; Banaszek, J.; Sikora, J.; Wiktorowicz, K. Heavy metals effect on cyanobacteria *synechocystis aquatilis* study using absorption, fluorescence, flow cytometry, and photothermal measurements. *Int. J. Thermophys.* **2011**, *32*, 762–773.
54. Berden-Zrimec, M.; Drinovec, L.; Zrimec, A. Delayed Fluorescence. In *Developments in Applied, Chlorophyll Fluorescence in Aquatic Science: Methods and Applications*; Suggett, D.J., Prášil, O., Borowitzka, M.A., Eds.; Springer: Berlin, Germany, 2010; Volume 4, pp. 293–309.
55. Komura, M.; Yamagishi, A.; Shibata, Y.; Iwasaki, I.; Itoh, S. Mechanism of strong quenching of photosystem II chlorophyll fluorescence under drought stress in a lichen, *Physciella melanchla*, studied by subpicosecond fluorescence spectroscopy. *Biochim. Biophys. Acta* **2010**, *1797*, 331–338.
56. Rahbarian, R.; Khavari-Nejad, R.; Ganjeali, A.; Bagheri, A.; Najafi, F. Drought stress effects on photosynthesis, chlorophyll fluorescence and water relations in tolerant and susceptible chickpea (*Cicer Arietinum* L.) genotypes. *Acta Biol. Crac. Bot.* **2011**, *53*, 47–56.
57. Rapacz, M.; Sasal, M.; Gut, M. Chlorophyll fluorescence-based studies of frost damage and the tolerance for cold-induced photoinhibition in freezing tolerance analysis of triticale (*×Triticosecale* Wittmack). *J. Agron. Crop Sci.* **2011**, *197*, 378–389.
58. Cerovic, Z.G.; Moise, N.; Agati, G.; Latouche, G.; Ghazlen, N.B.; Meyer, S. New portable optical sensors for the assessment of winegrape phenolic maturity based on berry fluorescence. *J. Food. Compos. Anal.* **2008**, *21*, 650–654.